Studies on Syntheses and Properties of TCNQ based Porous Coordination Polymers

Satoru Shimomura

2011

Preface

The study in this thesis has been carried out under the direction of Professor Susumu Kitagawa during April 2006 –March 2011 at the Department of Synthetic Chemistry and Biological Chemistry, Graduate School of Engineering, Kyoto University.

The author is greatly indebted to Professor Susumu Kitagawa for his significant guidance, continuous encouragement, and beneficial suggestion. The author wishes to express his hurtful gratitude to Professor Masaaki Ohba (Kyushu University) for his helpful advices and warm encouragements. The author is extremely grateful to Associate Professor Ryotaro Matsuda for his continuous encouragement and advice throughout this work. The author wishes to express his sincere gratitude to Associate Professor Takafumi Ueno, Ho-Chol Chang (Hokkaido University), Takashi Uemura, Shuhei Furukawa, and Assistant Professor Masakazu Higuchi and Satoshi Horike for their helpful suggestions and hearty encouragements. The author is deeply grateful to Emeritus Professor Takashi Kawamura (Gifu University) for his kind suggestion and helpful advice, in particular for the syntheses, and EPR and impedance measurements. The author is thankful to Professor Shigeyoshi Sakaki (iCeMS, Kyoto University) for his shrewd advice and discussion in theoretical calculation. The author wishes to thank Professor Tatsuo C. Kobayashi (Okayama University) for the helpful advice and experimental supports in SPring-8. The author also deeply thanks to Dr. Masaki Takata and Dr. Akihiro Hori (RIKEN SPring-8 center) for their fruitful discussion and encouragement. The author is deeply grateful to Associate Professor Yoshiki Kubota (Osaka Prefecture University) for his dedicated support in SPring-8 and informative suggestion about XRPD analysis. The author thanks Research Associate Keizo Mita (Osaka University) for his help in the measurement of Raman spectroscopy. The author acknowledges Ms. Arisa Yoshimura, Ms. Naomi Yasukawa, Ms. Hiroko Hano, Ms. Chiharu Minakata, Ms. Mariko Miyamura, and Mr. Yasushi Wanikawa for their experimental help in SPring-8.

The author deeply thanks Mr. Takashi Tsujino for his early training of experiment and utmost support. The author is also grateful to Associate Professor Shin-ichi Noro (Hokkaido University), Dr. Katsunori Mochizuki, Assistant Professor Daisuke Tanaka (Osaka University), Dr. Wakako Kaneko, Dr. Ko Yoneda, Dr. Hirotoshi Sakamoto, Assistant Professor Daisuke Kiriya (University of Tokyo), Dr. Sareeya Bureekaew, Mr. Yoshinori Kinoshita, Mr. Shinji Kato, Mr. Shinpei Hasegawa, Mr. Keisuke Kishida, and Mr. Keiji Nakagawa for their valuable discussion and continuous encouragement.

The author is indebted to Assistant Professor Hiroshi Sato for informative discussions and kind advices. The author also thanks to Dr. Seo Joobeom, Dr. Mio Kondo, Lecturer Takaaki Tsuruoka (Konan University), Dr. Charlotte Bonneau, Dr. Wataru Kosaka, Ms. Nao Horike, and Mr. Junichi Hataoka for their corporations and valuable discussions.

The author wishes to express appreciation to Dr. Yohei Takashima for his valuable suggestions and encouragements whether public or private. The author wishes to thank Mr. Yuh Hijikata, Mr. Nobuhiro Yanai, Mr. Daisuke Hiramatsu and Mr. Takeshi Ohmori for their helpful comments, encouragements and offering the environment for friendly competition. The author expresses his gratitude to Assistant Professor Tomomi Koshiyama (Kyushu University), Dr. Satoshi Abe, Dr. Maw Lin Foo, Ms. Mizue Abe, Mr. Kenji Hirai, Mr. Ryo Otani, Mr. Tomohiro Fukushima, Mr. Masashi Arai, and Mr. Daiki Umeyama for their valuable suggestions, kind supports and continuous encouragements. The author is deeply grateful to Mr. Kazuya Asano for his corporation and efforts to create a good research environment.

The author is thankful to Ms. Hiroko Hirohata, Ms. Kiyo Yamashita, Ms. Yoshiko Shimizu, Ms. Satoko Konishi, and Ms. Ritsuko Okamoto for their secretarial works and warm encouragement. Acknowledgements are to all other members of the group of Professor Kitagawa for their hearty encouragement and friendship during his time in the laboratory.

The author is much indebted for the financial support of Research Fellowship of the Japan Society for the Promotion of Science for Young Scientists.

Finally the author wishes to offer special thanks to his father, Yoshihiro Shimomura, his sister, Eri Naito, and his grandparents, Yoshitsugu Shimomura and Yoriko Shimomura for their all patience, constant financial supports and endearing encouragements.

Satoru Shimomura

Department of Synthetic Chemistry and Biological Chemistry
Graduate School of Engineering, Kyoto University
January, 2011

Contents

General Introduction

Porous materials

The history of porous materials goes back to the beginnings of human civilization and advances together with the development of humankind. Activated carbons, which are oldest and most famous porous materials, were used in a medical setting from as early as 1500 B.C.[1] Industrial applications originated in the late 18th century, when it was discovered that activated carbons could adsorb gases and remove color bodies from solution. These features come from the randomness of the amorphous structure with various pore sizes and pore shapes. Activated carbons have been being used extensively in manifold applications because of the inexpensive and convenient source and the simple synthetic method.[1, 2] Then, many kinds of porous materials, such as Zeolites were discovered and synthesized one after the other and used in various situations. Zeolites, which were found in the middle of the 18th century, are crystalline hydrated alkaline or alkaline-earth aluminosilicates containing pores and cavities.[3] Today, they are widely used in industrial applications with their crystallographically defined pore structures and high thermal and chemical stabilities.[4, 5]

At the end of the 20th century, the appearance of the new porous compound with inorganic-organic hybrid framework made an impact on the field of porous materials and added a new category to the conventional classification. Porous coordination polymers (PCPs), also known as metal organic frameworks (MOFs), have complete regular micropores, resulting in the quite large pore surface area, and highly designable framework, pore-shape, pore-size and surface functionality.[6-28] Their structures are constructed by the organic ligands as linkers and the metal centers as the connectors. PCPs get both variety and functionality of the organic materials and directivity and regularity of the inorganic materials. These components are connected by coordination bonds and other weak interactions or non-covalent bonds (H-bonds, π-electron stacking or van der Waals interaction) to form an infinite network. These interactions with smaller binding energy than that of a covalent bond cause the structural flexibility and dynamics in the crystalline state, which heightens a singularity of PCPs in the field of porous materials.[29]

Over the past dozen years since the beginning of PCPs, They have been attracting the attention of many scientists from various fields because of interest in the creation of amazingly versatile nanometer-sized spaces and the novel phenomena that occur in them. Currently, Studies on PCPs involve not only basic coordination chemistry but a wide range of fields such as Synthetic organic chemistry and Physical chemistry. This kind of hybridization of the scientific fields leads to give epochal advances in this field and create a new chemistry. Among them, approaches from chemistry

of organic conductors and charge transfer complexes increase their presence. While the previous researchs on PCPs focused on a construction and analysis of nano-porous structure, these approaches exploring unexpected electronic properties with redox active modules contribute to further development of PCPs. In this field, Tetracyanoquinodimethane (TCNQ) is one of the most famous redox active molecules, and there are an enormous number of researches using this molecule and they are still increasing.[30-36] Also in the field of PCPs, some porous frameworks based on TCNQ have been synthesized and showing various phenomena depending on the unique electronic property of TCNQ.

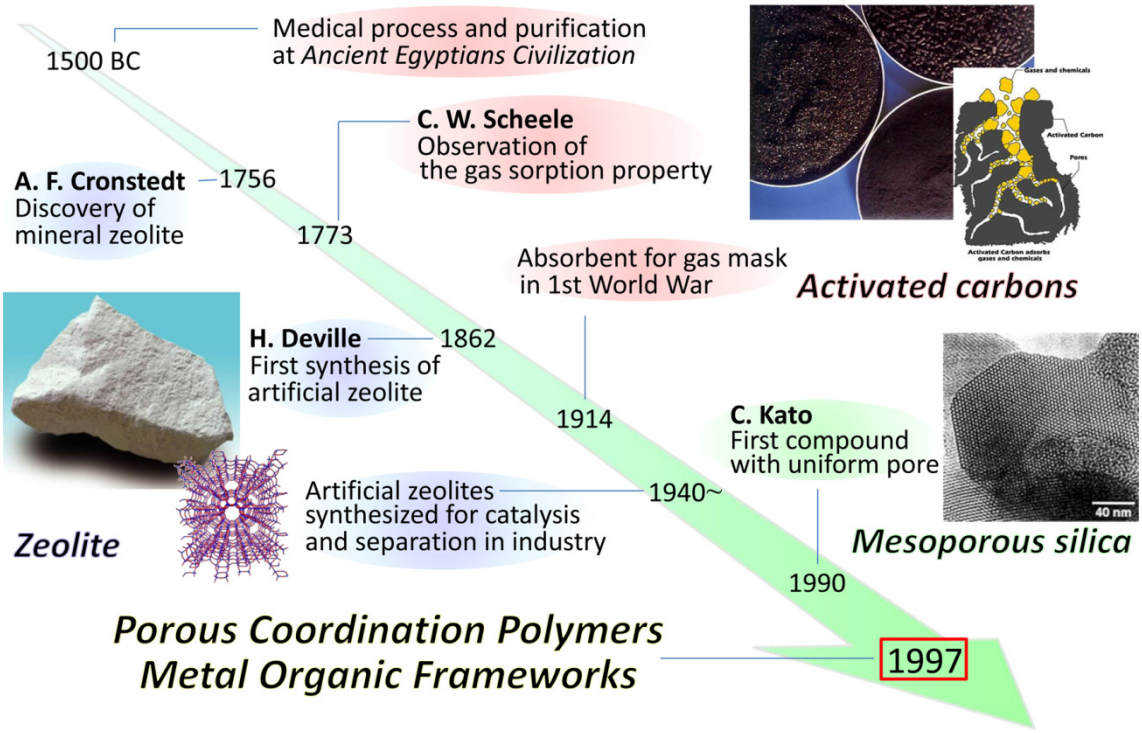

Figure 1. History of porous materials

TCNQ chemistry

TCNQ first appeared in 1960 by E. I. du Pont de Nemours and Company.[37] TCNQ is the historical example of an acceptor molecule which can be easily reduced to form the open shell anion radical $TCNQ^{\cdot -}$ when it is placed in contact with electron donors. TCNQ is also known as a decent multi-redox-active molecule; it can easily accommodate two extra electrons and, in some case, the radical trianion can even be formed. Diverse kinds of charge transfer complexes have been created with inorganic and organic donors. A charge transfer complex with a strong organic donor Tetrathiafulvalene (TTF); TTF-TCNQ particularly received the attention of the entire world at that time when it was synthesized.[38] TTF-TCNQ is the prototype of the charge-transfer compounds where HOMO and LUMO bands of the open shell donors and acceptors, respectively, contribute to the conduction. It has also been the first organic conductor to present a large conductivity in a wide temperature domain down to 59 K, where a sharp metal to insulator transition is observed.[39] The exceptional charge-transfer characters of them leaded to such unexpected electron properties. In this system, they are uniformly segregated and stacking with π orbitals contributing to two conduction bands. The π stacked column structure like this is common among the TCNQ based compounds and becomes the basis of their great electric and magnetic properties.

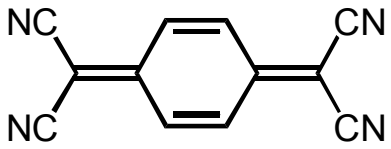

Tetracyanoquinodimethane (TCNQ)

On the other hands, one of the important factors to be considered in the compounds of TCNQ is the high σ-donor ability of TCNQ species. The presence of four widely separated cyano groups which can act as coordination sites renders TCNQ as potentially polydentate bridging ligands capable of binding up to four metal centers.[34, 35] Various kinds of metal-TCNQ complexes have been synthesized with the several coordination modes, such as μ_1, *syn*-μ_2, *cis*-μ_2, μ_3, and μ_4. Because of the structural and electronic diversity of TCNQ, a number of scientists have been interested in the interactions of TCNQ and metal ions leading to the studies of electron transfer phenomena and the unusual physical properties in solid state.

One of the typical coordination polymers are TCNQ radical anion complexes with monovalent metal ions: M(TCNQ) (M = Cu(I), Ag(I)).[33, 40] These were synthesized early in the history of TCNQ, and exhibited bistable switching phenomena in electron conductivity, which were induced by electric field and photo irradiation.[41, 42] Despite the extensive effort devoted to understanding this unique properties of these compound[43] and, especially in the case of Ag(TCNQ), the structural analysis was

succeeded,[40] there still remained skepticism regarding the validity of the mechanism, which were proposed in the original report. Meanwhile, Dunbar and co-workers reported the critical insights into the mechanism.[44] They characterized the structures and the conducting properties of two polymorphs of Cu(TCNQ) (phase I and phase II) and suggested these two phases with different electron conductivities are deeply involved with the switching phenomena. In phase I the TCNQ units form close π-stacking column structure at about 3.24 Å intervals whereas in phase II the closest distance of the π surfaces are about 6.8 Å. The column structure of TCNQ significantly affects the conducting mechanism, and this is why the difference of electron conductivities in phase I and II was observed. From this report to the present, many researchers have reported about this compound to achieve the construction and the control of nanostructure and the incorporation into nano-device system.[45-47]

About some dozens of coordination polymers with TCNQ have been synthesized so far. However there are not so many compounds, various studies about the magnetic properties based on the organic-inorganic hybrid infinite networks have been energetically carried out. In particular, Miyasaka, Dunbar and co-workers have synthesized various kinds of crystal structures of coordination polymers with TCNQ and its derivatives, and revealed their unique magnetic behaviors. The 2D coordination network systems composed of the paddlewheel-type dimetal units and TCNQ derivatives are one of the platforms which were adopted by their group to create the molecular based magnetic-conducting materials.[48-50] In these systems, the dimetal units acting as electron donors and the TCNQ derivatives acting as electron acceptors form charge transfer complexes and showing a charge transfer resonance, which leads to the long range strong magnetic interactions and/or metallic properties. These properties are deeply affected by the degree of charge transfer between the dimetal units and the TCNQ derivatives. Only the compound with the diruthenium $[Ru_2^{II,II}(O_2CCF_3)_4]$ units and $TCNQF_4$ exhibits 3-D long-range antiferromagnetic order at 95 K because of the full charge transfer from $[Ru_2^{II,II}]$ to $TCNQR_x$ to give the formal resonance form $[\{Ru_2^{4.5+}\}\text{-}(TCNQF_4^{\bullet -})\text{-}\{Ru_2^{4.5+}\}]$, compared with the isostructural compounds which are in the quasi-static state of $[\{Ru_2^{4+}\}\text{-}(TCNQR_x^{0})\text{-}\{Ru_2^{4+}\}]$ without charge transfer between the $[Ru_2^{II,II}]$ and $TCNQR_x$. The charge transfer capability and properties as organic radical of TCNQ derivatives should be beneficial in the construction of the long range magnetic interactions in molecular-based magnets.

TCNQ can provide various coordination architectures as a multidentate ligand as described above. In addition, TCNQ sometimes shows the formation of multimeric complexes which expands the structural diversity of the coordination frameworks, and especially, dimerization of the TCNQ radicals with σ bond leads to the enormous changes of molecular structure and electronic state.[51] The σ bonded dimer, (TCNQ−TCNQ) is formed by the linking of two TCNQ radical anions and a divalent anion. The π-conjugated structure of whole TCNQ molecule is ruptured by the *sp*3 type bond formation and the negative charges localize in each TCNQ moieties. However there are few reports about the σ bonded $(TCNQ{-}TCNQ)^{2-}$ and in most cases $(TCNQ{-}TCNQ)^{2-}$ have no

interaction with the metal fragment, coordination polymers with Mn and $(TCNQ{-}TCNQ)^{2-}$ have been synthesized and show fascinating structures and unique properties.[52, 53] The structure of $[Mn(TCNQ{-}TCNQ)(MeOH)_4]$ involves a 2D network composed of six-coordinate Mn ions equatorially bound to the four cyanide groups of $(TCNQ{-}TCNQ)^{2-}$ ligands. The axial sites are coordinated by the two MeOH molecules. The as-synthesized compound exhibits Curie-Weiss behavior with a small contribution from antiferromagnetic coupling at low temperature. On the other hand, when the compound was heated at 160 ºC, it exhibited a ferromagnetic transition at about 50 K. This drastic change of magnetic property comes from the cleavage of the weak σ bond in $(TCNQ{-}TCNQ)^{2-}$ and the generation of TCNQ radical anions from this process. As the case of this compound, TCNQ is the versatile unit to produce the conducting or magnetic properties and the switchable systems because of the electronic and structural diversity.

Chemistry of porous coordination polymer

Coordination polymers represent supramolecular compounds with infinite structure formed by metal ions and organic ligands with coordination bonding.(Scheme 1) The name "coordination polymer" was first used at 1916, and an enormous number of compounds have been synthesized and reported so far. They also included the potential porous systems, possessing pore spaces which were filled with solvent molecules or counter ions. However, the researches about the porous properties of them have begun in earnest in the end of the twentieth century, and the history of porous coordination polymers is not so long.

From when the gas storage or sorption properties are discovered,[54] PCPs have attracted worldwide attention as new porous materials with highly regular micropores. At that time, there are not so many compounds which can show porous properties among them. Even when the compounds possess the pore space in the structure, some of them cannot maintain the open framework then collapse or irreversibly transfer to the other structure in the guest removal process.[6] The fragility comes from the coordination bonds which are weaker than covalent and ionic bonds constituting the other conventional porous materials. In addition, the stability of the framework decreases as the porosity increase because of the principle 'nature abhors a vacuum'. Therefore, a lot of scientists have aimed to construct the robust framework with high porosity.

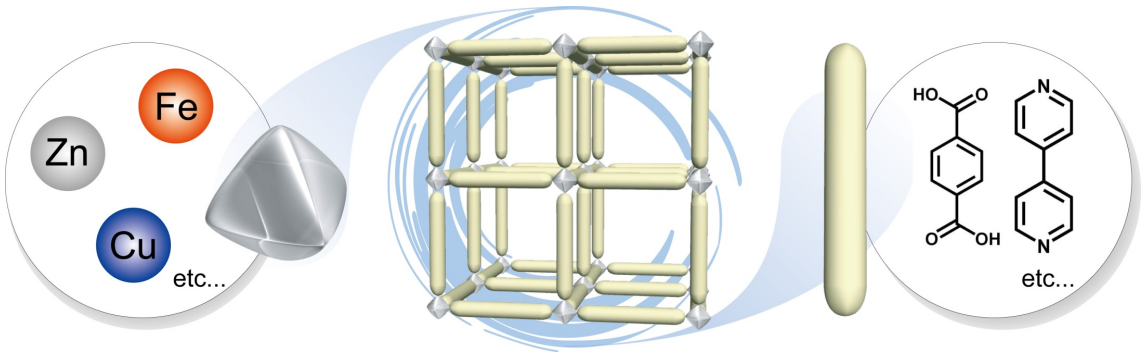

Scheme 1

Metal organic frameworks (MOFs) composed of Zn_4O clusters connected by the organic linkers are one of the famous series of porous motifs and embody the current of study for high porosity. $[Zn_4O(BDC)_3]$ (MOF-5) was synthesized early in the PCPs history and possess a cubic structure with 1,4-benzenedicarboxylate (BDC) as a organic linker.[55] On the basis of this motif, many porous compounds have been synthesized with using other dicarboxylate linkers, and this approach leads to some positive results to increase the pore volume according to the length and shape of the organic ligand.[56] The tricarboxylate linkers systems such as $[Zn_4O(BTB)_2]$ (MOF-177) and $[Zn_4O(BBC)_2]$

(MOF-200) also possess quite high porosity; the pore volumes reach as high as 90 percent of the lattice in the latter case.[57, 58] The 3D framework $[Cu_3(TMA)_2(H_2O)_3]$ (HKUST-1) including Cu_2 paddle wheel units linked by the Trimesic acid (TMA) is also one of the early PCP and a highly porous system.[59] This compound possesses a face-centered-cubic crystal structure and a 3D channel with a pore size of 1 nm and an accessible porosity of about 40 percent in the solid. This compound has been used for various studies because of the thermal stability and the aqueous durability of this motif. Therefore, some isostructural frameworks have been synthesized with longer tricarboxylate units and in the case of $Cu_3(TATB)_2(H_2O)_3$ (PCN-6), containing 4,4′,4″-*s*-triazine-2,4,6-triyltribenzoate (TATB) as a organic linker instead of TMA, the average diameter of the void inside the cuboctahedron is as large as 30.3 Å. [60] Despite the 2-fold interpenetration of the frameworks, PCN-6 is still sufficiently porous with the pore volume of 74 percent of the lattice. There are porous systems with a quite large pore size and a highly porosity composed of only small and simple components. $[Cr_3F(H_2O)O(BDC)_3]$ (MIL-101) is made from the linkage of BDC units and chromium trimers units that consist of three Cr cations and the μ_3O oxygen anion.[61] This compound possesses a extra-large cell volume and pore size; the pore space is constructed of the two cage units with the diameters of 29 Å and 34 Å which are connected with the window with the diameter of 12 Å and 14.5 Å, respectively.

Enhancement of thermal and chemical stability of porous structure is also important topic for PCPs. The compound $[Zn(MeIM)_2]$ (MeIM = 2-methylimidazolate) (ZIF-8, ZIF = zeolitic imidazolate framework) showed a one good design for this topic.[62] This compound is composed of Zn cations and MeIM linkers and they make a Zn–MeIM–Zn angle, close to 145°, which is coincident with the Si–O–Si angle which is preferred and commonly found in many zeolites. This framework possesses high thermal resistivity (up to 550°C in N_2) and chemical stability (in boiling water or 8 M NaOH aqueous solution). This exceptionally stable porous structure comes from the combination of a hydrophobicity of the pore surface and strong coordination bond between Zn and MeIM. As described above, various studies for the robustness and high porosity have been performed and are still going.

In contrast to the approach for robust porous framework, there are researches in which the fragility of PCPs is perceived as the flexibility and the dynamic properties. We can identify the compound showing guest accommodation with reversible nonporous to porous transformation as a porous material even if the compound cannot maintain the porous structure in guest removal process. These compounds are categorized as “third generation” PCPs[6] and later as “Soft Porous Crystals”,[29] and subjected to study due to their unique properties. The adsorption isotherms of these compounds sometimes cannot be classified according to the conventional IUPAC classification[63] because of the dynamic guest accommodation behavior. For instance, a ‘gate type’ sorption profile shows no uptake at low concentration of the guest molecules, and an abrupt increase in adsorption after a threshold

concentration. This so-called gate-opening pressure is a representative characteristic of them. The behavior is associated with a structural transformation from a non-porous to a porous phase.

The compound {[Cu(bpy)(H_2O)$_2$(BF_4)$_2$](bpy)} is the first example of the gate type sorption phenomena in PCPs.[64] This compound transforms from a 3D interpenetrated structure to a 2D square-grid layer structure [Cu(BF_4)$_2$(bpy)$_2$] by dehydration.[65] However this 2D sheet structure has no space to accommodate the guest molecules, the interlayer distance between the neighboring sheets increases and forms micropores with CO_2 adsorption. The gate type sorption behavior for CO_2 is associated with this expansion/shrinkage dynamic modulation. 2D layer structure is a good motif for the gate type sorption behavior because it is readily transformable system to respond to the guest accommodation. In particular, interdigitation is one of most useful structures because we can control interaction between sheets by modification of parts to be interdigitated. [Cu_2(dhbc)$_2$(bpy)]$_n$ (dhbc = 2,5-dihydroxybenzoate) has an interdigitation with π–π stacking interaction of dhbc moieties as a pillar in the adjacent sheets.[66] The π–π stacking of the pillar parts provides a moderate interaction for stabilization of the structure, and the sliding motion of π–π stacking is feasible when a guest is adsorbed to form an open structure. The compound [Zn(ip)(bpy)] (ip = isophthalate) (CID-1, CID = coordination polymers with an interdigitated structure) exhibits the basic structure of CID series in which it is easy to design the interaction between the 2D layer motifs.[67] The 2D layer in CID is composed of V-shaped dicarboxylate ligands, bpy and dinuclear metal units, and the dicarboxylate ligands impact on the interaction with the next layers and eventually the gate type sorption behaviors.

Some 3D porous network systems also show the flexible feature because of the variability of coordination bond; bond cleavage and change of coordination geometry are typical triggers, and these flexibilities promote long-range structural transformation. The compound [Cu_2(pzdc)$_2$(dpyg)] (pzdc = pyrazine-2,3-dicarboxylate, dpyg = 1,2-dipyridylglycol) constructed from the neutral 2D layer with Cu and pzdc, and pillar ligand, dpyg, which form 3D pillared layer structure.[68] This compound shows remarkable contraction of cell volume and especially of the interlayer distance by the removal of included guest molecules. The resultant framework whose channel size is not large enough to pass the molecules is classified to non-porous structure. However, the non porous phase can adsorb some solvent molecules because the transformation is reversible and the gate opening process and large hysteretic sorption isotherms can be observed. This is the first case of flexible 3D framework showing gate type sorption behavior as well as 2D layer systems. In the recent years, several researches about the gate type sorption behaviors for gas and organic molecules, and the mechanisms of them have been reported. For instance, the compound [Co(BDP)] (BDP = 1,4-benzenedipyrazolate) possessing large 1D square channels in as-synthesized state shows this type hysteretic sorption behavior even for H_2.[69] Understanding of these sorption phenomena will be a linchpin of a kinetic-based storage and separation of gases.

Although the gate type sorption was not observed, flexible features of frameworks were often determined by X-ray diffraction analysis. $[Ni_2(4,4'\text{-bpy})_3(NO_3)_4]$ have the interposing chiral bilayers of opposite handedness to form a tongue-and-groove type structure.[70] The crystal structures of this compound before and after guest removal revealed the slight shrinkage of the framework based on a subtle scissor-like action of the bilayers, leading to a distortion in the configuration of the bilayers. [V(OH)(BDC)] (MIL-47) have a 3D orthorhombic structure with rhomboid-shaped channel which is delimited by four walls of benzyl units and four chains of corner-shared vanadium octahedra.[71] This compound and derivatives showed the expansion of the framework with guest removal and later, was used for the separation of xylene isomers in the liquid phase.[72] $[Zn_2(bdc)_2(dabco)]$ (dabco = 1,4-diazabicyclo[2.2.2]octane) is an ancestral compound with typical tetragonal porous structure.[73] This structure is composed of square-grid 2D layer with Zn_2 paddle wheel units and BDC, and pillar ligand, dabco. This compound shows the reversible induced-fit type guest accommodation behaviors with the distortion of the framework. There are many derivative compounds using other dicarboxylate ligands and/or other pillar ligands,[74-76] and among them, $[Zn_2(bdc)_2(bpy)]$ (MOF-508) which has interpenetrating frameworks, can separate linear and branched isomers of pentane and hexane as a gas chromatographic column in the GC separation system with using the distortion and slippage motions of the frameworks.[77] These structural dynamics in crystalline materials lead to the varied unique porous properties of PCPs.[78, 79]

Apart from these studies focused on the construction of the framework, pore surface modification has been the important topic for PCPs. A sorption property of PCPs is strongly depended on the interactions between host framework and adsorbed guest molecules. In other words, design of host-guest interaction by adjustment of the pore surface is a shortcut to control the sorption properties of PCPs. Open or accessible metal sites are one of the popular interaction sites not only for PCPs but conventional porous materials. In early PCPs, these metal sites were accidentally produced from the "node" parts of the framework. Dimetal paddle wheel units are good motifs to create the open metal sites by removal of coordinated molecule in axial site. The Cu paddle wheel units in HKUST-1 act as a binding site for several gas molecules and a Lewis acidic site for the catalytic reactions.[80] $[Cu_2(BPTC)]$ (MOF-505, BPTC = 3,3′,5,5′-biphenyltetracarboxylate) also possesses the Cu paddle wheel units linked by the BPTC and shows a good H_2 storage capacity under low temperature condition,[81, 82] which is probably enhanced by the open metal sites. Metal-oxygen clusters are also one of the good candidates to provide the open metal sites stably. $[Ni_2(DHBDC)]$ (CPO-27-Ni or Ni-MOF-74), containing 3D honeycomb network with 1D large channels on which the open metal sites are uncovered after dehydration, shows the CO_2 binding structure with Ni-OCO bond and high sorption energy for several gas molecules.[83, 84] On the other hand, construction of the framework with metallo-ligands is a common strategy for introduction of open metal site on the pore surface of PCPs.[85] Metallo-ligands are metal complexes that contain two or more Lewis-base sites that are able

to bridge with other metal ions. The pioneering compounds with this type ligands are [Cu(II)(tpp)Cu(I)] and [Cu(II)(tcp)Cu(I)] (tpp = 5,10,15,20-tetra(4-pyridyl)-21H,23H-porphine, tcp = 5,10,15,20-tetrakis(4-cyanophenyl)-21H,23H-porphine).[86] Although these porphyrin-containing frameworks do not survive removal of guest molecules, the methodology have impacted on the recent researches. The metalloporphyrin network [CoT(p-CO_2)PP$Co_{1.5}$] with large, refillable 3D channels shows selective absorption properties with regard to the hydrophilicity of guest species based on the extraordinary hydrophilic character of the open metal sites on the pore surfaces.[87] The salen complex units are also a good metallo-ligand. The compound containing chiral salen units [Zn_2(bpdc)$_2$L] (bpdc = biphenyldicarboxylate, L = (R,R)-(2)-1,2-cyclohexanediamino-N,N′-bis(3-tert-butyl-5-(4-pyridyl)salicylidene)Mn^{III}Cl) is effective as an asymmetric catalyst for olefin epoxidation.[88] Various kinds of functional frameworks with open metal sites have been synthesized and these studies have been increasing.[89-91]

Here, we should mention about the postsynthetic approach; metal ions providing open metal sites are introduced into the already-formed network and entrapped by an organic linker in a pore wall.[92, 93] [$Cd_3L_4(NO_3)_6$] (L = (R)-6,6'-dichloro-2,2'-dihydroxy-1,1'-binaphthyl-4,4'-bipyridine) possesses the asymmetric 3D interpenetrating structure and shows enantioselective catalytic properties by the introduction of Lewis acidic metal centers (namely, Ti(OiPr)$_4$).[94] This postsynthetic approach is also used in the pore surface modification with organic functional groups and continues to expand rapidly.

There are huge numbers of studies about the pore surface modification with organic ligands and they have achieved to provide various kinds of porous properties and functions by controlling the pore environment such as Lewis acidity, hydrophilicity, and polarity. As described above, a lot of compounds with various kinds of porous properties in the series of [$Zn_4O(R_1)_3$] or [$Zn_2(R_1)_2(R_2)$] (R_1 = dicarboxylate, R_2 = pillar ligands) have been synthesized with using derivatives of dicarboxylate and pillar ligands.[56, 74, 76] Amino-MIL-53, which is the isostructure of MIL-53 with 2-aminoterephthalic acid instead of BDC, was synthesized to enhance the affinity for CO_2, resulting in a large selectivity in CO_2/CH_4 separations.[95] In addition, This Amino-MIL-53 was used for the further postsynthetic surface modification with the synthetic organic chemical approach, and these modifications affected the selective gas sorption properties.[96] In the case of [Zn(N_3-ipa)(bpy)] (CID-N_3), the pore surface properties can be changed by photoirradiation with using the photochemical reaction from azide to nitrene and this photoactivation enhances the sorption capability for O_2.[97]

However, there are few reports about the PCPs showing the strong guest accommodation by the complexation with guest molecules by the electron or charge transfer.[98-100] These systems should be able to achieve the good separation and/or the unusual selectivity which it is not easy to achieve by the conventional porous compounds. To establish these systems, redox active organic molecules,

which are used for organic conductors, are being used to construct the open frameworks. The hybridization of the scientific field is happening in this instant of time.

Hybridization of TCNQ in PCPs

Although some potential TCNQ based porous frameworks containing solvent molecules in the open framework have already reported in earlier times, there were few cases in which the compounds were recognized as host materials and attention focused on the release and accommodation of the guest molecules. This is because their interesting magnetic and electric properties are interesting enough to distract the attentions from their porous properties. However, they should show the unique porous properties and physical phenomena caused by the host-guest charge transfer interactions. The aim of this study was to create the new TCNQ based porous coordination polymers and to develop the unique porous properties which are difficult to achieve with the conventional porous materials (Scheme 2).

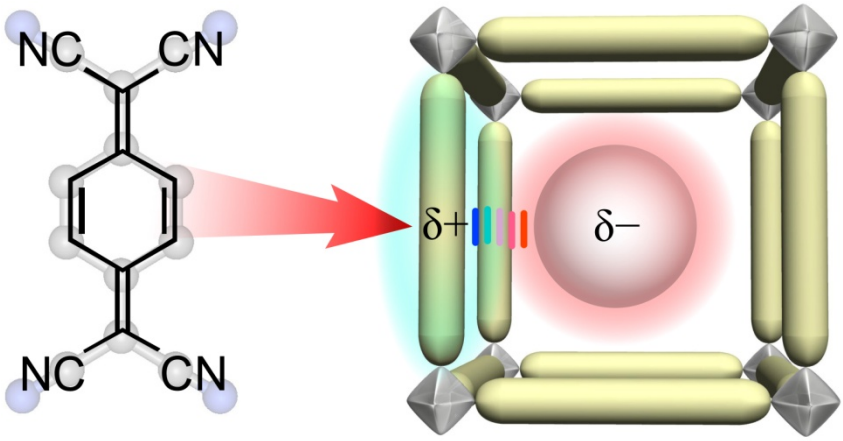

Scheme 2

Survey of this thesis

Chapter 1 described the synthesis, characteristics and guest accommodation properties of TCNQ dianion-based PCP, [Zn(TCNQ)bpy] (TCNQ = 7,7,8,8-tetracyano-*p*-quinodimethane, bpy = 4,4′-bipyridyl). The reaction of $Zn(NO_3)_2 \cdot 6H_2O$ with LiTCNQ and bpy in MeOH solution provided this compound. The X-ray diffraction analysis revealed that this compound possesses the 2D layer of [Zn(TCNQ)] linked by pillar ligands, bpy, and forms 3D pillared layer structure with 2D porous system. This compound showed the good electron donating property for aromatic molecules because the highly reduced TCNQs array on the pore surface. This electron donating property leaded to the host guest charge transfer complexation accompanying with crystal color change. In the result, this open framework obtained a sensing capability for several aromatics with crystal to crystal transformation and strong accommodation, which are based on charge transfer interaction with them. This result will be useful to the design and synthesis of new framework-guest hybrid compounds with unique physical properties and/or chemical reactions.

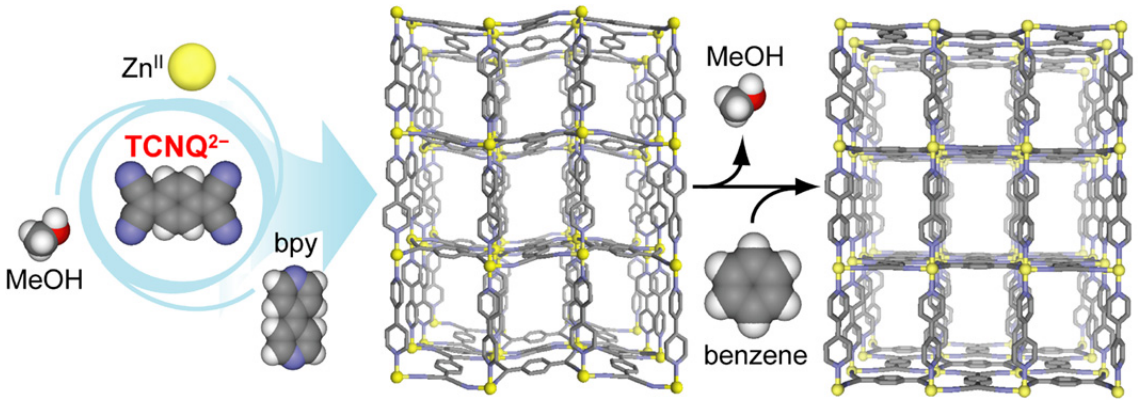

Chapter 2 described the synthesis and comparison of a series of TCNQ-dianion-based porous coordination polymers with divalent metal cations [M(TCNQ)bpy] (M = Fe, Zn, Mn, Co, Cd). The synthesis reactions of these compounds are promoted by the addition of ascorbic acid, which is the key to obtaining a high yield. They form almost identical three-dimensional pillared layer structures with the M–TCNQ two-dimensional layers linked by bpy pillar ligands. The electronic properties of these compounds vary depending on the constitutional metal ions and guest molecules. We found that the electronic interaction between metal ions and TCNQ moieties in the frameworks strongly impacted the electronic properties of the compounds.

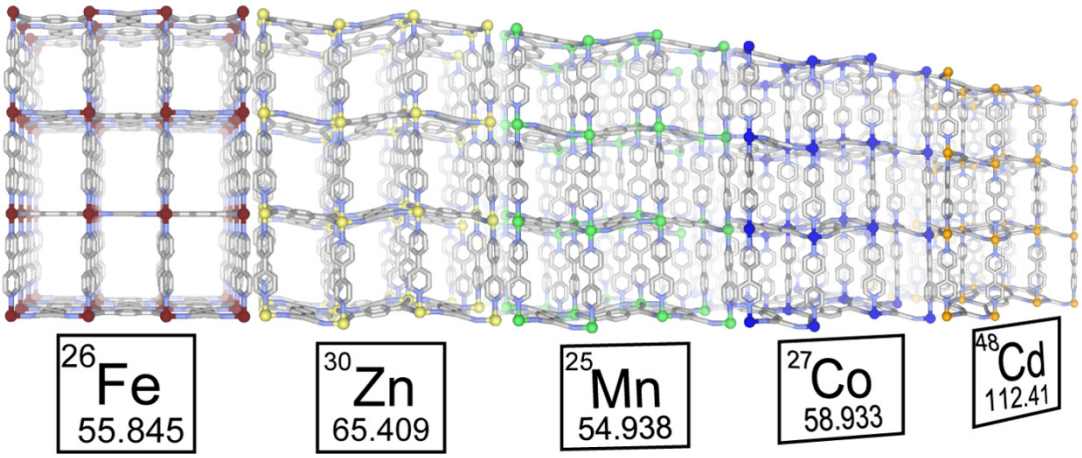

Chapter 3 described the synthesis and characteristics of TCNQ-dimer-based PCPs [Zn(TCNQ-TCNQ)bpy]. The reaction of $Zn(NO_3)_2 \cdot 6H_2O$ with LiTCNQ and bpy (= 4,4′-bipyridine) in an MeOH/benzene mixture (1:1) provided a 3D open framework composed of 1D chains of [Zn(bpy)] and TCNQ dimers acting as cross-linkers. TCNQ dimer is derived from a sigma dimerization of two TCNQ radical anions. This framework formed the undulating channel which is adequate to accommodate a benzene molecule because of the suitability of the cavity's size and thickness. Adsorption measurement and X-ray powder diffraction measurement revealed this framework possessed the good affinity for benzene molecule and showed the structural flexibility in the guest-removal process. Based on these natures, this framework showed a selective adsorption property of benzene with gate open type sorption behavior and separation properties for benzene from cyclohexane. Synergy of the structural flexibility to adapt to the target molecular shape, and, with the interaction site located in the right position of the pore surface, makes PCPs an effective separation system.

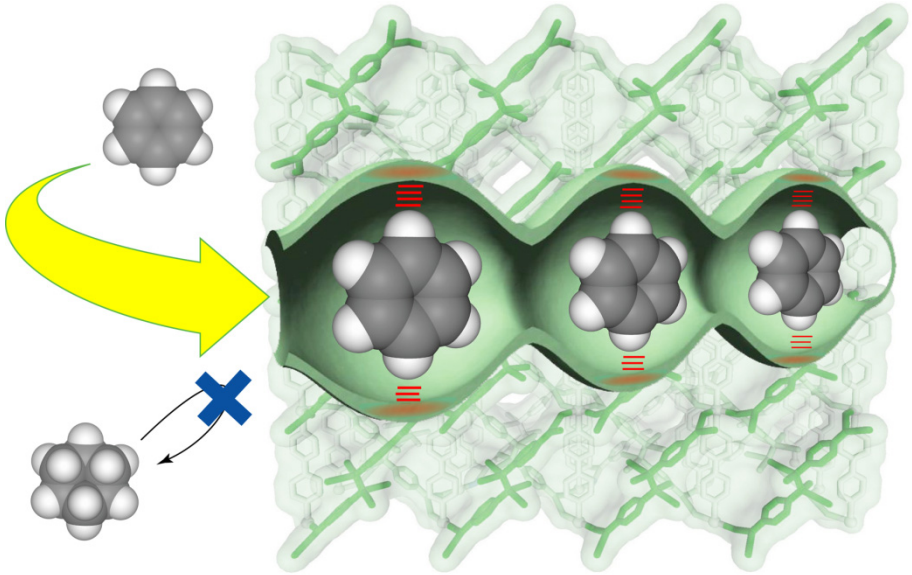

Chapter 4 described the unusual selective gas sorption property of TCNQ dimer based PCP, [Zn(TCNQ-TCNQ)bpy]. This compound showed selective recognition of O2 and NO molecules over a variety of other gas molecules (C_2H_2, Ar, CO_2, N_2 and CO). X-ray diffraction analysis and spectroscopic measurements (IR, Raman) provided the information about this unique phenomenon. This framework showed the closed–open type structural transition accompanying with gas adsorption and IR spectra of TCNQ dimer unit and Raman spectra of adsorbed O2 molecule indicated the existence of charge transfer interaction between them. The key to this selectivity is a combination of the structural dynamics and electron-donating function of the framework, which can be induced by the soft crystallinity and designability of PCPs. PCPs therefore show promise as selective adsorption systems for small gas molecules.

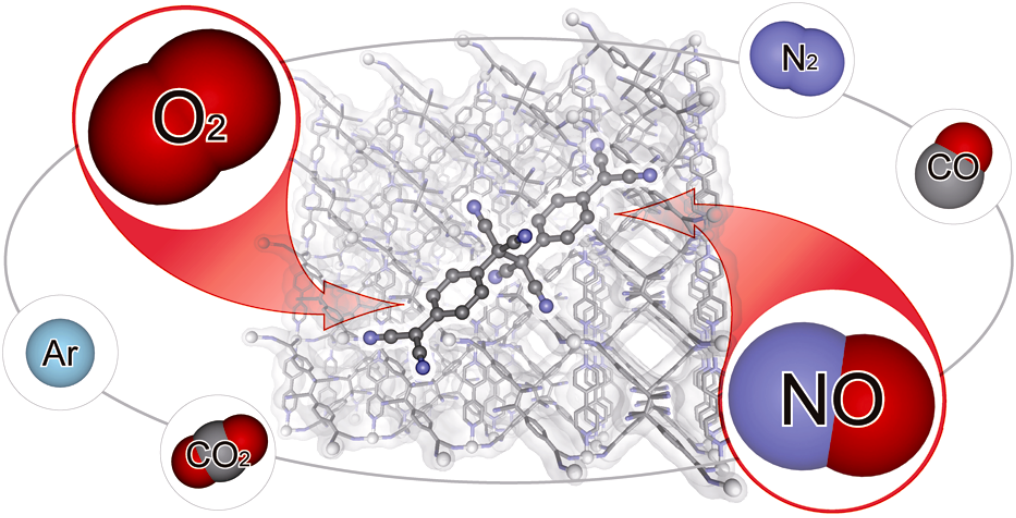

Chapter 5 described the relationship between the structural flexibility and selective sorption properties of PCPs. Two PCPs [M(TCNQ-TCNQ)bpy] (M = Mn, Zn) consisting of the same components except for the metal cations and forming identical structures have been prepared to compare their selective sorption and separation properties. In contrast to the crystal to amorphous transformation of Mn compound, Zn compound showed crystal to crystal transformation in the guest removal process. DSC measurements indicated that an energy gap between the guest-accommodating phase and the guest-free phase of Zn compound is larger than that of Mn compound. In these systems, the high selective guest accommodation of the Zn complex is based on the crystal-to-crystal transformation with a large energy gap. The results indicate that the flexibility of the framework is one of the important factors determining the porous properties. Tuning the flexibility of PCPs based on designability of the frameworks will offer a new approach to control sorption behavior and a new function based on the dynamic properties of PCPs.

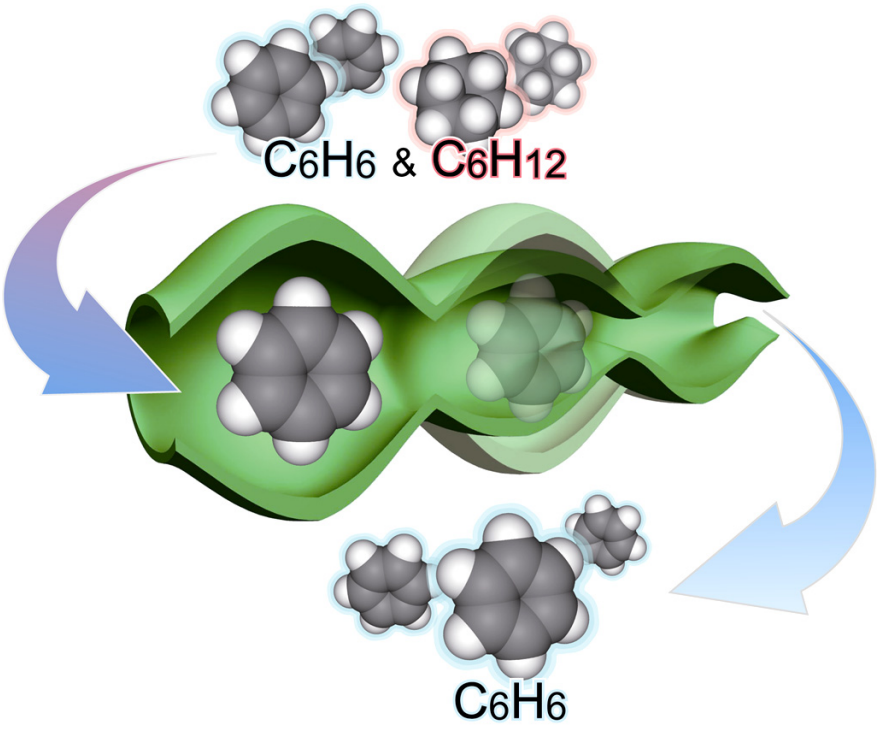

References

[1] Matisova, E.; Skrabakova, S., *J. Chromatogr. A* **1995,** *707*, 145-179.

[2] Wigmans, T., *Carbon* **1989,** *27*, 13-22.

[3] Davis, M. E.; Lobo, R. F., *Chem. Mater.* **1992,** *4*, 756-768.

[4] Ozin, G. A.; Kuperman, A.; Stein, A., *Angew. Chem. Int. Ed. Engl.* **1989,** *28*, 359-376.

[5] Cheetham, A. K.; Ferey, G.; Loiseau, T., *Angew. Chem. Int. Ed.* **1999,** *38*, 3268-3292.

[6] Kitagawa, S.; Kondo, M., *Bull. Chem. Soc. Jpn.* **1998,** *71*, 1739-1753.

[7] Yaghi, O. M.; Li, H. L.; Davis, C.; Richardson, D.; Groy, T. L., *Acc. Chem. Res.* **1998,** *31*, 474-484.

[8] Batten, S. R.; Robson, R., *Angew. Chem. Int. Ed.* **1998,** *37*, 1460-1494.

[9] Blake, A. J.; Champness, N. R.; Hubberstey, P.; Li, W. S.; Withersby, M. A.; Schröder, M., *Coord. Chem. Rev.* **1999,** *183*, 117-138.

[10] Moulton, B.; Zaworotko, M. J., *Chem. Rev.* **2001,** *101*, 1629-1658.

[11] Eddaoudi, M.; Moler, D. B.; Li, H. L.; Chen, B. L.; Reineke, T. M.; O'Keeffe, M.; Yaghi, O. M., *Acc. Chem. Res.* **2001,** *34*, 319-330.

[12] James, S. L., *Chem. Soc. Rev.* **2003,** *32*, 276-288.

[13] Côté, A. P.; Shimizu, G. K. H., *Coord. Chem. Rev.* **2003,** *245*, 49-64.

[14] Papaefstathiou, G. S.; MacGillivray, L. R., *Coord. Chem. Rev.* **2003,** *246*, 169-184.

[15] Janiak, C., *Dalton Trans.* **2003**, 2781-2804.

[16] Kitagawa, S.; Kitaura, R.; Noro, S., *Angew. Chem. Int. Ed.* **2004,** *43*, 2334-2375.

[17] Rao, C. N. R.; Natarajan, S.; Vaidhyanathan, R., *Angew. Chem. Int. Ed.* **2004,** *43*, 1466-1496.

[18] Fletcher, A. J.; Thomas, K. M.; Rosseinsky, M. J., *J. Solid State Chem.* **2005,** *178*, 2491-2510.

[19] Müller, U.; Schubert, M.; Teich, F.; Puetter, H.; Schierle-Arndt, K.; Pastré, J., *J. Mater. Chem.* **2006,** *16*, 626-636.

[20] Maspoch, D.; Ruiz-Molina, D.; Veciana, J., *Chem. Soc. Rev.* **2007,** *36*, 770-818.

[21] Morris, R. E.; Wheatley, P. S., *Angew. Chem. Int. Ed.* **2008,** *47*, 4966-4981.

[22] Lee, J.; Farha, O. K.; Roberts, J.; Scheidt, K. A.; Nguyen, S. T.; Hupp, J. T., *Chem. Soc. Rev.* **2009,** *38*, 1450-1459.

[23] Ferey, G.; Serre, C., *Chem. Soc. Rev.* **2009,** *38*, 1380-1399.

[24] Murray, L. J.; Dinca, M.; Long, J. R., *Chem. Soc. Rev.* **2009,** *38*, 1294-1314.

[25] Fischer, R. A.; Woll, C., *Angew. Chem. Int. Ed.* **2009,** *48*, 6205-6208.

[26] Li, J. R.; Kuppler, R. J.; Zhou, H. C., *Chem. Soc. Rev.* **2009,** *38*, 1477-1504.

[27] Ma, L. Q.; Abney, C.; Lin, W. B., *Chem. Soc. Rev.* **2009,** *38*, 1248-1256.

[28] Chen, B. L.; Xiang, S. C.; Qian, G. D., *Acc. Chem. Res.* **2010,** *43*, 1115-1124.

[29] Horike, S.; Shimomura, S.; Kitagawa, S., *Nat. Chem.* **2009,** *1*, 695-704.

[30] Acker, D. S.; Hertler, W. R., *J. Am. Chem. Soc.* **1962,** *84*, 3370-3374.

[31] Hertler, W. R.; Acker, D. S.; Benson, R. E.; Hartzler, H. D., *J. Am. Chem. Soc.* **1962,** *84*, 3387-3393.

[32] Hertler, W. R.; Benson, R. E., *J. Am. Chem. Soc.* **1962,** *84*, 3474-3478.

[33] Melby, L. R.; Mahler, W.; Mochel, W. E.; Harder, R. J.; Hertler, W. R.; Benson, R. E., *J. Am. Chem. Soc.* **1962,** *84*, 3374-3387.

[34] Kaim, W.; Moscherosch, M., *Coord. Chem. Rev.* **1994,** *129*, 157-193.

[35] Ballester, L.; Gutierrez, A.; Perpinan, M. F.; Azcondo, M. T., *Coord. Chem. Rev.* **1999,** *192*, 447-470.

[36] Jerome, D., *Chem. Rev.* **2004,** *104*, 5565-5591.

[37] Acker, D. S.; Harder, R. J.; Hertler, W. R.; Mahler, W.; Melby, L. R.; Benson, R. E.; Mochel, W. E., *J. Am. Chem. Soc.* **1960,** *82*, 6408-6409.

[38] Ferraris, J.; Walatka, V.; Perlstei.Jh; Cowan, D. O., *J. Am. Chem. Soc.* **1973,** *95*, 948-949.

[39] Coleman, L. B.; Cohen, M. J.; Sandman, D. J.; Yamagish.Fg; Garito, A. F.; Heeger, A. J., *Solid State Commun.* **1973,** *12*, 1125-1132.

[40] Shields, L., *J. Chem. Soc., Faraday Trans. 2* **1985,** *81*, 1-9.

[41] Potember, R. S.; Poehler, T. O.; Cowan, D. O., *Appl. Phys. Lett.* **1979,** *34*, 405-407.

[42] Potember, R. S.; Poehler, T. O.; Benson, R. C., *Appl. Phys. Lett.* **1982,** *41*, 548-550.

[43] Gu, Z. Z.; Wu, H. M.; Wei, Y.; Liu, J. Z., *J. Phys. Chem.* **1993,** *97*, 2543-2545.

[44] Heintz, R. A.; Zhao, H. H.; Xiang, O. Y.; Grandinetti, G.; Cowen, J.; Dunbar, K. R., *Inorg. Chem.* **1999,** *38*, 144-156.

[45] Liu, H. B.; Zhao, Q.; Li, Y. L.; Liu, Y.; Lu, F. S.; Zhuang, J. P.; Wang, S.; Jiang, L.; Zhu, D. B.; Yu, D. P.; Chi, L. F., *J. Am. Chem. Soc.* **2005,** *127*, 1120-1121.

[46] O'Mullane, A. P.; Fay, N.; Nafady, A.; Bond, A. M., *J. Am. Chem. Soc.* **2007,** *129*, 2066-2073.

[47] Flannigan, D. J.; Lobastov, V. A.; Zewail, A. H., *Angew. Chem. Int. Ed.* **2007,** *46*, 9206-9210.

[48] Miyasaka, H.; Campos-Fernandez, C. S.; Clerac, R.; Dunbar, K. R., *Angew. Chem. Int. Ed.* **2000,** *39*, 3831-3832.

[49] Miyasaka, H.; Izawa, T.; Takahashi, N.; Yamashita, M.; Dunbar, K. R., *J. Am. Chem. Soc.* **2006,** *128*, 11358-11359.

[50] Miyasaka, H.; Motokawa, N.; Matsunaga, S.; Yamashita, M.; Sugimoto, K.; Mori, T.; Toyota, N.; Dunbar, K. R., *J. Am. Chem. Soc.* **2010,** *132*, 1532-1544.

[51] Dong, V.; Endres, H.; Keller, H. J.; Moroni, W.; Nothe, D., *Acta Crystallogr., Sect. B: Struct. Sci.* **1977,** *33*, 2428-2431.

[52] Zhao, H. H.; Heintz, R. A.; Dunbar, K. R.; Rogers, R. D., *J. Am. Chem. Soc.* **1996,** *118*, 12844-12845.

[53] Zhao, H.; Heintz, R. A.; Ouyang, X.; Dunbar, K. R.; Campana, C. F.; Rogers, R. D., *Chem. Mater.*

1999, *11*, 736-746.

[54] Kondo, M.; Yoshitomi, T.; Seki, K.; Matsuzaka, H.; Kitagawa, S., *Angew. Chem. Int. Ed. Engl.* **1997,** *36*, 1725-1727.

[55] Li, H.; Eddaoudi, M.; O'Keeffe, M.; Yaghi, O. M., *Nature* **1999,** *402*, 276-279.

[56] Eddaoudi, M.; Kim, J.; Rosi, N.; Vodak, D.; Wachter, J.; O'Keeffe, M.; Yaghi, O. M., *Science* **2002,** *295*, 469-472.

[57] Chae, H. K.; Siberio-Perez, D. Y.; Kim, J.; Go, Y.; Eddaoudi, M.; Matzger, A. J.; O'Keeffe, M.; Yaghi, O. M., *Nature* **2004,** *427*, 523-527.

[58] Furukawa, H.; Ko, N.; Go, Y. B.; Aratani, N.; Choi, S. B.; Choi, E.; Yazaydin, A. O.; Snurr, R. Q.; O'Keeffe, M.; Kim, J.; Yaghi, O. M., *Science* **2010,** *329*, 424-428.

[59] Chui, S. S. Y.; Lo, S. M. F.; Charmant, J. P. H.; Orpen, A. G.; Williams, I. D., *Science* **1999,** *283*, 1148-1150.

[60] Sun, D. F.; Ma, S. Q.; Ke, Y. X.; Collins, D. J.; Zhou, H. C., *J. Am. Chem. Soc.* **2006,** *128*, 3896-3897.

[61] Ferey, G.; Mellot-Draznieks, C.; Serre, C.; Millange, F.; Dutour, J.; Surble, S.; Margiolaki, I., *Science* **2005,** *309*, 2040-2042.

[62] Park, K. S.; Ni, Z.; Cote, A. P.; Choi, J. Y.; Huang, R. D.; Uribe-Romo, F. J.; Chae, H. K.; O'Keeffe, M.; Yaghi, O. M., *Proc. Natl. Acad. Sci. USA* **2006,** *103*, 10186-10191.

[63] Sing, K. S. W.; Everett, D. H.; Haul, R. A. W.; Moscou, L.; Pierotti, R. A.; Rouquerol, J.; Siemieniewska, T., *Pure Appl. Chem.* **1985,** *57*, 603-619.

[64] Li, D.; Kaneko, K., *Chem. Phys. Lett.* **2001,** *335*, 50-56.

[65] Kondo, A.; Noguchi, H.; Ohnishi, S.; Kajiro, H.; Tohdoh, A.; Hattori, Y.; Xu, W. C.; Tanaka, H.; Kanoh, H.; Kaneko, K., *Nano Lett.* **2006,** *6*, 2581-2584.

[66] Kitaura, R.; Seki, K.; Akiyama, G.; Kitagawa, S., *Angew. Chem. Int. Ed.* **2003,** *42*, 428-431.

[67] Horike, S.; Tanaka, D.; Nakagawa, K.; Kitagawa, S., *Chem. Commun.* **2007**, 3395-3397.

[68] Kitaura, R.; Fujimoto, K.; Noro, S.; Kondo, M.; Kitagawa, S., *Angew. Chem. Int. Ed.* **2002,** *41*, 133-135.

[69] Choi, H. J.; Dinca, M.; Long, J. R., *J. Am. Chem. Soc.* **2008,** *130*, 7848-7850.

[70] Kepert, C. J.; Rosseinsky, M. J., *Chem. Commun.* **1999**, 375-376.

[71] Barthelet, K.; Marrot, J.; Riou, D.; Ferey, G., *Angew. Chem. Int. Ed.* **2002,** *41*, 281-284.

[72] Alaerts, L.; Kirschhock, C. E. A.; Maes, M.; van der Veen, M. A.; Finsy, V.; Depla, A.; Martens, J. A.; Baron, G. V.; Jacobs, P. A.; Denayer, J. E. M.; De Vos, D. E., *Angew. Chem. Int. Ed.* **2007,** *46*, 4293-4297.

[73] Dybtsev, D. N.; Chun, H.; Kim, K., *Angew. Chem. Int. Ed.* **2004,** *43*, 5033-5036.

[74] Chun, H.; Dybtsev, D. N.; Kim, H.; Kim, K., *Chem. Eur. J.* **2005,** *11*, 3521-3529.

[75] Ma, B. Q.; Mulfort, K. L.; Hupp, J. T., *Inorg. Chem.* **2005,** *44*, 4912-4914.

[76] Farha, O. K.; Hupp, J. T., *Acc. Chem. Res.* **2010,** *43*, 1166-1175.

[77] Chen, B. L.; Liang, C. D.; Yang, J.; Contreras, D. S.; Clancy, Y. L.; Lobkovsky, E. B.; Yaghi, O. M.; Dai, S., *Angew. Chem. Int. Ed.* **2006,** *45*, 1390-1393.

[78] Zhang, J. P.; Chen, X. M., *J. Am. Chem. Soc.* **2008,** *130*, 6010-6017.

[79] Galli, S.; Masciocchi, N.; Colombo, V.; Maspero, A.; Palmisano, G.; Lopez-Garzon, F. J.; Domingo-Garcia, M.; Fernandez-Morales, I.; Barea, E.; Navarro, J. A. R., *Chem. Mater.* **2010,** *22*, 1664-1672.

[80] Schlichte, K.; Kratzke, T.; Kaskel, S., *Microporous Mesoporous Mater.* **2004,** *73*, 81-88.

[81] Chen, B. L.; Ockwig, N. W.; Millward, A. R.; Contreras, D. S.; Yaghi, O. M., *Angew. Chem. Int. Ed.* **2005,** *44*, 4745-4749.

[82] Lin, X.; Jia, J. H.; Zhao, X. B.; Thomas, K. M.; Blake, A. J.; Walker, G. S.; Champness, N. R.; Hubberstey, P.; Schroder, M., *Angew. Chem. Int. Ed.* **2006,** *45*, 7358-7364.

[83] Dietzel, P. D. C.; Panella, B.; Hirscher, M.; Blom, R.; Fjellvag, H., *Chem. Commun.* **2006**, 959-961.

[84] Dietzel, P. D. C.; Johnsen, R. E.; Fjellvag, H.; Bordiga, S.; Groppo, E.; Chavan, S.; Blom, R., *Chem. Commun.* **2008**, 5125-5127.

[85] Kitagawa, S.; Noro, S.; Nakamura, T., *Chem. Commun.* **2006**, 701-707.

[86] Abrahams, B. F.; Hoskins, B. F.; Michail, D. M.; Robson, R., *Nature* **1994,** *369*, 727-729.

[87] Kosal, M. E.; Chou, J. H.; Wilson, S. R.; Suslick, K. S., *Nat. Mater.* **2002,** *1*, 118-121.

[88] Cho, S. H.; Ma, B. Q.; Nguyen, S. T.; Hupp, J. T.; Albrecht-Schmitt, T. E., *Chem. Commun.* **2006**, 2563-2565.

[89] Zou, R. Q.; Sakurai, H.; Han, S.; Zhong, R. Q.; Xu, Q., *J. Am. Chem. Soc.* **2007,** *129*, 8402-8403.

[90] Tonigold, M.; Lu, Y.; Bredenkotter, B.; Rieger, B.; Bahnmuller, S.; Hitzbleck, J.; Langstein, G.; Volkmer, D., *Angew. Chem. Int. Ed.* **2009,** *48*, 7546-7550.

[91] Murray, L. J.; Dinca, M.; Yano, J.; Chavan, S.; Bordiga, S.; Brown, C. M.; Long, J. R., *J. Am. Chem. Soc.* **2010,** *132*, 7856-7857.

[92] Mulfort, K. L.; Hupp, J. T., *J. Am. Chem. Soc.* **2007,** *129*, 9604-9605.

[93] Himsl, D.; Wallacher, D.; Hartmann, M., *Angew. Chem. Int. Ed.* **2009,** *48*, 4639-4642.

[94] Wu, C. D.; Lin, W. B., *Angew. Chem. Int. Ed.* **2007,** *46*, 1075-1078.

[95] Couck, S.; Denayer, J. F. M.; Baron, G. V.; Remy, T.; Gascon, J.; Kapteijn, F., *J. Am. Chem. Soc.* **2009,** *131*, 6326-6327.

[96] Volkringer, C.; Cohen, S. M., *Angew. Chem. Int. Ed.* **2010,** *49*, 4644-4648.

[97] Sato, H.; Matsuda, R.; Sugimoto, K.; Takata, M.; Kitagawa, S., *Nat. Mater.* **2010,** *9*, 661-666.

[98] Ohmori, O.; Kawano, M.; Fujita, M., *J. Am. Chem. Soc.* **2004,** *126*, 16292-16293.

[99] Cheon, Y. E.; Suh, M. P., *Angew. Chem. Int. Ed.* **2009,** *48*, 2899-2903.

[100] Yao, Q. X.; Pan, L.; Jin, X. H.; Li, J.; Ju, Z. F.; Zhang, J., *Chem. Eur. J.* **2009,** *15*, 11890-11897.

Chapter 1

TCNQ Dianion-Based Coordination Polymer Whose Open Framework Shows Charge-Transfer Type Guest Inclusion

Abstract

A three-dimensional coordination framework constructed with 7,7,8,8-tetracyano-*p*-quinodimethane (TCNQ) diainon have been synthesized and structurally characterized. This open framework possessing highly electron rich surface has optical sensing cavity for several aromatics with crystal to crystal transformation and strong accommodation, which are based on charge transfer interaction with them.

Introduction

Porous coordination polymers have attracted the attention of chemists who have scientific interest in developing nanometer-sized pores providing novel guest assemblies, and in guest-stressed and guest-activated phenomena.[1] For these purposes, functionalization of the pore surfaces is very attractive idea for applications in storage,[2] separation[3] and catalysis.[3a,4] Porous frameworks in this category can be designed and synthesized by using appropriate ligands with interaction sites, such as hydrogen bonding sites,[3d,5] and open metal sites.[2d,4a,6]

On the other hand, charge transfer (CT) interactions play a significant role in various functional materials, although only a few examples of this type of interaction in porous compounds have been seen to date.[7] With this background, we have designed electrically flexible pore surfaces to achieve CT between a host framework and a guest molecule by incorporating a redox active module into the framework to act as an interaction site, which can provide selective accommodation or sensing properties based on the combination of CT and van der Waals interactions. 7,7,8,8-tetracyano-*p*-quinodimethane (TCNQ) is a well-known multi-redox active ligand that can act as a good acceptor and a weak or a strong donor when its valence is 0, –1, or –2, respectively. We predicted that a CT interaction between a host framework and a guest molecule would occur if TCNQ were directly incorporated into the pore walls of a polymer. Here, we show a new redox active three-dimensional (3D) coordination framework containing TCNQ with Zn ions and 4,4′-bipyridine (bpy), and demonstrate unusual guest accommodations accompanying the CT interaction.

Results and discussion

Yellow crystals of {[Zn(TCNQ)bpy]·6MeOH}$_n$ (**1**⊃MeOH) were synthesized by reacting $Zn(NO_3)_2 \cdot 6H_2O$ with LiTCNQ and bpy in MeOH. Figure 1 shows the crystal structure of **1**⊃MeOH. The Zn ions are octahedrally coordinated to the four cyanide nitrogen atoms of TCNQ in the equatorial plane and the two nitrogen atoms of the bpy at the axial sites. The Zn ions are linked by TCNQ molecules to give a two-dimensional (2D) corrugated layer in the *ab* plane. The bpy ligands act as pillars, with the Zn ions in the adjacent layers linked to form a 3D pillared layer structure. This crystal possesses 2D channels with cross-sections of approximately 3.4 × 5.9 Å^2 and a void space of about 50.7%, if the van der Waals radii of the constituting atoms are considered.[8]

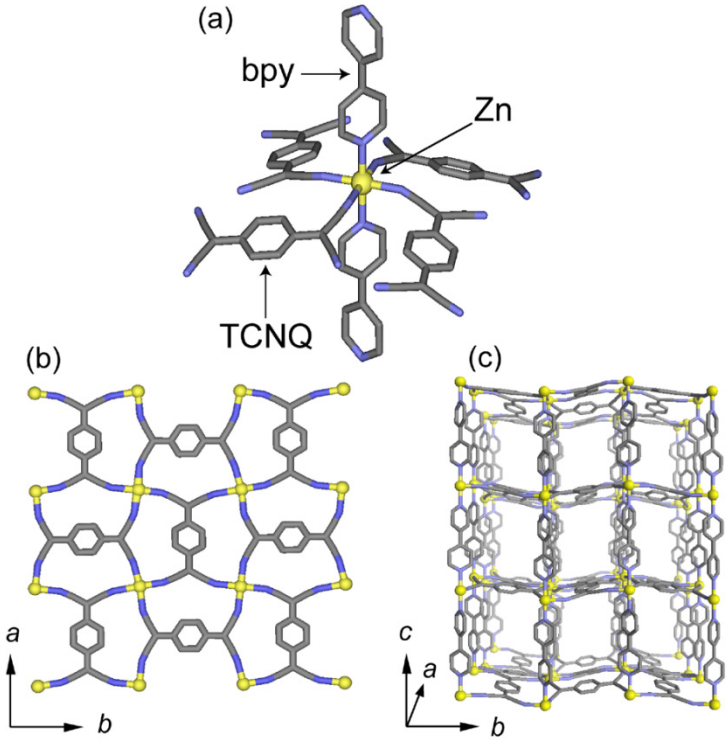

Figure 1. (a) Coordination environment of Zn^{II} ion and (b) top view and (c) side view of **1**⊃MeOH. One of the doubly disordered bpy, the hydrogen atoms and guest molecules are omitted for clarity.

Considering the charge balance of the framework, charge number of the TCNQ is estimated to be –2 (Zn: +2, TCNQ: –2, bpy: 0), because no counter anion is observed in the cavity by both X-ray structure and IR spectrum. In addition, the molecular bond length, which reflects charge number, indicates almost –2 form, especially bond **a** and **c** (Table 1).[9-11] There have been many reports on the relationship between the bond distances and the charged state of TCNQ[9]. As the negative charges on the TCNQ molecules increases, the **a** and **c** bond distances increase, while the **b** and **d** bond

distances decrease. The bond distances of TCNQ in 1 clearly indicate the $TCNQ^{2-}$ anion, and are different from the bond distances of $TCNQ^{-}$, especially in bond distance **c**. Moreover, the Infrared ν_{CN} stretching frequencies of TCNQ molecules also indicate the oxidation states. In general, the ν_{CN} bands shift to the lower frequency region as the negative charge on TCNQ molecules increases. A $TCNQ^{-}$ molecule shows ν_{CN} bands at 2220−2175 cm^{-1} (s) and 2170−2150cm^{-1} (s), [10−12] while a $TCNQ^{2-}$ in Na_2TCNQ affords at 2164 cm^{-1} (s) and 2096 cm^{-1} (vs). [13] The bands at 2194 cm^{-1} (s) and 2121 cm^{-1} (vs) in **1** also support the form of $TCNQ^{2-}$ (Figure 2). The ν_{CN} stretching frequencies of **1** higher than the typical $TCNQ^{2-}$ is attributable to a σ-donation of the TCNQ molecules to the Zn^{II} ions.[14] In addition, the absence of the band of NO_3^{-} around 1390 cm^{-1} indicates the oxidation states of TCNQ molecules in **1** are $TCNQ^{2-}$. The production process of resulting $TCNQ^{2-}$ is not clear, but that may be a disproportionation reaction of $TCNQ^{-}$.[15]

Table 1. Bond lengths (Å) of TCNQ molecules in **1** and related compounds.

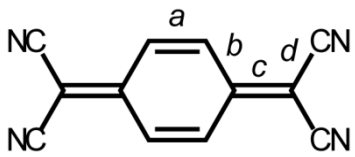

	a	**b**	**c**	**d**
$TCNQ^{-}$ [a]	1.358−1.378	1.385−1.435	1.402−1.431	1.407−1.440
$TCNQ^{2-}$ [b]	1.371−1.380	1.380−1.395	1.481−1.491	1.370−1.392
1⊃CH_3OH	1.380(6)	1.402(6)	1.472(5)	1.405(5)

[a] reference 10. [b] reference 11.

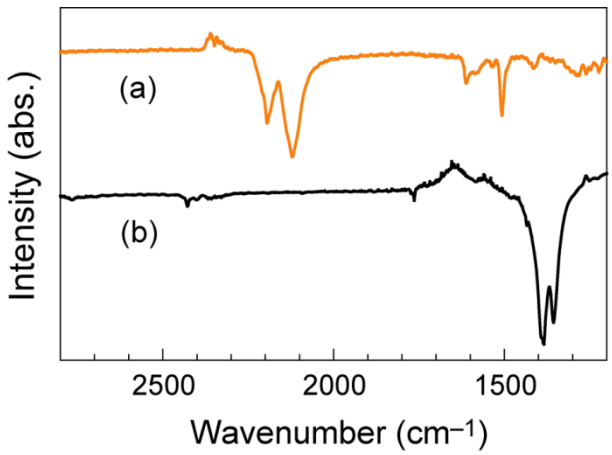

Figure 2. IR spectra of (a) {[Zn(TCNQ)bpy]$_n$·6MeOH} (**1**⊃MeOH) and (b) $Zn(NO_3)\cdot 6H_2O$.

As a result, a dense array of strong donor sites ($TCNQ^{2-}$) is formed on the pore surface of the open framework of **1**, providing a highly electron rich surface for the guest molecules. Only one coordination polymer composed of $TCNQ^{2-}$ has been reported to date,[11] and **1** is the first example of a regular array of $TCNQ^{2-}$ embedded in the pore wall of a 3D open framework.

Given the exceptional highly electron-rich surface of **1**, we sought to test its ability to accommodate various aromatic guest molecules. When the crystal of **1**⊃MeOH was immersed into benzene, the guest MeOH can be exchanged with benzene to form **1**⊃benzene within ten seconds, which is red rather than the yellow of the parent compound. (Figure 3) This is a guest-induced crystal-to-crystal transformation. Marked changes were observed in the crystal structure of **1**⊃benzene, while the coordination environment around the Zn ion was similar to the MeOH analogue. The layer based on TCNQ and Zn ion in **1**⊃benzene was planar, although that in **1**⊃MeOH was considerably corrugated. Furthermore, the cell volume increased slightly by 2%, and the pore size expanded to approximately 3.5 × 7.9 $Å^2$.[8]

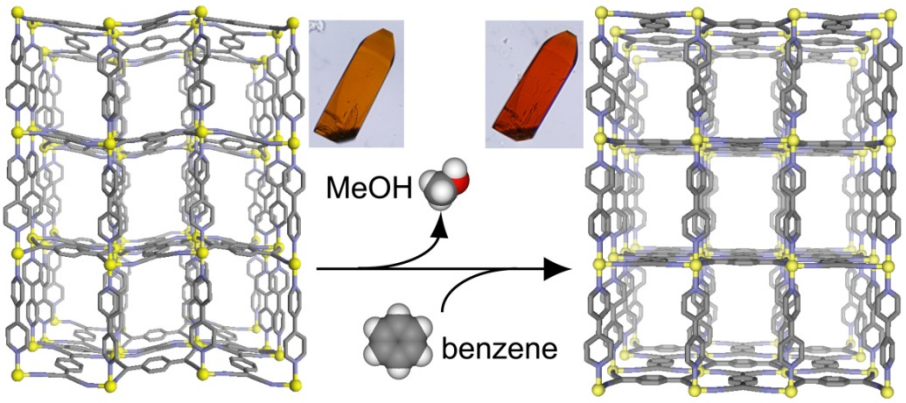

Figure 3. Structural transformation and color change from **1**⊃MeOH to **1**⊃benzene by guest exchange.

The two benzene molecules per Zn ion filled the channel, and were located between the pillar ligands at right angles to the layer, with a unique interaction between the host and the guest molecule. The C(12) carbon atoms of the benzene molecule were located only 3.63(2) Å away from the most negative charged carbon atom, the C(5) atom of TCNQ (Figure 4).[16] This exceptionally short C(5)···H(8)−C(12) bond distance is shorter than the sum of the van der Waals radii between the C(5) and C(12), which results from a C−H···C-type hydrogen bonding, representing the existence of an electrostatic and/or CT interaction between the TCNQ and the benzene. This crystal transformation is attributed to an accommodation of the benzene molecules into **1** with a dilatation of the channels, and this maintains the pore size by pillaring the layer on host-guest interaction.

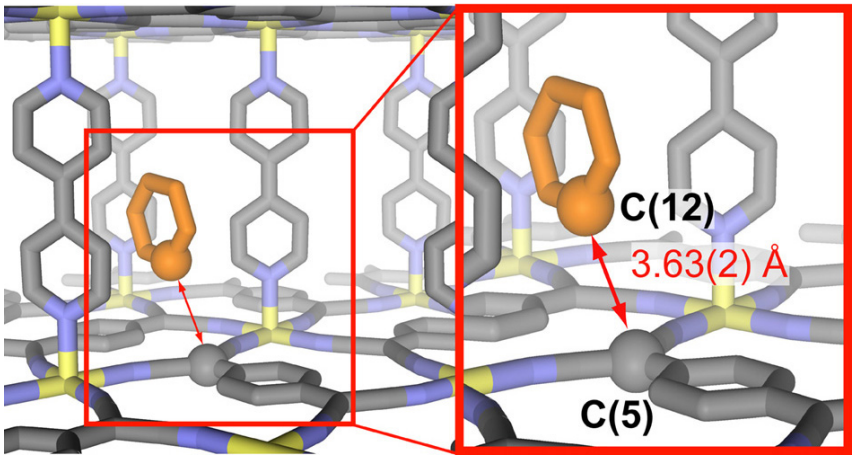

Figure 4. View of the nearest C−C distance between benzene molecule and TCNQ moiety. The occupancy of benzene molecule is 0.5.

For other guests (toluene, ethylbenzene, anisole, benzonitrile, and nitrobenzene), changes in color different to **1**⊃MeOH, similar to that for benzene were seen, except for anisole and nitrobenzene, where the occlusion of anisole and nitrobenzene formed light yellow and dark brown crystals, respectively. The color of the crystals is specific to the guest, and the guest exchange is reversible upon removal/accommodation of the guests. **1** is unstable to guest removal: the framework irreversibly collapses and changes to the other crystal phase. This compound is not suitable to sorption measurement and doesn't possess the permanent porosity. However, the guests in **1** can be reversibly exchanged each other by immersion. This possesses the accessible channel to exchange the guests.

Figure 5 shows the UV-vis spectra of **1** with anisole (1⊃anisole), benzene (1⊃benzene), and nitrobenzene (1⊃nitrobenzene). The visible spectra showed absorption bands in the 400–700 nm region in the following order: 1⊃anisole (418 nm), 1⊃benzene (445 nm), and 1⊃nitrobenzene (480 nm), which were associated with the electron-accepting characteristics of the guest molecule. In particular, the band associated with 1⊃nitrobenzene was quite broad, extending out to 800 nm. This is ascribed to the CT interaction between TCNQ and the aromatic molecule.[17]

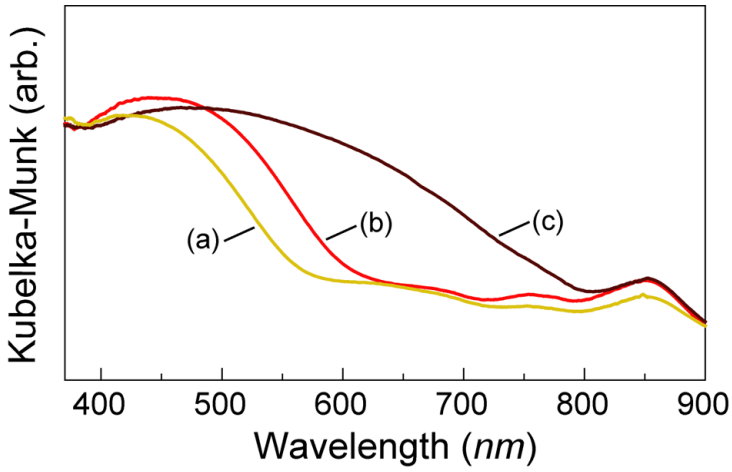

Figure 5. Diffuse reflectance UV-vis spectra of (a) **1**⊃anisole, (b) **1**⊃benzene and (c) **1**⊃nitrobenzene.

Conclusion

In summary, we have synthesized a new coordination polymer with a redox active module, due to the CT interaction between the host framework and guest molecule. The CT interaction sites incorporated into framework will be useful to design and synthesis of new framework-guest hybrid compounds with unique physical properties and/or chemical reactions.

Experimental Section

Materials. 7,7,8,8-tetracyano-p-quinodimethane and 4,4'-Bipyrizine were obtained from Tokyo Kasei Industrial and $Zn(NO_3)_2 \cdot 6H_2O$ were obtained from Wako and used without further purification. LiTCNQ was prepared by the literature method.[17]

Synthesis of Coordination Polymer {[Zn(TCNQ)bpy]·6MeOH}$_n$ (1⊃MeOH). Single crystal of **1** was prepared by the following procedure. This procedure was carried out under N_2 atmosphere using Schlenk technique. A solution of LiTCNQ (0.2 mmol, 42 mg) and bpy (0.2 mmol, 31 mg) in MeOH (50 ml) was carefully layered on the top of a solution of $Zn(NO_3)_2 \cdot 6H_2O$ (0.2 mmol, 59.5 mg) in MeOH (50 ml). Yellow crystals began to form in a few weeks. One of these crystals was used for X-ray crystallography. The bulk product was obtained by the following procedure. Slow addition of a solution of LiTCNQ (0.3 mmol, 69.6 mg) and bpy (0.3 mmol, 51.5 mg) in MeOH (100 ml) and a solution of $Zn(NO_3)_2 \cdot 6H_2O$ (0.3 mmol, 98.3 mg) in MeOH (100 ml) to MeOH (100 ml) at 293 K under N_2 atmosphere. The yellow powder obtained was collected by filtration, washed with flesh MeOH soon. (yield ca. 10 %)

Guest Exchange of 1⊃MeOH with Aromatic Guests. The single crystal of **1**⊃MeOH with dimensions of 0.15 × 0.04 × 0.03 mm^3 was immersed into about 2 ml of benzene in ten seconds. Herein the color of the crystal abruptly changed to red from yellow, and the resultant crystals were examined by XRPD, which clearly indicates **1**⊃MeOH dissimilar to that of **1**⊃MeOH. This crystals encounters a swift guest exchange without any destruction of the framework. The other aromatic guests (toluene, ethylbenzene, anisole, benzonitrile, and nitrobenzene) were exchanged in a manner similar to benzene.

X-ray Crystal Analysis. Single crystal X-ray diffraction data collection was carried out on a Rigaku mercury diffractometer with a graphite monochromated MoKα radiation (γ = 0.71069 Å) and a CCD detector. The crystal structure was solved by a direct method (SHELX97) and Patterson Methods (DIRDIF99 PATTY) and refined by full-matrix least-squares refinement using the CRYSTALS computer program. The positions of non-hydrogen atoms were refined with anisotropic displacement factors, except for the guest molecules. The hydrogen atoms were positioned geometrically and refined using a riding model.

Physical Measurements. Thermal gravimetry analysis (TGA) was carried out with a Rigaku Instrument TG8120 in a nitrogen atmosphere. IR spectra were recoded on a Perkin-Elmer 2000 FTIR spectrophotometer with samples prepared in KBr pellets. Xray powder diffraction (XRPD)

data were collected on a Rigaku RINT-2200HF (Ultima) diffractometer with Cu-Kα radiation. UV-vis spectra were recorded on a HITACHI U-3500/U-4000 spectrometer.

Table 2. Crystal data and Structure Solution and Refinement of **1**⊃MeOH.

Empirical Formula	$C_{28}H_{30}N_6O_6Zn$
Formula Weight	611.96
Crystal System	tetragonal
Lattice Parameters	a = 17.355(1) Å
	c = 22.740(2) Å
	V = 6848.7(10) Å^3
Space Group	P4/ncc (#130)
Z value	8
D_{calc}	1.187 g/cm^3
F_{000}	2544.00
μ (MoKα)	7.61 cm^{-1}
Radiation	MoKα (λ = 0.71070 Å)
	graphite monochromated
$2\theta_{max}$	55.0^o
No. of Reflections Measured	Total: 68046
	Unique: 3919 (R_{int} = 0.069)
Completeness	99.1%
Refinement	Full-matrix least-squares on F^2
$2\theta_{max}$ cutoff	0.0^o
Anomalous Dispersion	All non-hydrogen atoms
No. Observations (I>2.50σ(I))	2210
No. Variables	206
Reflection/Parameter Ratio	10.73
Residuals: R1 (I>2.50σ(I))	0.074
Residuals: wR2 (I>2.50σ(I))	0.081
Goodness of Fit Indicator	1.087
Max Shift/Error in Final Cycle	0.000
Maximum peak in Final Diff. Map	1.29 e$^-$/Å^3
Minimum peak in Final Diff. Map	-0.56 e$^-$/Å^3

R1 = $\Sigma||Fo| - |Fc||/\Sigma|Fo|$. wR2 = $[\Sigma w(Fo^2 - Fc^2) /\Sigma w(Fo^2)^2]^{1/2}$.

Table 3. Crystal data and Structure Solution and Refinement of **1**⊃benzene.

Empirical Formula	$C_{34}H_{24}N_6Zn$
Formula Weight	581.98
Crystal System	tetragonal
Lattice Parameters	a = 12.384(2) Å
	c = 22.765(3) Å
	V = 3491.2(8) Å^3
Space Group	I4/mcm (#140)
Z value	4
D_{calc}	1.107 g/cm^3
F_{000}	1200.00
μ (MoKα)	7.32 cm^{-1}
Radiation	MoKα (λ = 0.71070 Å)
	graphite monochromated
$2\theta_{max}$	55.0^o
No. of Reflections Measured	Total: 14384
	Unique: 1100 (R_{int} = 0.071)
Completeness	100.0%
Refinement	Full-matrix least-squares on F
$2\theta_{max}$ cutoff	0.0^o
Anomalous Dispersion	All non-hydrogen atoms
No. Observations (I>1.30σ(I))	937
No. Variables	87
Reflection/Parameter Ratio	10.77
Residuals: R (I>1.30σ(I))	0.066
Residuals: R (I>2.00σ(I))	0.054
Residuals: Rw (I>1.30σ(I))	0.070
Goodness of Fit Indicator	1.027
Max Shift/Error in Final Cycle	0.000
Maximum peak in Final Diff. Map	0.45 e$^-$/Å^3
Minimum peak in Final Diff. Map	-0.42 e$^-$/Å^3

$R = \Sigma||Fo| - |Fc||/\Sigma|Fo|$. $Rw = [\Sigma w(Fo^2 - Fc^2) / \Sigma w(Fo^2)^2]^{1/2}$.

References

[1] (a) Kitagawa, S.; Kitaura, R.; Noro, S.-i. *Angew. Chem. Int. Ed. Engl.* **2004**, *43*, 2334-2375.(b) Yaghi, O. M.; O'Keeffe, M.; Ockwig, N. W.; Chae, H. K.; Eddaoudi, M,; Kim, J. *Nature* **2001**, *423*, 705-724. (c) Ferey, G.; Mellot-Draznieks, C.; Serre, C.; Millange, F. *Acc. Chem. Res.* **2005**, *38*, 217-225. (d) Bradshaw, D.; Claridge, J. B.; Cussen, E. J.; Prior, T. J.; Rosseinsky, M. J. *Acc. Chem. Res.* **2005**, *38*, 273-283. (e) Moulton, B.; Zaworotko, M. J. *Chem. Rev.* **2001**, *101*, 1629-1658.

[2] (a) Ferey, G. ; Mellot-Draznieks, C.; Serre, C.; Millange, F.; Dutour, J.; Surble, S.; Margiolaki, I. *Science* **2005**, 309, 2040-2042. (b) Chae, H. K.; Siberio-Perez, D. Y.; Kim, J.; Go, Y.; Eddaoudi, M,; Matzger, A. J.; O'Keeffe,M.; Yaghi, O. M. *Nature* **2004**, *427*, 523-527.(c) Zhao, X.; Xiao, B.; Fletcher, A. J.; Thomas, K. M.; Bradshaw, D.; Rosseinsky, M. J. *Science* **2004**, *306*, 1012-1015. (d) Kaye, S. S.; Long, J. R. *J. Am. Chem. Soc.* **2005**, *127*, 6506-6507. (e) Seki, K.; Mori, W. *J. Phys. Chem. B* **2002**, *106*, 1380-1385. (f) Chandler, B. D.; Cramb, D. T.; Shimizu, G. K. H. *J. Am. Chem. Soc.* **2006**, *128*, 10403-10412. (g) Halder, G. J.; Kepert, C. J. *J. Am. Chem. Soc.* **2005**, *127*, 7891-7900.

[3] (a) Seo, J. S.; Whang, D.; Lee, H.; Jun, S. I.; Oh, J.; Jeon, Y. J.; Kim, K. *Nature* **2000**, *404*, 982-986. (b) Evans, O. R.; Ngo, H. L.; Lin, W. *J. Am. Chem. Soc*. **2001**, *123*, 10395-10396. (c) Pan, L.; Olson, D. H.; Ciemnolonski, L. R.; Heddy, R.; Li, J. *Angew. Chem. Int. Ed.* **2006**, *45*, 616-619. (d) Matsuda, R.; Kitaura, R.; Kitagawa, S.; Kubota, Y.; Belosludov, R. V.; Kobayashi, T. C.; Sakamoto, H.; Chiba, T.; Takata, M.; Kawazoe, Y.; Mita, Y. *Nature* **2005**, *436*, 238-241.

[4] (a) Wu, C.-D.; Hu, A.; Zhang, L.; Lin, W. *J. Am. Chem. Soc.* **2005**, *127*, 8940-8941. (b) Ohmori, O.; Fujita, M. *Chem. Commun.* **2004**, 1586-1587.

[5] Custelcean, R.; Gorbunova, M. G. *J. Am. Chem. Soc.* **2005**, *127*, 16362-16363

[6] (a) Rowsell, J. L.C.; Yaghi, O. M. *Angew. Chem. Int. Ed.* **2005**, *44*, 4670-4679. (b) Chen, B.; Fronczek, F. R.; Maverick, A. W. *Inorg. Chem.* **2004**, *43*, 8209-8211.

[7] (a) Suh, M. P.; Moon, H. R.; Lee, E. Y.; Jang, S. Y. *J. Am. Chem. Soc.* **2006**, *128*, 4170-4718. (b) Moon, H. R.; Kim, J. H.; Suh, M. P. *Angew. Chem. Int. Ed.* **2005**, *44*, 1261-1265. (c) Ohmori, O.; Kawano, M.; Fujita, M. *J. Am. Chem. Soc.* **2004**, *126*, 16292-16293. (d) Choi, H. J.; Suh, M. P. *J. Am. Chem. Soc.* **2004**, *126*, 15844-15851.

[8] Kistenmacher, T. J.; Emge, T. J.; Bloch, A. N.; Cowan, D. O. *Acta Cryst.* **1982**, *B38*, 1193-1199.

[9] (a) Ballester, L.; Gutiérrez, A.; Perpiñán, F. M.; Azcondo, M. T. *Coord. Chem. Rev.* **1999**, *190-192*, 447-470. (b) Miyasaka, H.; Campos-Fernández, C. S.; Clérac, R.; Dunbar, K.R. *Angew. Chem. Int. Ed.* **2000**, *39*, 3831-3835. (c) Shields, L. *J. Chem. Soc., Faraday trans. 2*

1985, *81*, 1-9. (d) Zhao, H.; Heintz, R A.; Ouyang, X.; Dunbar, K. R.; Campana, C. F.; Rogers, R. D. *Chem. Mater.* **1999**, *11*, 736-746.

[10] Oshio, H.; Ino, E.; Ito, T.; Maeda, Y. *Bull. Chem. Soc. Jpn.* **1995**, *68*, 889-897.

[11] Kaim, W.; Moscherosch, M. *Coord. Chem. Rev.* **1994**, *129*, 157-193.

[12] Khatkale, M. S.; Devlin, J. P. *J. Chem. Phys.* **1979**, *70*, 1851-1859.

[13] Hartmann, H.; Kaim, W.; Wanner, M.; Klein, A.; Frantz, S.; Duboc-Toia, C.; Fiedler, J.; Zalis, S. *Inorg. Chem.* **2003**, *42*, 7018-7025.

[14] Grossel, M. C.; Duke, A. J.; Hibbert, D. B.; Lewis, I. K.; Seddon, E. A.; Horton, P. H.; Weston, S. W. *Chem. Mater.* **2000**, *12*, 2319-2323.

[15] Miller, J. S.; Zhang, J. H.; Reiff, W. M.; Dixon, D. A.; Preston, L. D.; Reis, A. H., Jr.; Gebert, E.; Extine, M.; Troup, J.; Epstein, A. J.; Ward, M. D. *J. Phys. Chem.* **1987**, *91*, 4344-4360.

[16] (a) Chen, C.; Iion, M. *Energy & Fuels* **1999**, *13*, 1105-1106. (b)Acker, D. S.; Hertler, W. R. *J. Am. Chem. Soc.* **1962**, *84*, 3370-3374.

Chapter 2

Impact of Metal-ion Dependence on the Porous and Electronic Properties of TCNQ-dianion-based Porous Coordination Polymers

Abstract

A series of TCNQ-dianion-based porous coordination polymers [M(TCNQ)bpy] (M = Fe, Zn, Mn, Co, Cd) have been synthesized and characterized. The synthesis reactions of these compounds are promoted by the addition of ascorbic acid, which is the key to obtaining a high yield. They form almost identical three-dimensional pillared layer structures with the M–TCNQ two-dimensional layers linked by bpy pillar ligands. The electronic properties of these compounds vary depending on the constitutional metal ions and guest molecules. We found that the electronic interaction between metal ions and TCNQ moieties in the frameworks strongly impacted the electronic properties of the compounds.

Introduction

Soft porous crystals (SPCs) with the cooperative integration of "softness" and "regularity" are attractive materials showing unconventional porous properties and unique host–guest interactions.[1] Within the field of SPCs, porous coordination polymers (PCPs) have attracted much attention from scientists because of the remarkably rich diversity of structures and properties.[2-11] In addition, there have been many studies on PCPs having switchable properties that depend on guest molecules and they have had important ramifications in materials science.[12-28]

PCPs possess an enormous diversity of structures and properties. In many cases, the diversity derives from the infinite variation of organic ligands. The molecular shapes of the organic ligands, which form the pore walls, directly affect the size, shape, and dimensionality of the pore. In addition, their electronic natures and physical properties critically influence the pore surface properties. In contrast, metal ions contribute to the diversity of PCPs in a different way. However, there is only a finite variation of metal ions, which is much less than that of organic ligands, providing the structural multiplicity of the coordination geometry, including coordination number and distortion of bond angles. Moreover, they provide high diversity, such as flexibility based on the dynamics of coordination bonds and electronic/magnetic properties based on their charge states. Usually, metal ions act as the nodes of the framework and have less opportunity to interact directly with guest molecules. However, it is conceivable that metal ions could strongly impact the host–guest interaction if they interact electronically with the organic ligands.

We have previously reported several PCPs with 7,7,8,8-tetracyano-*p*-quinodimethane (TCNQ) as an organic ligand,[29, 30] focusing on the electrical and structural properties of this organic molecule. TCNQ is a well-known multiredox active organic molecule that can act as a good acceptor and a weak or a strong donor when its valence is 0, –1, or –2, respectively.[31-34] In addition, TCNQ is suitable for forming high-dimensional coordination networks because of the coordination and structural diversities based on its multidentate nature and dimerization reaction.[35-42] The TCNQ in the frameworks acts as a good interaction site for guest adsorption and recognition, resulting in it showing unique sorption properties such as selective organic and gas sorption,[30] as well as guest-responsive color changes based on the charge-transfer (CT) interaction.[29] In contrast to the organic ligands, the metal ions are not considered to be the important component for the unique porous properties in these PCP systems. However, an exploration of the metal-dependent porous properties of PCPs is also an intriguing topic and has great potential for exploiting a new field of PCPs. In this paper, five PCPs [M(TCNQ)bpy] (M = Fe(II), Zn(II), Mn(II), Co(II), Cd(II), bpy = 4,4′-bipyridyl) consisting of the same components except for the metal cations and forming identical structures were prepared to compare the metal-dependent porous and electronic properties.

Results and discussion

The crystals of [M(TCNQ)bpy] were obtained by the complexation reaction of the divalent metal cations, TCNQ dianion, and bpy in solution at room temperature. Two synthesis methods have been previously reported: a disproportionation reaction of TCNQ radical anions[29, 43] and a deprotonation reaction of TCNQH2 to generate TCNQ dianion.[44] We optimized the reaction conditions of the former method and found that the disproportionation reaction of TCNQ radical anions to produce TCNQ dianion was facilitated by the presence of ascorbic acid in the solution. Ascorbic acid, which is a good reducing agent, promotes the reduction reaction even on radical anionic molecules, forming dianion species. In the absence of ascorbic acid, some side reactions easily occurred and it was very difficult to obtain the pure [M(TCNQ)bpy] compounds by this method. The latter method was recently reported and adopted by Robson and co-workers.[44] The as-synthesized compounds immediately show an irreversible transformation on exposure to air because of the immediate removal of guest molecules of methanol, resulting in a nonporous compound. However, these compounds undergo guest exchange from the methanol to aromatic molecules, such as nitrobenzene, when they are immersed in the neat solvent. The aromatic guest molecules, which have rather high boiling points, make the compounds air stable because of the strong interaction between the guest molecules and the framework. Single-crystal X-ray analysis of [M(TCNQ)bpy] revealed tetragonal structures in which the metal ions were connected by TCNQ dianions to form two-dimensional sheet motifs parallel to the ab-plane, and they were linked by bpy ligands along the c-axis to give three-dimensional pillared layer-type networks (Figures 1, 2). The structure of the Mn complex is similar to the structure that has already been reported.[44] The as-synthesized two-dimensional motifs of metal ions and TCNQ dianions mainly show corrugated layer structures at the measurement temperature except for the Fe complex. At low temperature (133 K), the Fe complex also shows a similar corrugated layer structure (Figure 2(a)). However, the layer transforms to a flattened structure and the symmetry changes from primitive lattice (P) to body-centered lattice (I) when the compound is heated to 243 K (Figure 2(b)). In this transformation, a slight tetragonal distortion, with expansion in the Fe–N(bpy) axial bonds (from 2.18 Å to 2.21 Å, on average) and almost no change in the Fe–N(TCNQ) equatorial bonds (from 2.15 Å to 2.14 Å), and a reduction in the deviation of the π-surface of TCNQ from the *ab*-plane were observed. In addition, the structure of TCNQ in the framework changes with this transformation. In the context of electronic issues, the most important structural features in TCNQ complexes are the bond lengths within the TCNQ ligand. The C–C distances within the TCNQ ring are a good indicator of the oxidation state.[33, 40, 45] The small decrease in the value of the relationship of bond lengths of TCNQ ($I = c/(b + d)$) implies that the ligand loses a partial negative charge in this transformation (Table 3). This would be strongly involved with the change of the Fe–TCNQ bond.

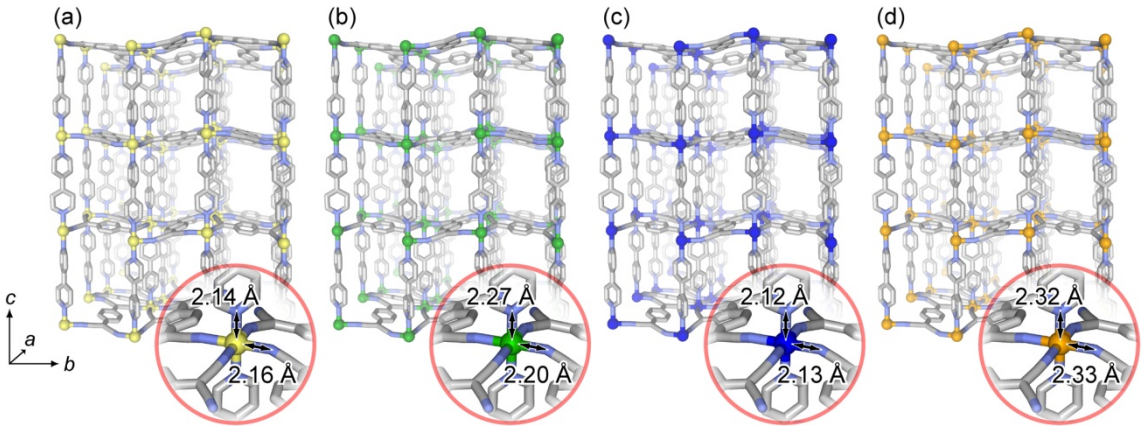

Figure 1. Crystal structures of [M(TCNQ)bpy]·*x*MeOH (M = (a) Zn, (b) Mn, (c) Co, (d) Cd) showing the pillared layer structures and the averaged coordination bond lengths. In the Mn complex, the values of bond lengths extracted from the structure measured at 223 K to remove the temperature effect. One of the doubly disordered bpy, the hydrogen atoms, and guest molecules, Methanol, are omitted for clarity.

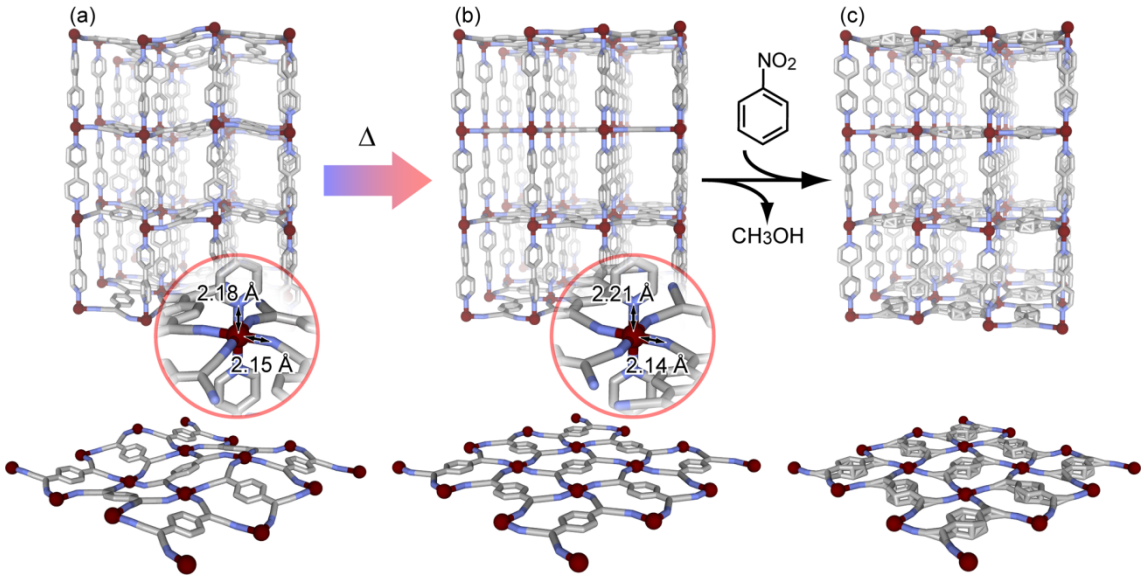

Figure 2. Crystal structures of [Fe(TCNQ)bpy]·*x*MeOH at (a) 133 K and (b) 243 K, and (c) obtained after guest exchange with nitrobenzene. Bottom parts show the forms of the two-dimensional layers [Fe(TCNQ)] in each structure. One of the doubly disordered bpy, the hydrogen atoms, and guest molecules are omitted for clarity.

Table 1. Crystallographic Data for [M(TCNQ)bpy]·*x*MeOH (M =Zn, Mn, Co, Cd)

M	Zn	Mn	Co	Cd
formula	$C_{28}H_{30}N_6O_6Zn$	$C_{57}H_{76}Mn_2N_{12}O_{13}$	C_{30} Co N_6 O_8	$C_{30}H_{10}CdN_6O_8$
fw	611.96	1247.18	631.30	694.85
cryst syst	tetragonal	tetragonal	tetragonal	tetragonal
space group	*P*4/*ncc* (#130)	*P*4/*ncc* (#130)	*P*4/*ncc* (#130)	*P*4/*ncc* (#130)
a, Å	17.355(1)	17.2551(4)	17.302(8)	17.571(14)
c, Å	22.740(2)	23.1856(7)	22.789(11)	23.404(18)
V, Å^3	6848.7(10)	6903.2(3)	6822(6)	7226(10)
Z	8	4	8	8
Temp, K	213	130	223	223
R1 [I > 2σ(I)] [a]	0.074	0.0517	0.0869	0.0504
wR2 [I > 2σ(I)] [a]	0.081	0.1336	0.1209	0.0560
GOF	1.087	0.906	1.059	1.052
reference	ref 29	ref 44	This work	This work

[a] $R1 = \Sigma||Fo| - |Fc||/\Sigma|Fo|$. $wR2 = [\Sigma w(Fo^2 - Fc^2) / \Sigma w(Fo^2)^2]^{1/2}$.

Table 2. Crystallographic data for [Fe(TCNQ)bpy]·guest at 133 K (Fe_133K), 243 K (Fe_243K), and with anisole (Fe⊃ani) and nitrobenzene (Fe⊃nb)

	Fe_133K	Fe_243K	Fe⊃ani	Fe⊃nb
formula	$C_{29}H_{33}FeN_6O_7$	$C_{30}H_{12}FeN_6O_8$	$C_{22}H_{12}FeN_6$	$C_{22}H_{12}FeN_6$
fw	633.46	640.31	416.22	416.22
cryst syst	tetragonal	tetragonal	tetragonal	tetragonal
space group	*P*-42$_1$*c* (#114)	*I*4/*mcm* (#140)	*I*4/*mcm* (#140)	*P*4/*ncc* (#130)
a, Å	17.2926(4)	12.413(20)	12.377(13)	17.4656(7)
c, Å	22.8962(8)	23.03(4)	22.90(2)	23.0745(11)
V, Å^3	6846.7(3)	3549(10)	3508(6)	7038.8(5)
Z	8	4	4	8
Temp, K	133	243	213	293
R1 [I > 2σ(I)] [a]	0.0749	0.0873	0.0853	0.1776
wR2 [I > 2σ(I)] [a]	0.1039	0.1036	0.0806	0.2072
GOF	1.139	1.041	0.841	1.069
reference	This work	This work	This work	This work

[a] $R1 = \Sigma||Fo| - |Fc||/\Sigma|Fo|$. $wR2 = [\Sigma w(Fo^2 - Fc^2) / \Sigma w(Fo^2)^2]^{1/2}$.

Table 3. Bond lengths (Å) of TCNQ moiety in [M(TCNQ)bpy]·*x*MeOH and related compounds.

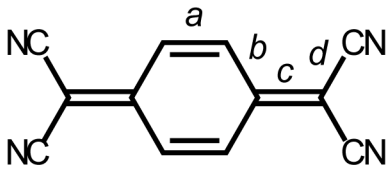

	a	*b*	*c*	*d*	$I = c / (b + d)$
$TCNQ^{-}$ [a]	1.373(4)	1.423(4)	1.420(4)	1.416(4)	0.5
$TCNQ^{2-}$ [b]	1.371(9)	1.39(1)	1.481(9)	1.38(1)	0.535
	1.380(9)	1.397(9)	1.491(9)	1.39(1)	0.535
Fe_133K	1.383(3)	1.397(3)	1.480(3)	1.394(3)	0.530
Fe_243K	1.362(4)	1.380(4)	1.462(4)	1.403(4)	0.525
Zn [c]	1.377(6)	1.398(6)	1.477(5)	1.392(5)	0.529
Mn [d]	1.376(4)	1.407(4)	1.461(4)	1.398(4)	0.521
Co	1.383(9)	1.386(8)	1.475(8)	1.399(8)	0.530
Cd	1.379(6)	1.395(6)	1.469(6)	1.391(6)	0.527

[a] Reference 33, [b] Reference 45, [c] Reference 29, [d] Reference 44.

The three-dimensional structures of [M(TCNQ)bpy] possess two-dimensional grid-like pores filled with the synthetic solvent, methanol molecules, as previously described. The accessible spaces are surrounded by TCNQ dianions, which have a strong electron-donating ability to make CT interactions with electron-accepting molecules. These frameworks show CT-induced color changes depending on the electron-accepting ability of the guest molecules.[29] We used two aromatic molecules, anisole and nitrobenzene, possessing different electron-accepting ability, to evaluate the CT character of these complexes. In the case of the Fe complex, despite a lack of color change with anisole, the red crystal quickly turns dark brown by guest exchange with nitrobenzene. We tried to elucidate the details of the difference by single-crystal X-ray diffraction analysis. The Fe complex with anisole (Fe⊃ani) shows a simple pillared layer structure with a planar two-dimensional layer, which was observed in the as-synthesized form at ambient temperature. TCNQ moieties in the framework do not have a disordered structure and the value of *I*, which is a good indicator of the oxidation state, is almost the same as that of the as-synthesized form. Only low electron density was observed in the pore and the positions of the guest molecules could not be determined, probably because of their disordered distributions. In contrast, in the Fe complex with nitrobenzene (Fe⊃nb), the TCNQ moieties in the framework have a chaotic structure; the TCNQ ring was strongly disordered in the vertical direction to the slightly corrugated two-dimensional layer (Figure 2(c)). Although the arrangement of the guest molecules in the pore also was not determined, some electron

density close to the π-surface of TCNQ can be observed. These results imply that there are some differences in electronic state between the TCNQ moieties of Fe⊃ani and Fe⊃nb, the differences being induced by the host–guest CT interactions, given the spectroscopic results described below. We also measured the X-ray powder diffraction patterns of all metal complexes after guest exchange (Figure 3). There were clear differences in the relative intensities between the patterns of the anisole forms and the nitrobenzene forms. However, we could not observe a clear metal dependence in the patterns with each guest molecule.

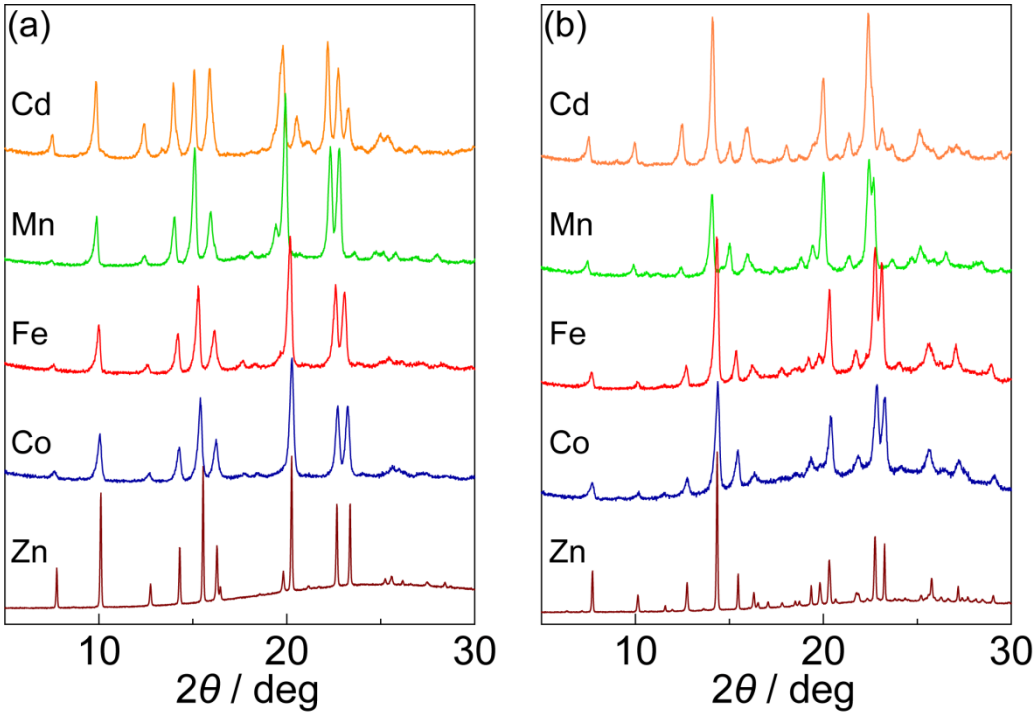

Figure 3. X-ray powder diffraction patterns of [M(TCNQ)bpy] (M = Fe, Zn, Mn, Co, Cd) with (a) anisole and (b) nitrobenzene as the guest molecules.

Figure 4 shows the UV-vis spectra of [M(TCNQ)bpy] with anisole and nitrobenzene. In previous work on the Zn complex, a shift in the absorption band associated with the electron-accepting characteristics of the guest molecule was observed.[29] All complexes also show guest-responsive absorption bands; a red shift of the adsorption bands of M⊃nb around 400–700 nm from the bands of M⊃ani (M⊃ani to M⊃nb, Fe: 472 nm to 478 nm, Zn: 418 nm to 480 nm, Mn: < 400 nm to 447 nm, Co: 595 nm to 626 nm, Cd: 424 nm to 462 nm). Furthermore, the absorption intensity and region of the nitrobenzene compounds tend to be stronger and broader than those of the anisole compounds, especially in the case of the Fe complex. This is ascribed to the CT interaction between the host frameworks and the aromatic molecules. The peak positions and the responsiveness to guest molecules vary according to the metal ions. If metal ions have no effect on the electronic state of

TCNQ in the frameworks, no differences would be observed in their absorption bands. It seems that the metal ions electronically interact with TCNQ and, although there are some differences of degree, affect the molecular orbitals of TCNQ. Infrared spectroscopy in the ν(C≡N) region is useful for assigning charge as well as predicting stacking modes in TCNQ complexes. However, analysis of the IR data for metal-bound TCNQ ligands is complicated by the fact that ν(C≡N) stretches can shift to higher energies if the TCNQ acts primarily as a σ-donor or to lower energies if there is significant metal-to-TCNQ π-back bonding.[36-38] Therefore, we compared the more informative infrared active modes, δ(C−H) bend, to understand the change in electronic states of the TCNQ moieties. All complexes exhibit a δ(C−H) mode at almost the same position around 825 cm^{-1} in accord with the presence of reduced TCNQ (Figure 5(b)).[38, 46] In contrast to the δ(C−H) modes, there are some differences depending on the metal ions in the ν(C≡N) modes (Figure 5(a)). The frequency of the ν(C≡N) mode decreases in the following order: Zn, Co, Mn, Fe. In the case of the Cd complex, peak splitting of the ν(C≡N) bands was observed, which comes from the existence of several ν(C≡N) modes in the complex. However, we have no structural information or additional spectroscopic data; the complete occupied *d*-orbitals and/or the size of the metal ion may lead to this peak splitting, considering the subtle but similar tendency in the Zn complex. The M–TCNQ coordination bonding characters such as σ-bonding and π-back bonding depend on the metal ions. This difference is the linchpin of the various properties of the whole framework in these systems.

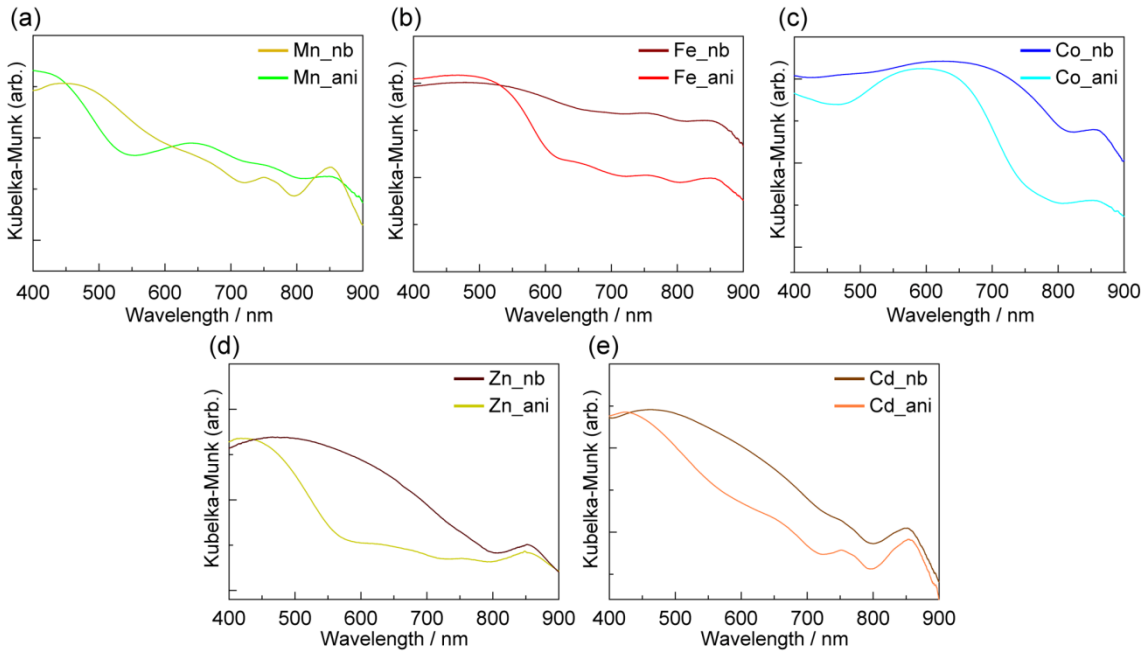

Figure 4. Diffuse reflectance UV-vis spectra of [M(TCNQ)bpy] (M = (a) Mn, (b) Fe, (c) Co, (d) Zn, (e) Cd) with anisole (M_ani) and nitrobenznen (M_nb).

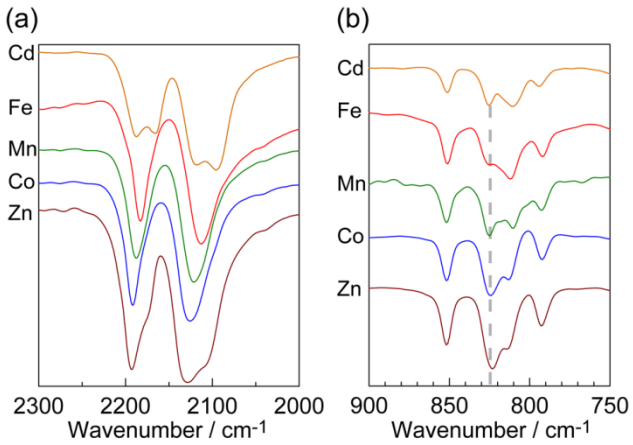

Figure 5. Infrared spectra around (a) the ν(C≡N) and (b) δ(C−H) region the of [M(TCNQ)bpy] (M = Fe, Zn, Mn, Co, Cd) with nitrobenzene.

As a preliminary experiment, we checked the electrical resistivity of these compounds at room temperature. They showed high resistivity in the region between semiconductor and insulator. The Fe complex showed the lowest resistivity (5.9×10^7 Ω cm) and the Zn complex showed the highest resistivity (> 10^{11} Ω cm) with nitrobenzene as the guest. When the guest was exchanged from nitrobenzene to anisole, the resistivity increased by about 100-fold. These results imply that the TCNQ units, metal ions, and guest molecules have an electronic relationship with each other.

Conclusion

This paper has described the synthesis and characterization of a series of TCNQ-dianion-based PCPs [M(TCNQ)bpy] (M = Fe, Zn, Mn, Co, Cd). They form three-dimensional pillared layer structures composed of M–TCNQ two-dimensional layers and bpy pillars regardless of the metal ions. They show metal-dependent guest-responsive color changes and electronic properties. This indicates that the metal ions acting as a node in the frameworks electronically interact with TCNQ moieties and affect the molecular orbitals of TCNQ. These systems with an electronic relationship between metal ions, organic ligands, and guest molecules are still not common, but should be important in creating new porous properties in the field of PCPs. They have the potential to provide a new platform to synthesize organic–inorganic hybrid functional materials.

Experimental Section

Materials. All chemicals and solvents used in the syntheses were reagent grade. LiTCNQ was prepared by the literature method; the solution of TCNQ (1.02 g, 5 mmol) and lithium iodide (1.00 g, 7.5 mmol) in acetonitrile (50 ml) was mixed in reflux condition for 12 h under an N2 atmosphere. After cooling, the purple powder was separated by filtration and washed with acetonitrile until the washings were bright green.

Synthesis of [M(TCNQ)bpy] (M = Fe, Zn, Mn, Co, Cd). All procedures were carried out under an N2 atmosphere using the Schlenk technique. Single crystals suitable for X-ray analysis were prepared by careful diffusion of a solution of LiTCNQ (0.1 mmol, 21 mg) and bpy (0.1 mmol, 16 mg) in methanol (20 ml) into a solution containing metal(II) nitrate hydrate (Mn, Co, Zn, Cd) or ammonium iron(II) sulfate hydrate (0.1 mmol), and a small amount of ascorbic acid in methanol/water mixture (10 ml/10 ml) in a straight glass tube. Crystals began to form in a few days. The bulk product was obtained by slow addition of a solution of LiTCNQ (1 mmol, 211 mg) and bpy (1 mmol, 156 mg) in methanol (20 ml) to a solution of metal(II) nitrate hydrate (Mn, Co, Zn, Cd) or ammonium iron(II) sulfate hydrate (1 mmol), and ascorbic acid (1 mmol, 176 mg) in methanol/water mixture (10 ml/10 ml). Powder samples were collected by filtration and washed with methanol, then immediately soaked in an aromatic solvent (such as nitrobenzene) to exchange the guest molecules without drying in the process. After further filtration, the powder samples were lightly dried.

Physical Measurements. Infrared spectra were measured using a KBr disk with a Perkin-Elmer Spectrum 2000 FT-IR system. X-ray powder diffraction (XRPD) data were collected on a Rigaku RINT-2200HF (Ultima) diffractometer with Cu-Kα radiation (λ = 1.54073 Å). UV-vis spectra were recorded on a HITACHI U-3500/U-4000 spectrometer.

Crystal Structure Determination. X-ray diffraction data of all compounds were collected on a Rigaku Mercury CCD system with graphite monochromated Mo Kα radiation and a Rigaku/MSC Saturn CCD diffractometer with confocal monochromated Mo Kα radiation (λ = 0.71070 Å). Single crystals were mounted in a quartz tube filled with solvent vapors to avoid drying, and kept at measurement temperature under flowing N_2 during collection of the diffraction data. The crystal structures were solved by a direct method (SIR2002 and SHELX97) and refined by full-matrix least-squares refinement using the CRYSTALS computer program. The positions of nonhydrogen atoms were refined with anisotropic displacement factors, except for the guest molecules. The hydrogen atoms were positioned geometrically and refined using a riding model. CCDC 784861 - 784866 contain the supporting crystallographic data for this paper.

References

[1] Horike, S.; Shimomura, S.; Kitagawa, S., *Nat. Chem.* **2009,** *1*, 695-704.

[2] Eddaoudi, M.; Moler, D. B.; Li, H. L.; Chen, B. L.; Reineke, T. M.; O'Keeffe, M.; Yaghi, O. M., *Acc. Chem. Res.* **2001,** *34*, 319-330.

[3] Kitagawa, S.; Kitaura, R.; Noro, S., *Angew. Chem. Int. Ed.* **2004,** *43*, 2334-2375.

[4] Fletcher, A. J.; Thomas, K. M.; Rosseinsky, M. J., *J. Solid State Chem.* **2005,** *178*, 2491-2510.

[5] Lin, X.; Jia, J. H.; Hubberstey, P.; Schroder, M.; Champness, N. R., *CrystEngComm* **2007,** *9*, 438-448.

[6] Kuppler, R. J.; Timmons, D. J.; Fang, Q. R.; Li, J. R.; Makal, T. A.; Young, M. D.; Yuan, D. Q.; Zhao, D.; Zhuang, W. J.; Zhou, H. C., *Coord. Chem. Rev.* **2009,** *253*, 3042-3066.

[7] Long, J. R.; Yaghi, O. M., *Chem. Soc. Rev.* **2009,** *38*, 1213-1214.

[8] Fischer, R. A.; Woll, C., *Angew. Chem. Int. Ed.* **2009,** *48*, 6205-6208.

[9] Ma, L. Q.; Abney, C.; Lin, W. B., *Chem. Soc. Rev.* **2009,** *38*, 1248-1256.

[10] Ferey, G.; Serre, C., *Chem. Soc. Rev.* **2009,** *38*, 1380-1399.

[11] Deng, H. X.; Olson, M. A.; Stoddart, J. F.; Yaghi, O. M., *Nat. Chem.* **2010,** *2*, 439-443.

[12] Beauvais, L. G.; Shores, M. P.; Long, J. R., *J. Am. Chem. Soc.* **2000,** *122*, 2763-2772.

[13] Ohmori, O.; Kawano, M.; Fujita, M., *J. Am. Chem. Soc.* **2004,** *126*, 16292-16293.

[14] Yao, Q. X.; Pan, L.; Jin, X. H.; Li, J.; Ju, Z. F.; Zhang, J., *Chem. Eur. J.* **2009,** *15*, 11890-11897.

[15] Yang, S. H.; Lin, X.; Blake, A. J.; Walker, G. S.; Hubberstey, P.; Champness, N. R.; Schroder, M., *Nat. Chem.* **2009,** *1*, 487-493.

[16] Mulfort, K. L.; Wilson, T. M.; Wasielewski, M. R.; Hupp, J. T., *Langmuir* **2009,** *25*, 503-508.

[17] Lee, E. Y.; Jang, S. Y.; Suh, M. P., *J. Am. Chem. Soc.* **2005,** *127*, 6374-6381.

[18] Tanaka, D.; Horike, S.; Kitagawa, S.; Ohba, M.; Hasegawa, M.; Ozawa, Y.; Toriumi, K., *Chem. Commun.* **2007**, 3142-3144.

[19] Hou, L.; Lin, Y. Y.; Chen, X. M., *Inorg. Chem.* **2008,** *47*, 1346-1351.

[20] Chen, B. L.; Wang, L. B.; Xiao, Y. Q.; Fronczek, F. R.; Xue, M.; Cui, Y. J.; Qian, G. D., *Angew. Chem. Int. Ed.* **2009,** *48*, 500-503.

[21] Allendorf, M. D.; Bauer, C. A.; Bhakta, R. K.; Houk, R. J. T., *Chem. Soc. Rev.* **2009,** *38*, 1330-1352.

[22] Muller, M.; Devaux, A.; Yang, C. H.; De Cola, L.; Fischer, R. A., *Photochem. Photobiol. Sci* **2010,** *9*, 846-853.

[23] Fuma, Y.; Ebihara, M.; Kutsumizu, S.; Kawamura, T., *J. Am. Chem. Soc.* **2004,** *126*, 12238-12239.

[24] Zeng, M. H.; Wang, Q. X.; Tan, Y. X.; Hu, S.; Zhao, H. X.; Long, L. S.; Kurmoo, M., *J. Am. Chem. Soc.* **2010,** *132*, 2561-2563.

[25] Maspoch, D.; Ruiz-Molina, D.; Wurst, K.; Domingo, N.; Cavallini, M.; Biscarini, F.; Tejada, J.; Rovira, C.; Veciana, J., *Nat. Mater.* **2003,** *2*, 190-195.

[26] Ohkoshi, S. I.; Arai, K. I.; Sato, Y.; Hashimoto, K., *Nat. Mater.* **2004,** *3*, 857-861.

[27] Ohba, M.; Yoneda, K.; Agusti, G.; Munoz, M. C.; Gaspar, A. B.; Real, J. A.; Yamasaki, M.; Ando, H.; Nakao, Y.; Sakaki, S.; Kitagawa, S., *Angew. Chem. Int. Ed.* **2009,** *48*, 4767-4771.

[28] Southon, P. D.; Liu, L.; Fellows, E. A.; Price, D. J.; Halder, G. J.; Chapman, K. W.; Moubaraki, B.; Murray, K. S.; Letard, J. F.; Kepert, C. J., *J. Am. Chem. Soc.* **2009,** *131*, 10998-11009.

[29] Shimomura, S.; Matsuda, R.; Tsujino, T.; Kawamura, T.; Kitagawa, S., *J. Am. Chem. Soc.* **2006,** *128*, 16416-16417.

[30] Shimomura, S.; Horike, S.; Matsuda, R.; Kitagawa, S., *J. Am. Chem. Soc.* **2007,** *129*, 10990-10991.

[31] Acker, D. S.; Harder, R. J.; Hertler, W. R.; Mahler, W.; Melby, L. R.; Benson, R. E.; Mochel, W. E., *J. Am. Chem. Soc.* **1960,** *82*, 6408-6409.

[32] Clarkson, S. G.; Lane, B. C.; Basolo, F., *Inorg. Chem.* **1972,** *11*, 662-664.

[33] Kistenmacher, T. J.; Emge, T. J.; Bloch, A. N.; Cowan, D. O., *Acta Crystallogr., Sect. B: Struct. Sci.* **1982,** *38*, 1193-1199.

[34] Miller, J. S.; Zhang, J. H.; Reiff, W. M.; Dixon, D. A.; Preston, L. D.; Reis, A. H.; Gebert, E.; Extine, M.; Troup, J.; Epstein, A. J.; Ward, M. D., *J. Phys. Chem.* **1987,** *91*, 4344-4360.

[35] Shields, L., *J. Chem. Soc., Faraday Trans. 2* **1985,** *81*, 1-9.

[36] Kaim, W.; Moscherosch, M., *Coord. Chem. Rev.* **1994,** *129*, 157-193.

[37] Ballester, L.; Gutierrez, A.; Perpinan, M. F.; Azcondo, M. T., *Coord. Chem. Rev.* **1999,** *192*, 447-470.

[38] Zhao, H.; Heintz, R. A.; Ouyang, X.; Dunbar, K. R.; Campana, C. F.; Rogers, R. D., *Chem. Mater.* **1999,** *11*, 736-746.

[39] Heintz, R. A.; Zhao, H. H.; Xiang, O. Y.; Grandinetti, G.; Cowen, J.; Dunbar, K. R., *Inorg. Chem.* **1999,** *38*, 144-156.

[40] Miyasaka, H.; Campos-Fernandez, C. S.; Clerac, R.; Dunbar, K. R., *Angew. Chem. Int. Ed.* **2000,** *39*, 3831-3835.

[41] Abrahams, B. F.; Hudson, T. A.; Robson, R., *Cryst. Growth Des.* **2008,** *8*, 1123-1125.

[42] Miyasaka, H.; Motokawa, N.; Matsunaga, S.; Yamashita, M.; Sugimoto, K.; Mori, T.; Toyota, N.; Dunbar, K. R., *J. Am. Chem. Soc.* **2010,** *132*, 1532-1544.

[43] Grossel, M. C.; Duke, A. J.; Hibbert, D. B.; Lewis, I. K.; Seddon, E. A.; Horton, P. N.; Weston, S. C., *Chem. Mater.* **2000,** *12*, 2319-2323.

[44] Abrahams, B. F.; Elliott, R. W.; Hudson, T. A.; Robson, R., *Cryst. Growth Des.* **2010,** *10*, 2860-2862.

[45] Oshio, H.; Ino, E.; Ito, T.; Maeda, Y., *Bull. Chem. Soc. Jpn.* **1995,** *68*, 889-897.

[46] Khatkale, M. S.; Devlin, J. P., *J. Chem. Phys.* **1979,** *70*, 1851-1859.

Chapter 3

Guest-Specific Function of a Flexible Undulating Channel in a TCNQ Dimer-based Porous Coordination Polymer

Abstract

We have designed and synthesized a flexible porous coordination polymer with highly selective capacity to separate benzene from cyclohexane. The undulating channel providing the suitable space for the benzene and the H–π interaction between the host framework and the guest molecules result in this high selectivity.

Introduction

In the field of porous coordination polymers (PCPs), separation is one of the most significant topics. PCPs have regularly ordered nanometer-size frameworks with readily modifiable pore surface properties and structural flexibility, which give them potential applications in separation,[1,2] storage[3] and catalyst.[4] The highly selective separation of hydrocarbons having similar physical properties, such as boiling point and molecular size, remains a significant challenge that has much scientific and commercial value. Because cyclohexane is usually produced by hydrogenation of benzene, in the benzene/cyclohexane-miscible system used in the petrochemical industry, separating their mixture is essential.[5] However, the separation is difficult because these substances have similar boiling points (benzene, 80.1 °C and cyclohexane, 80.7 °C), molecular geometry, and Lennard-Jones collision diameters.[6] To face this chemical similarity, we need to design the high recognition capability system, for instance, in biological system which requires the specific binding sites such as cation–π, H–π, and H-bonding-type interaction and the flexible structure to create suitable space for the target molecules.[7,8] 7,7,8,8-Tetracyano-*p*-quinodimethane (TCNQ) is a well-known molecule with a large π surface and redox activity. A PCP whose pore surface is formed by TCNQ will have an H–π-type interaction with benzene and achieve selective separation of benzene from cyclohexane with a suitable pore shape for benzene generated from the specific flexibility of the PCP.

Results and discussion

Green crystals of {[Zn(μ_4-TCNQ–TCNQ)bpy]·1.5benzene}$_n$ (**1**⊃benzene) were synthesized by reacting $Zn(NO_3)_2·6H_2O$ with LiTCNQ and bpy (= 4,4′-bipyridine) in an MeOH/benzene mixture (1:1). The Zn ions are octahedrally coordinated to the four cyanide nitrogen atoms of TCNQ in the equatorial plane and the two nitrogen atoms of the bpy at the axial sites (Figure 1a). The Zn ions are linked by bpy to give a one-dimensional (1D) chain in the direction of the *a*-axis. $[TCNQ–TCNQ]^{2–}$ acts as cross-linker connecting the four 1D chains of Zn ions and bpy to form a 3D open framework (Figure 1b). $[TCNQ–TCNQ]^{2–}$ is derived from a sigma dimerization of two $TCNQ^–$ anions. There are few reports about coordination polymers containing the TCNQ dimer, despite the scarcity, unique shape, and various coordination modes of the dimer making the structures interesting.[9] The dianionic ligand is a nonplanar, staircase motif because of the sp^3 C−C σ-bond connecting the two TCNQs, and the two electrons are separated and delocalized in each planar part of the TCNQ. The channels delimited by the ligands are of the undulating form, not a straight but a unique form comprising an alternating arrangement of two types of tubes of large and small diameter. The large diameter space is adequate to accommodate a benzene molecule because of the suitability of the cavity's size and thickness (Figure 1c). The guest benzene molecule is accommodated strongly in the cavity with the size effect and the H–π interaction with the host framework. The distance between the pore wall perpendicular to the benzene molecule, which comprises the electron-rich π surface of the TCNQ dimer and the center of the benzene molecule, is 5.05 Å. This is consistent with the existence of the H–π interaction between the host framework and the guest molecule (Figure 1c).[8] Only one benzene molecule per Zn^{II} ion was determined by crystallography to be in the cage of the undulating channel, and this is tightly fixed by the H-π interaction. The absence of other guest molecules in the channel of 1⊃benzene was attributed to the disorder of included guest molecules.

Interestingly, although the benzene molecule can be removed from and adsorbed to this compound, the aperture of the small tube is not large enough for the benzene molecule to pass through it, indicating that the framework is flexible. The X-ray powder diffraction (XRPD) patterns also show the structural flexibility of this compound, which is classified as a third-generation compound.[10] In the guest-removal process, the crystal is transformed to a guest-free crystal phase **2**. Alternatively, exposing **2** to benzene vapor for 5 h produced the other crystal phase, **3**⊃benzene whose XRPD pattern quite similar to **1**⊃benzene. The flexibility may originate in the freedom in the coordination mode of TCNQ.

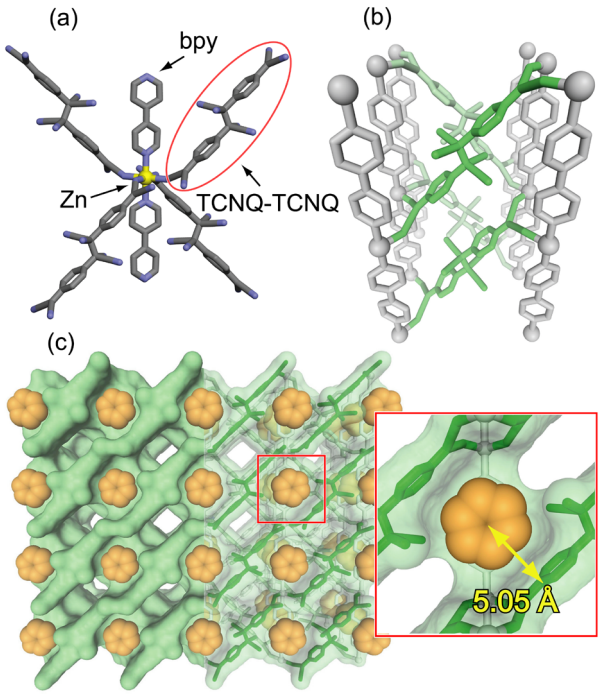

Figure 1. (a) Coordination environment of Zn(II) ion of **1**⊃benzene. (b) TCNQ dimer (green) connected to four 1D chains of Zn and bpy (gray). (c) Benzene arranged in the cage of the undulating channel of 1⊃benzene. The hydrogen atoms are omitted for clarity.

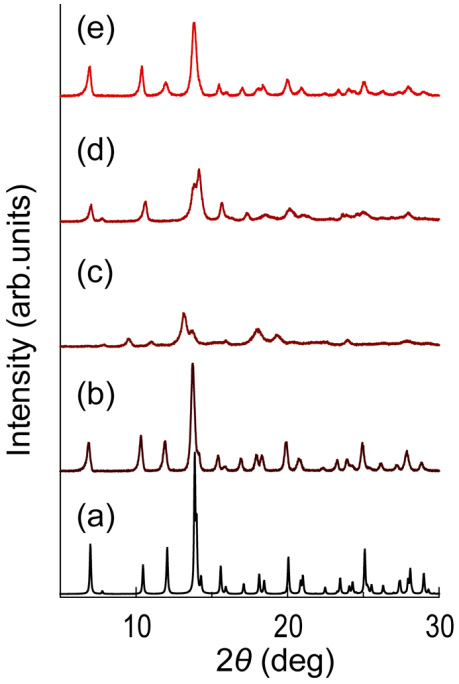

Figure 2. XRPD pattern of (a) simulation (**1**⊃benzene), (b) as synthesized state (**1**⊃benzene), (c) degassed state (**2**), (d) exposed to a vapor of benzene (**3**⊃benzene), (e) exposed to a vapor of benzene/MeOH mixture (**1**⊃benzene).

The guests of **1**⊃benzene were removed at 413 K for 10 h under low pressure, and the sorption isotherms of benzene and cyclohexane of **2** at 298 K were measured. The profiles differed obviously between each isotherm (Figure 3). In the case of benzene, a flat curve means no adsorption in the lower relative pressure region, although an abrupt increase in adsorption and decrease in relative pressure was observed in the process from point A to point B. In the measurement by BELSORP-18 Plus, measurer decides recorded points with an introduction pressure (P_i) of an adsorptive. P_i of an adsorptive is introduced into the cell and then it will achieve an equilibrium pressure (P_e). Then, the adsorption amount (A) are calculated and P_e and A are recorded. In this one cycle, there is no additional vapor-dosing of an adsorptive into the cell. This vapor dosing procedure is useful for the transition and kinetics evaluation of gas adsorption. This compound transforms from non porous (phase 2) to porous structure (phase 3) across the point A and suddenly starts to adsorb the benzene. Because adsorption isotherms of phase 2 and 3 are completely different, the pressure decreases to an equilibrium pressure (point B) and (rapid or sudden) uptake is observed. In the results, we get the isotherm with the break like Figure 3. Figure 4 shows the benzene isotherm and time dependent pressure change of this compound. This is similar to the gate-open type adsorption behavior,[2,11] which is related to the structural transformation of the host framework. The crystal initially has no gates large enough to receive benzene molecules in its cavities until a certain number of benzene molecules accumulate on the surface. Once the threshold concentration, the so-called gate opening pressure, is achieved, the crystal begins to accommodate the guests, and the sorption accelerates cooperatively, accompanied by the structural transformation. The driving force to open the gates could be the presence of a higher-affinity interaction of the pore surface and guest molecules. In contrast, no adsorption of cyclohexane occurs even in the higher relative pressure region, indicating the gates remain closed for cyclohexane.

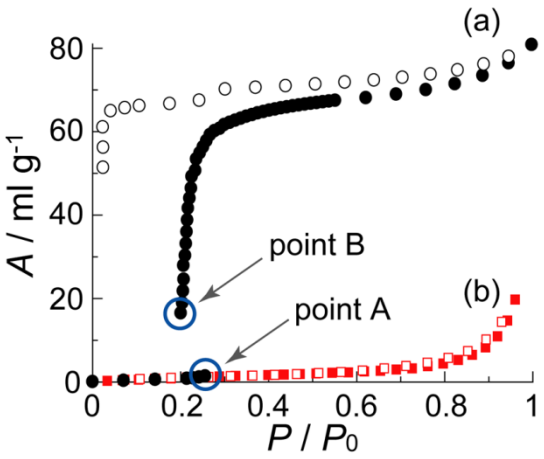

Figure 3. Sorption isotherm for each adsorbate in **2** at 298 K. (a) Benzene adsorption (filled circles) and desorption (open circles). (b) Cyclohexane adsorption (full squares) and desorption (open squares).

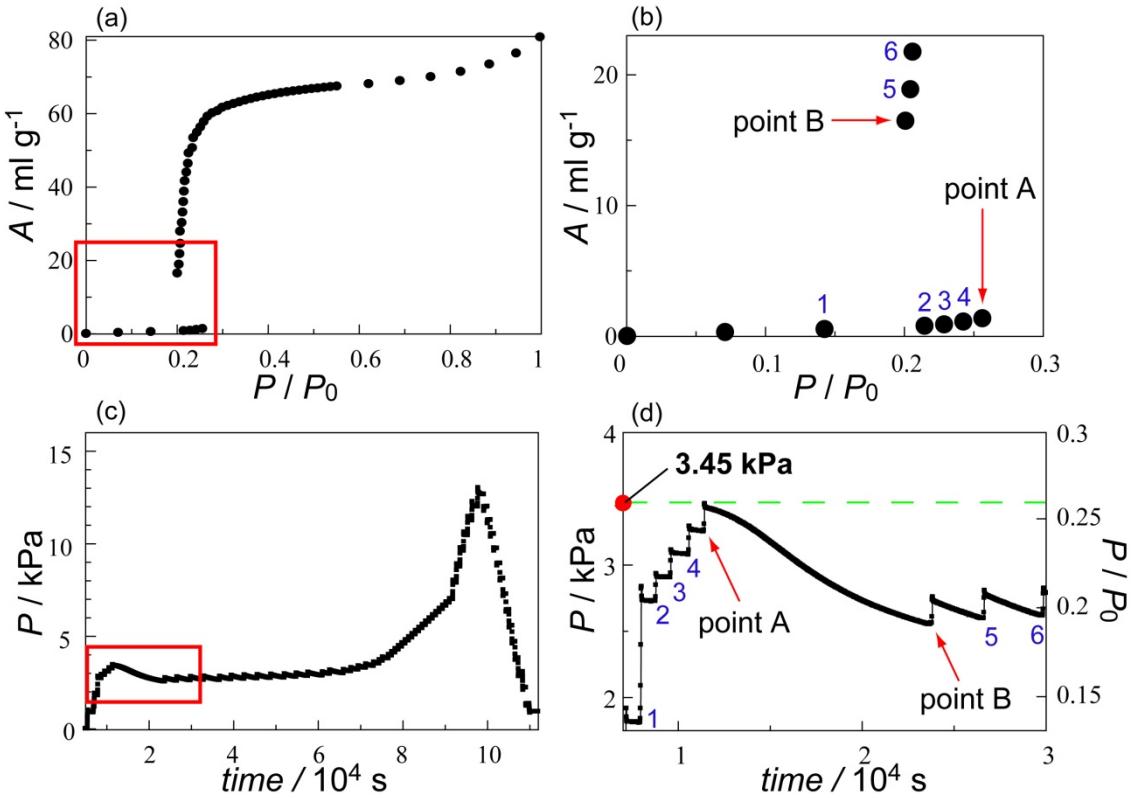

Figure 4. (a)(b) The benzene adsorption isotherm and the detail around the break. (c)(d) The time dependent pressure change in this measurement and the detail around the break. The labeled numbers of each point in (b) are directly corresponded to in (d). From (d), the adsorption starts above the pressure 3.45 kPa.

The guest-free phase **2** was exposed to the vapor of benzene/cyclohexane mixture at a ratio of 1:1 at room temperature for 5 h. The XRPD pattern was transformed from the guest-free state **2** to the benzene-adsorbed state **3**⊃benzene. This sample was decomposed, and all the organic components were dissolved in DMSO-d_6. The ^{1}H NMR spectrum showed that the ratio of benzene and cyclohexane of this compound was 96:4 (Figure 5). This compound maintained the high separation efficiency at least for three times (98:2 (second), 97:3 (third)). At other benzene/cyclohexane mixture ratios (1:3, 1:10), benzene was also selectively adsorbed (96:4, 95:5, respectively). This compound also preferentially adsorbed 1,4-cyclohexadiene from a mixture of equal parts of 1,3-cyclohexadiene and 1,4-cyclohexadiene (23:77), which have almost the same molecular shape and boiling point and differ only in the position of protons in the molecular plane. These properties are linked directly to the strength of the H–π interaction with the host framework. Considering the crystallographic results of **1,** 1,4-cyclohexadiene can interact with this compound with four protons, unlike 1,3-cyclohexadiene, which interacts with three protons. The keys to the success of the separation are the H–π-type host–guest interaction, which triggers the structural transformation from the closed form (**2**) to the open form (**3**) in the sorption process, and the undulating channel with cages fitting tightly to the shape of benzene.

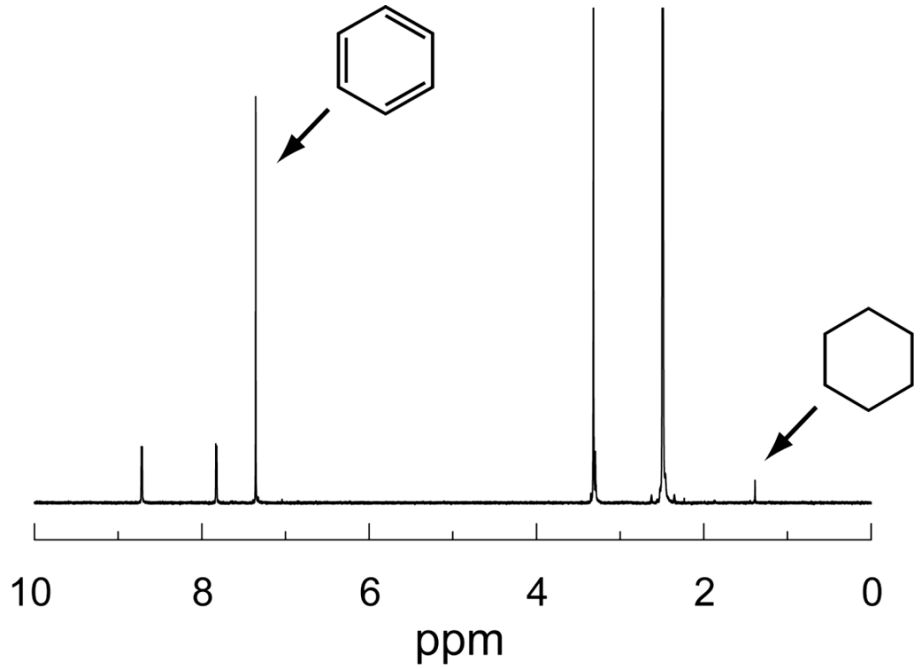

Figure 5. 1H-NMR spectra of degassed [Zn(μ_4-TCNQ-TCNQ)bpy] (**2**) exposed to a vapor of a benzene/cyclohexane mixture (1:1) for 5 hours. The ratio of benzene and cyclohexane in this compound is 96:4

Conclusion

In conclusion, we have designed and synthesized a PCP with highly selective capacity to separate benzene from cyclohexane. Synergy of the undulating channel formed gives the PCP structural flexibility to adapt to the target molecular shape, and, with the interaction site located in the right position of the pore surface, makes PCPs an effective separation system.

Experimental Section

Materials. 7,7,8,8-tetracyano-p-quinodimethane and 4,4'- Bipyridine were obtained from Tokyo Kasei Industrial and $Zn(NO_3)_2 \cdot 6H_2O$ were obtained from Wako and used without further purification. LiTCNQ was prepared by the literature method.

Synthesis of Porous Coordination Polymer {[Zn(TCNQ-TCNQ)bpy]·1.5benzene}$_n$ (1⊃benzene). Single crystal of **1** was prepared by the following procedure. All procedure were carried out under N_2 atmosphere using Schlenk technique. A solution of LiTCNQ (0.1 mmol, 21 mg) and bpy (0.1 mmol, 16 mg) in MeOH/benzene mixture (20 ml) was carefully layered on the top of a solution of $Zn(NO_3)_2 \cdot 6H_2O$ (0.1 mmol, 30 mg) in MeOH/benzene mixture (20 ml). Green crystals began to form in a few days. The bulk product was obtained by the following procedure. Slow addition of a solution of LiTCNQ (2 mmol, 422 mg) and bpy (1 mmol, 156 mg) in MeOH/benzene mixture (100 ml) to a solution of $Zn(NO_3)_2 \cdot 6H_2O$ (1 mmol, 297 mg) in MeOH/benzene mixture (100 ml) at 293 K under N_2 atmosphere. The green powder obtained was collected by filtration. (yield 93%) Elemental analysis calcd. for $C_{43}H_{25}N_{10}Zn$: C, 69.17; H, 3.37; N, 18.75, Found: C, 68.48; H, 3.58; N, 18.65.

X-ray Crystal Analysis. Single crystal X-ray diffraction data collection was carried out on a Rigaku mercury diffractometer with a graphite monochromated MoKα radiation (γ = 0.71069 Å) and a CCD detector. The crystal structure was solved by a direct method (SIR2002) and refined by full-matrix least-squares refinement using the CRYSTALS computer program. The positions of non-hydrogen atoms were refined with anisotropic displacement factors, except for the guest molecules. The hydrogen atoms were positioned geometrically and refined using a riding model.

Physical Measurements. The elemental analysis was carried out on a Flash EA 1112 series, Thermo Finnigan instrument. Thermal gravimetry analysis (TGA) was carried out with a Rigaku Instrument TG8120 in a nitrogen atmosphere. X-ray powder diffraction (XRPD) data were collected on a Rigaku RINT-2200HF (Ultima) diffractometer with Cu-Kα radiation. The adsorption isotherms of CO2 (195 K), acetone and benzene (298K) were measured in the gaseous state by using BELSORP18-Plus volumetric adsorption equipment from BEL Japan, Inc. VT 1H NMR spectra were recorded on a JEOL A-500 spectrometer and referenced to residual protons of DMSO-d_6 solvent.

Table 1. Crystal data and Structure Solution and Refinement of **1**⊃benzene.

Empirical Formula	C40H22N10Zn
Formula Weight	708.06
Crystal System	monoclinic
Lattice Parameters	*a* = 11.361(5) Å
	b = 12.645(6) Å
	c = 14.775(7) Å
	V = 2122.4(18) Å3
Space Group	Pccm (#49)
Z value	2
Dcalc	1.108 g/cm3
F000	724.00
μ(MoKα)	6.155 cm-1
Radiation	MoKα (λ= 0.71070 Å)
	graphite monochromated
2θmax	54.9°
No. of Reflections Measured	Total: 15080
	Unique: 2521 (Rint = 0.041)
Completeness	99.8%
Refinement	Full-matrix least-squares on F2
2θmax cutoff	0.0°
Anomalous Dispersion	All non-hydrogen atoms
No. Observations (I>2.50□(I))	2210
No. Variables	206
Reflection/Parameter Ratio	10.73
Residuals: R1 (I>2.00□(I))	0.0586
Residuals: R (All reflections)	0.0660
Residuals: wR2 (All reflections)	0.0591
Goodness of Fit Indicator	1.082
Max Shift/Error in Final Cycle	0.000
Maximum peak in Final Diff. Map	1.12 e-/Å3
Minimum peak in Final Diff. Map	-0.41 e-/Å3

$R = \Sigma||Fo| - |Fc||/\Sigma|Fo|$. $Rw = [\Sigma w(Fo^2 - Fc^2) / \Sigma w(Fo^2)^2]^{1/2}$.

References

[1] (a) Yaghi, O. M.; Li, G. M.; Li, H. L. *Nature* **1995**, *378*, 703-706. (b) Chen, B. L.; Liang, C. D.; Yang, J.; Contreras, D. S.; Clancy, Y. L.; Lobkovsky, E. B.; Yaghi, O. M.; Dai, S. *Angew. Chem. Int. Ed.* **2006**, *45*, 1390-1393. (c) Pan, L.; Olson, D. H.; Ciemnolonski, L. R.; Heddy, R.; Li, J. *Angew. Chem. Int. Ed.* **2006**, *45*, 616-619. (d) Choi, E. Y.; Park, K.; Yang, C. M.; Kim, H.; Son, J. H.; Lee, S. W.; Lee, Y. H.; Min, D.; Kwon, Y. U. *Chem. Eur. J.* **2004**, *10*, 5535-5540. (e) Makinen, S. K.; Melcer, N. J.; Parvez, M.; Shimizu, G. K. H. *Chem. Eur. J.* **2001**, *7*, 5176-5182. (f) Matsuda, R.; Kitaura, R.; Kitagawa, S.; Kubota, Y.; Belosludov, R. V.; Kobayashi, T. C.; Sakamoto, H.; Chiba, T.; Takata, M.; Kawazoe, Y.; Mita, Y. *Nature* **2005**, *436*, 238-241.

[2] Llewellyn, P. L.; Bourrelly, S.; Serre, C.; Filinchuk, Y.; Ferey, G. *Angew. Chem. Int. Ed.* **2006**, *45*, 7751-7754.

[3] (a) Chen, B. L.; Ockwig, N. W.; Millward, A. R.; Contreras, D. S.; Yaghi, O. M. *Angew. Chem. Int. Ed.* **2005**, *44*, 4745-4749. (b) Dinca, M.; Dailly, A.; Liu, Y.; Brown, C. M.; Neumann, D. A.; Long, J. R. *J. Am. Chem. Soc.* **2006**, *128*, 16876-16883. (c) Ferey, G.; Mellot-Draznieks, C.; Serre, C.; Millange, F.; Dutour, J.; Surble, S.; Margiolaki, I. *Science* **2005**, *309*, 2040-2042. (d) Halder, G. J.; Kepert, C. J. *J. Am. Chem. Soc.* **2005**, *127*, 7891-7900. (e) Lee, E. Y.; Jang, S. Y.; Suh, M. P. *J. Am. Chem. Soc.* **2005**, *127*, 6374-6381. (f) Lin, X.; Jia, J. H.; Zhao, X. B.; Thomas, K. M.; Blake, A. J.; Walker, G. S.; Champness, N. R.; Hubberstey, P.; Schroder, M. *Angew. Chem. Int. Ed.* **2006**, *45*, 7358-7364. (g) Zhao, X. B.; Xiao, B.; Fletcher, A. J.; Thomas, K. M.; Bradshaw, D.; Rosseinsky, M. J. *Science* **2004**, *306*, 1012-1015.

[4] (a) Cho, S. H.; Ma, B. Q.; Nguyen, S. T.; Hupp, J. T.; Albrecht-Schmitt, T. E. *Chem. Commun.* **2006**, 2563-2565. (b) Dybtsev, D. N.; Nuzhdin, A. L.; Chun, H.; Bryliakov, K. P.; Talsi, E. P.; Fedin, V. P.; Kim, K. *Angew. Chem. Int. Ed.* **2006**, *45*, 916-920. (c) Gomez-Lor, B.; Gutierrez-Puebla, E.; Iglesias, M.; Monge, M. A.; Ruiz-Valero, C.; Snejko, N. *Chem. Mater.* **2005**, *17*, 2568-2573. (d) Ohmori, O.; Fujita, M. *Chem. Commun.* **2004**, 1586-1587. (e) Wu, C. D.; Hu, A.; Zhang, L.; Lin, W. B. *J. Am. Chem. Soc.* **2005**, *127*, 8940-8941.

[5] Bai, Y. X.; Qian, J. W.; Zhao, Q.; Xu, Y.; Ye, S. R. *J. Appl. Polym. Sci.* **2006**, *102*, 2832-2838.

[6] (a) Gade, S. K.; Tuan, V. A.; Gump, C. J.; Noble, R. D.; Falconer, J. L. *Chem. Commun.* **2001**, 601-602. (b) Lu, L. Y.; Peng, F. B.; Jiang, Z. Y.; Wang, J. H. *J. Appl. Polym. Sci.* **2006**, *101*, 167-173. (c) Lu, L. Y.; Sun, H. L.; Peng, F. B.; Jiang, Z. Y. *J. Membr. Sci.* **2006**, *281*, 245-252. (d) Pandey, L. K.; Saxena, C.; Dubey, V. *J. Membr. Sci.* **2003**, *227*, 173-182. (e

Peng, F. B.; Lu, L. Y.; Sun, H. L.; Wang, Y. Q.; Liu, J. Q.; Jiang, Z. Y. *Chem. Mater.* **2005**, *17*, 6790-6796.

[7] Davis, A. M.; Teague, S. J. *Angew. Chem. Int. Ed.* **1999**, *38*, 737-749.

[8] Meyer, E. A.; Castellano, R. K.; Diederich, F. *Angew. Chem. Int. Ed.* **2003**, *42*, 1210-1250.

[9] (a) Mikami, S.; Sugiura, K.; Miller, J. S.; Sakata, Y. *Chem. Lett.* **1999**, 413-414. (b) Zhao, H.; Heintz, R. A.; Ouyang, X.; Dunbar, K. R.; Campana, C. F.; Rogers, R. D. *Chem. Mater.* **1999**, *11*, 736-746. (c) Zhao, H. H.; Heintz, R. A.; Dunbar, K. R.; Rogers, R. D. *J. Am. Chem. Soc.* **1996**, *118*, 12844-12845.

[10] Kitagawa, S.; Kitaura, R.; Noro, S. *Angew. Chem. Int. Ed.* **2004**, *43*, 2334-2375.

[11] (a) Li, D.; Kaneko, K. *Chem. Phys. Lett.* **2001**, *335*, 50-56. (b) Seki, K. *Phys. Chem. Chem. Phys.* **2002**, *4*, 1968-1971. (c) Kitaura, R.; Seki, K.; Akiyama, G.; Kitagawa, S. *Angew. Chem. Int. Ed.* **2003**, *42*, 428-431. (d) Kondo, A.; Noguchi, H.; Ohnishi, S.; Kajiro, H.; Tohdoh, A.; Hattori, Y.; Xu, W. C.; Tanaka, H.; Kanoh, H.; Kaneko, K. *Nano Lett.* **2006**, *6*, 2581-2584. (e) Chen, B. L.; Ma, S. Q.; Zapata, F.; Fronczek, F. R.; Lobkovsky, E. B.; Zhou, H. C. *Inorg. Chem.* **2007**, *46*, 1233-1236.

Chapter 4

Selective Sorption of Oxygen and Nitric Oxide by an Electron-Donating Flexible Porous Coordination Polymer

Abstract

Porous coordination polymers (PCPs) are exciting porous materials, formed by metal ions bridged together by organic linkers, that can combine two seemingly contradictory properties - crystallinity with flexibility. PCPs can therefore create highly regular yet dynamic nanoporous domains that are particularly promising for sorption applications. Here we describe the effective selective sorption of dioxygen and nitric oxide by a structurally and electronically dynamic PCP built from zinc centres and 7,7,8,8-tetracyano-*p*-quinodimethane (TCNQ) as a linker. In contrast with a variety of other gas molecules (C_2H_2, Ar, CO_2, N_2 and CO), O_2 and NO are accommodated in its pores. This unprecedented preference arises from the concerted effect of the charge-transfer interaction between TCNQ and these guests, and the switchable gate opening and closing of the pores of the framework. This system provides further insight into the efficient recognition of small gas molecules.

Introduction

Recognition and selective accommodation of gas molecules are vital challenges in the environmental and industrial fields, and are fascinating subjects for scientific study. High efficiency separation of small gases such as CH_4, C_2H_2, CO_2, N_2, O_2, NO_x, without a large expenditure of energy is becoming increasingly important from energetical and biological standpoints. Enhancing the molecular recognition ability of the nanoporous domain is an important aim of such research; achieving this aim requires providing good affinity for the target molecule and a means to avoid the uptake of other molecules. In cases of conventional porous materials, there are few applicable molecules for selective accommodation because of the difficulty in designing structures having the properties mentioned above. On the other hand, porous coordination polymers (PCPs) or metal organic frameworks (MOFs) have attracted attention as strong candidates for this purpose[1-9] because they possess designability that provides various kinds of host–guest interactions in nanoporous domains, and flexibility that allows guest-responsive dynamic accommodation extending over the mesoscopic domain (10 – 100 nm). Pore surface design that includes modification of building block functionality in the nanoporous domain is one of the important methods to increase the affinity for target molecules, attaining selective accommodations.[10-14] In the mesoscopic domain, structural flexibility, causing the closed/open-type structural transformation, is the linchpin for the gated effect, which enhances the selectivity. Flexible crystalline porous material, which we call soft porous crystal,[15] should provide an ideal sorption system with highly selective recognition and efficient use of the whole pore space only for storage of the target molecule.

There has recently been a lot of interest in physisorption of gases by PCPs, such as selective sorption properties for CH_4 and CO_2,[16-18] and temperature dependent gate sorption phenomena.[19] These results are associated with the advantage of soft PCPs dissimilar to conventional porous materials. In many cases of conventional porous materials, the selective gas sorption properties depend on the size and shape effect. Therefore, it is difficult to achieve the retrograde tendency of the selectivity to these factors. For example, the sorption property with selectivity only for O_2 and NO is unusual for porous materials.[20-28] The Table 1 shows the structural, physical, and electronic parameters for the adsorbate molecules.[22, 23, 29] Focusing on O_2 as a target adsorbate molecule presents some difficulties for designing the O_2-recognition mechanism from N_2 and Ar, which have similar molecular shape or size to O_2. In addition, CO_2 is a good adsorbate for microporous and mesoporous materials because of the small kinetic diameter and good affinity for the adsorbent. There are few cases in which the adsorbent shows no uptake of CO_2 even though it possesses porosity for O_2. The selective sorption of O_2 over CO_2 is one of the most crucial challenges for any porous materials. In this manuscript, we report on a PCP possessing an exceptional selective sorption property for O_2 and NO, and we characterize this unprecedented mechanism.

Table 1. The list of physical, and electronic parameters for the adsorbate molecules. The red letters mean the highest value among these molecules. The reduction energy is defined as the energy difference between the neutral-state and the reduction-state.

	NO	CO_2	C_2H_2	Ar	O_2	N_2	CO
							
Kinetic diameter (Å)	3.17	3.3	3.3	3.4	3.46	3.64	3.76
Dipole Moment (D)	0.161	0	0	0	0	0	0.117
Quadrupole moment $10^{40}\ \theta(Cm^2)$	11	13.4	20.4	0	1.3	4.7	8.3
Polarizability ($Å^3$)	1.70	2.65	3.59	1.66	1.60	1.76	1.95
Reduction energy ($kJmol^{-1}$)	32.1	351.4	172.0	331.6	4.1	241.5	185.8

Results and discussion

Structural transformation of the gate-opening properties to target molecules is a potential mechanism for selective accommodation.[20] We have previously reported that [Zn(TCNQ-TCNQ)bpy](**1**) has a flexible three dimensional structure constructed from Zn(II) cation, 4,4′-bipyridyl (bpy), and TCNQ dimer, which is the interactive dianion unit for the guest molecule (Fig. 1), and shows the closed/open-type structural transformation accompanying the adsoption/desorption process.[30] These properties make **1** a good candidate as an adsorbent for selective separation. Compound **1** can effectively separate benzene from the benzene/cyclohexane-miscible system.

In addition to the benzene molecule, TCNQ dimer in **1** forms durable CH-π-type interactions with aromatic protons possessing partial positive charge. Based on this affinity, the framework of **1** showed host–guest complexations with several aromatic molecules, and these accommodating structures were detected by single crystal X-ray diffraction analysis (Fig. 2). The channels delimited by TCNQ dimer are of the undulating form, not a straight but a unique form, comprising an alternating arrangement of two types of tubes of large and small diameter. The aromatic molecules are held by the two TCNQ dimers from both sides of the channel wall, and the aromatic protons are directed to the π surfaces of the TCNQ dimers. The distances between the pore walls perpendicular to the aromatic molecules also indicate that they are accommodated strongly in the channels with CH-π-type interactions and confinement effects.[31]

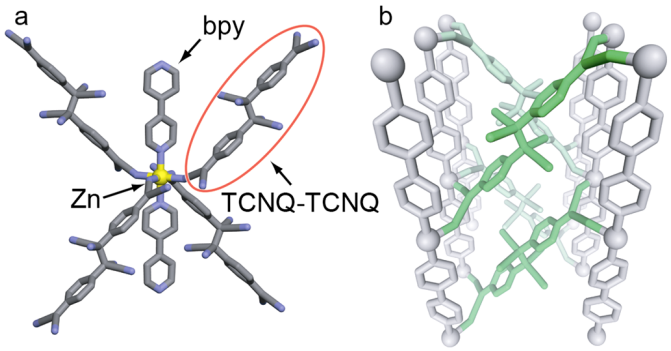

Figure 1. The details of crystal structure of 1 (open form). The coordination environment of Zn(II) cation in 1 (a). Bpy coordinates to the axial sites of Zn to form one dimensional chain (gray) and TCNQ dimer (green) coordinates to the equatorial sites of Zn to connect the one dimensional chains (b).

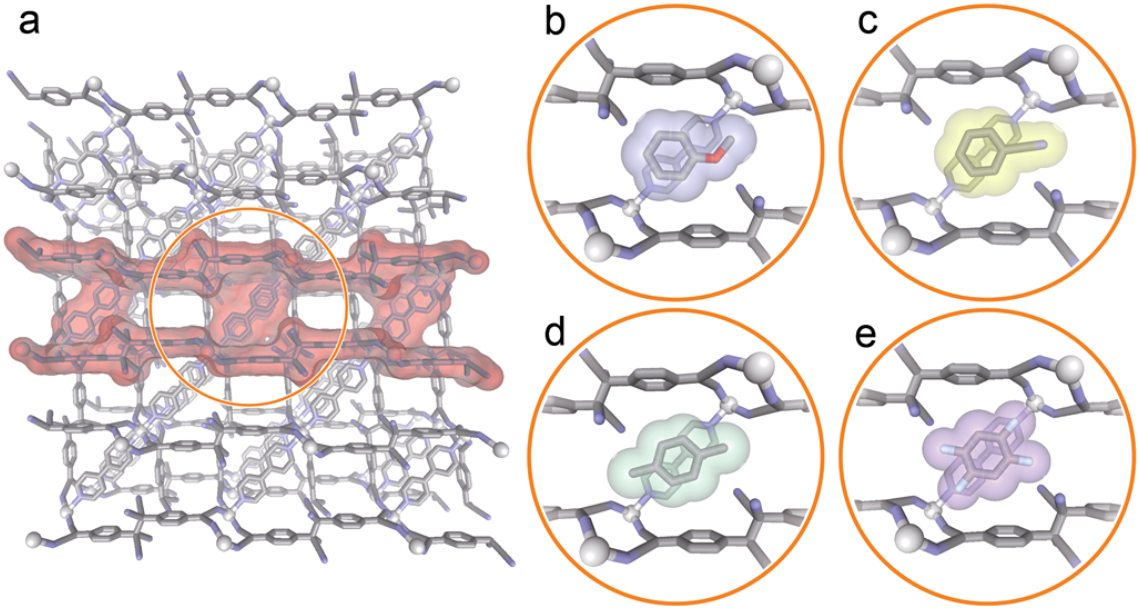

Figure 2. Guest-accommodating structures of 1 (open form). This framework possesses the undulating channel structure showing in red colored part (a) and the several aromatic molecules are accommodated in the large diameter spaces of this channel (anisole (b), benzonitrile (c), *p*-xylene (d), 1,2,4,5-tetrafluorobenzene(e)). b-e, the volume occupied by each of the four aromatic molecules is highlighted in blue, yellow, green and purple, respectively. In cases of b and c, however the guest molecules are disordered in the two oppositely-oriented positions along the undulating channel, one of them are omitted for clarity.

The electron-rich pore surfaces of **1** should also have a good affinity for electron-accepting molecules. This tendency can be observed in the case of gas molecules. The sorption isotherms of several kinds of gas molecules were measured on the closed form **1** (Fig. 3). Only in the cases of O_2 and NO, this compound shows the sorption phenomena characteristic of the gate-type sorption behaviour: no uptake in the low concentration region and an abrupt increase in adsorption after the threshold concentration. This behaviour based on the closed/open-type structural transformation was detected by X-ray powder diffraction (XRPD) analysis (Fig. 4). The XRPD patterns of the open form and closed form are distinctly different from each other. Le Bail analysis shows that the closed form possesses a different unit cell with less symmetry than that of the open form. Accompanying the accommodation of O_2 and NO, the patterns changed from the closed form to the new phases with almost the same unit cells as those of the open form. The saturation-adsorbed amounts of O_2, 268 cm^3(at STP)g^{-1}, and NO, 322 cm^3(at STP)g^{-1}, correspond to 7.5 and 9 molecules per formula, respectively. In contrast, no sharp uptake over one molecule per formula was observed in the other gas molecules (N_2, CO, CO_2, C_2H_2, or Ar).

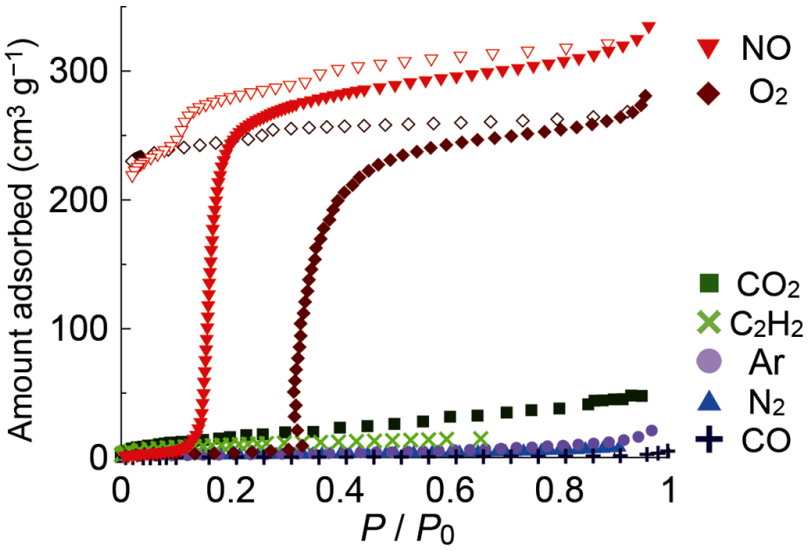

Figure 3. Adsorption isotherms of several gas molecules. The sorption measurements were carried out under the following conditions: N_2, O_2, CO at 77 K, Ar at 87 K, NO at 121 K, and CO_2, C_2H_2 at 195 K. Filled and open symbols represent adsorption and desorption data, respectively. The desorption isotherms for O_2 and NO shows the large hysteresis that indicate good interaction between host and guests. The desorption isotherms for other gas molecules are omitted for clarity.

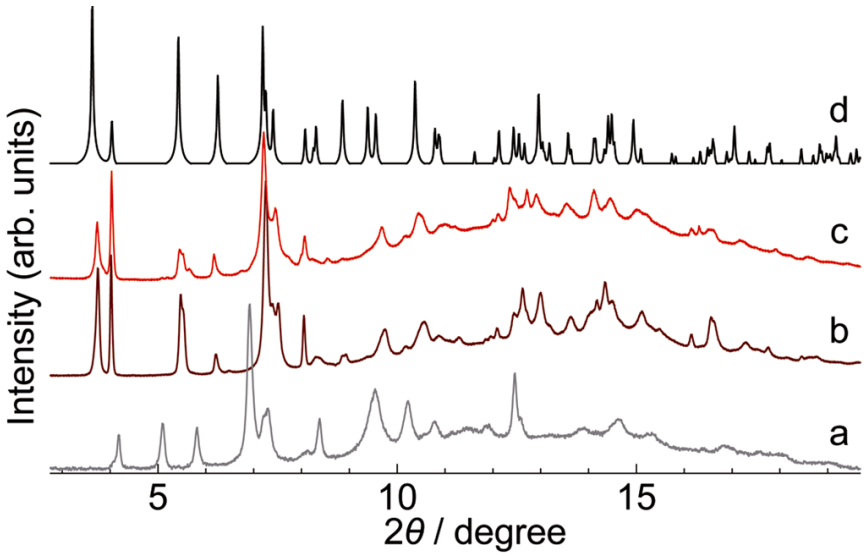

Figure. 4. **Structural transformation of 1 accompanying with guest sorption.** XRPD patterns of no guest state (a), O_2 adsorbed state(b), NO adsorbed state(c), and simulated as-synthesized state (d). The XRPD patterns of the open (a) and closed (d) forms of the framework are very different. On sorption of O2 (b) and NO (c), the framework becomes more similar to the open form.

In this phenomena, the closed/open transition is important because the trigger of the transformation—the interaction between the host and guest—is an overriding factor for this selectivity. Considering the case of no uptake of CO_2 and C_2H_2, the quadrupole moment and polarizability, which have a strong effect on the dispersion force of the molecule, have no bearing on this selectivity. In contrast with the case of NO, no uptake of CO indicates that the electric dipole moment of guest molecules is not associated with this phenomenon. From these results and background, **1** seems to respond to and recognize some sort of properties common to O_2 and NO.

We used a spectroscopic approach to try to elucidate the state of **1** and O_2 in the sorption process. Infrared spectroscopy in the ν(C≡N) stretches and the δ(C−H) band is useful for assigning the charge state of the TCNQ unit.[32, 33] The spectrum of the no guest sample exhibited ν(C≡N) bands at 2192 and 2138 cm^{-1} and δ(C-H) bands at 805 cm^{-1}, which are characteristic of the TCNQ dimer (Fig. 5). When the sample was exposed to O_2 atmosphere at 93 K, the peaks of the ν(C≡N) bands shifted to 2213 and 2156 cm^{-1}. In the reduction state of TCNQ, the cyano groups become involved in a malonodinitrilato-type structure with decreased C-N but increased C-C bond order. Therefore, the C-N bond closes back to triple bond caused by the decrease in the conjugated electron in the TCNQ π system. This peak shift corresponds to the decrease in electron density on TCNQ, implying the charge-transfer (CT) interaction between the framework and O_2 molecule.[34-36] The Raman spectrum of **1** under the O_2 sorption condition confirms this conclusion. The ν(O□O) stretch band, which is the index of the physical and chemical state of the O_2 molecule, can be detected directly.[37-40] As the sorption of $^{16}O_2$ molecule progressed, two peaks were observed: a sharp peak at 1454 cm^{-1} and a broad peak at 1449 cm^{-1} (Fig. 6). Both peaks disappeared with removal of the guest. The broad band arises from the framework transformation accompanying the O_2 sorption because this band was observed under $^{18}O_2$ atmosphere instead of $^{16}O_2$. However, the sharp band was not observed under $^{18}O_2$ atmosphere. Considering that no bands appeared around 1550 cm^{-1}, the sharp band can be assigned as the ν(O=O) stretching mode in the pore of **1**. In published papers to date, O_2 molecules are incorporated in the microporous materials to form molecular aggregation, even in the weak interaction of guest molecules and the pore surface. This is so-called a confinement effect.[41, 42] When O_2 was adsorbed on a microporous compound, a slight blue shift of the ν(O=O) stretching band by about 10 cm^{-1} is induced by this effect.[10] On the other hand, the case of **1** shows a different propensity to that shown in the previous result. The large red shift of the ν(O=O) band by about 100 cm^{-1}, in other words, the decrease in the bonding force constant (therefore, bond order), cannot be induced by the confinement effect, which might make a slight influence on the bonding properties of the oxygen molecule. The decrease in the bond order of O_2 are commonly caused by electron acceptance of the antibonding π^* orbitals. Compared with the reported peak positions of ν(O□O) stretching in the various electronic states, the band suggests that O_2 molecules accommodated in **1** have a partial negative charge and that there is no redox reaction with one-electron transfer.[43-45] This

is direct evidence of the existence of the CT interaction between the framework and O_2 molecules and that they are in an exceptional state with an electronic effect and a confinement effect.

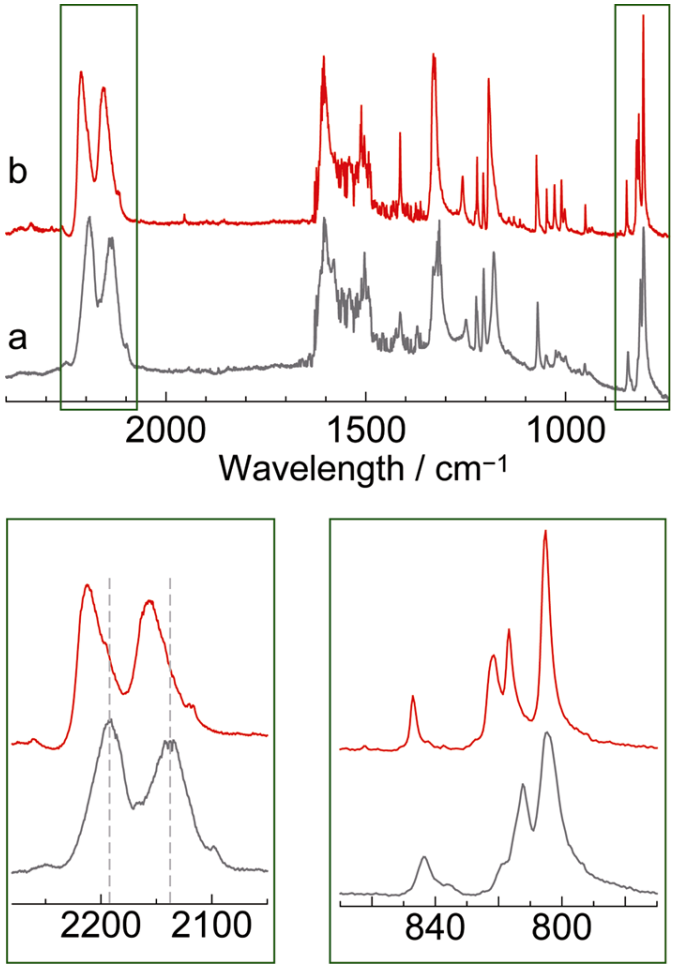

Figure. 5. **Infrared spectra of each states of 1**. Closed form of **1** in air at room temperature, which treated under vacuum at 373 K for 12 hours (a), and under O_2 at 93 K (b). The definite peak shifts of the ν(C≡N) bands at 2192 and 2138 cm^{-1} to 2213 and 2156 cm^{-1}, respectively, and no changes of the δ(C–H) band have been observed in the O_2 sorption process. This means the decrease in the conjugated electron in the TCNQ dimers.

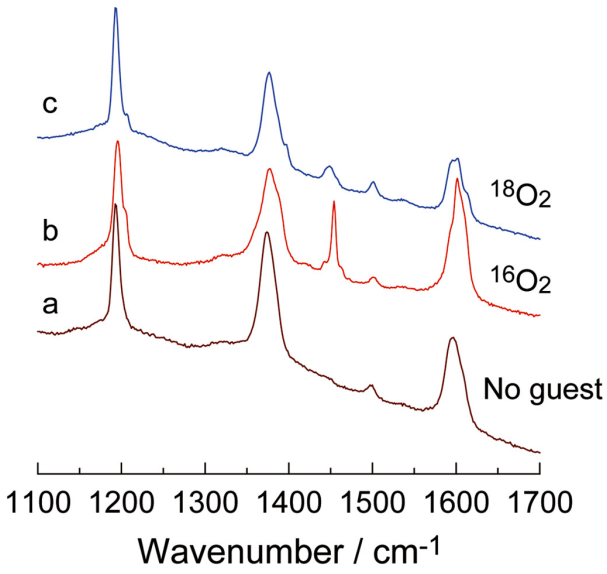

Figure. 6. **Atmosphere control Raman spectroscopy of 1**. After the guest removal treatment, the Raman spectra of **1** were measured under air (a), under $^{16}O_2$ at 90 K (b), and under $^{18}O_2$ at 90 K (c). The peak of ν(O=O) stretching band of $^{16}O_2$ have been observed with a large red shift from that in the gas state (b). This significant decrease in the bond order of O_2 are commonly caused by electron acceptance of the antibonding π^* orbitals. The $^{18}O_2$ stretching band, which is calculated to be about 1371(5) cm^{-1} from that of $^{16}O_2$, occurs in the region of the framework moieties and overlaps with them.

We calculated the reduction energies of gas molecules at MP2/6-311+G* level to check the electron acceptability of them. O_2 and NO have low reduction energies and good electron acceptability compared with the other gas molecules (Table 1). This electron acceptability plays the critical role in this system. These results distinguish O_2 and NO from the other guest gas molecules. Cooperative effect of acceptor guest and donor framework is important in this sorption behaviour. Because of a partial charge delocalization, the framework is maintained over adsorption/desorption cycle, exhibiting the stability and recyclability. This is also corroborated by the Raman spectroscopy. In addition, The total stabilization energy depending on the distance between one TCNQ dimer and single gas molecules have been calculated at MP2/6-311+G* level. However NO shows a higher affinity for TCNQ dimer than the other gas molecules, we cannot get the results suggesting the primacy of O_2 over the other molecules and supporting the experimental results. These results imply the selective sorption of this compound should not be based on the interaction between single TCNQ dimer and single gas molecules but the other mechanism, such as the interaction between TCNQ dimers and aggregated gas molecules. Relatively high gate opening pressure of O_2 sorption isotherm is consistent with this assumption.

Conclusion

In conclusion, we have discovered that **1** shows selective recognition of O_2 and NO molecules. This specific sorption ability is ascribed to the closed/open-type structural transformation triggered by the CT interaction between the host framework and guest molecule. The key to this selectivity is the combination of structural dynamics and electron-donating function of the framework, which can be induced by the soft crystallinity and designability of PCPs. PCPs will provide a new platform for selective adsorption systems for small gas molecules.

Experimental Section

Synthesis of [Zn(TCNQ-TCNQ)bpy]•1.5benzene (1⊃benzene).

Slow addition of a solution of LiTCNQ (2 mmol, 422 mg) and bpy (1 mmol, 156 mg) in MeOH/benzene mixture (1:1, 100 ml) to a solution of $Zn(NO_3)_2$•$6H_2O$ (1 mmol, 297 mg) in MeOH/benzene mixture (1:1, 100 ml) at 293 K under N_2 atmosphere. The green powder obtained was collected by filtration, washed with MeOH/benzene mixture (1:20), and dried under reduced pressure. (yield 93%) Elemental analysis calcd. for $C_{43}H_{25}N_{10}Zn$: C, 69.17; H, 3.37; N, 18.75, Found: C, 68.48; H, 3.58; N, 18.65. The compound accommodating other aromatic guests are synthesized by a method similar to 1⊃benzene with using other aromatic molecule as a solvent instead of benzene.

Crystal Structure Determination

Single crystal X-ray diffraction data collection was carried out on a Rigaku mercury diffractometer with a graphite monochromated MoKα radiation (γ = 0.71069 Å) and a CCD detector. The crystal structure was solved by a direct method (SHELX97) and refined by full-matrix least-squares refinement using the CRYSTALS computer program. The positions of non-hydrogen atoms were refined with anisotropic displacement factors, except for the guest molecules. The hydrogen atoms were positioned geometrically and refined using a riding model. The void space of all compounds along the c axis is occupied by the disordered guest molecules. The case of 1⊃1,2,4,5-tetrafluorobenzene, Due to the disorder of the guest molecules, U(eq) of the some atoms of guest molecules are underestimated. The other alerts derive from the disordered guest molecules which could not be completely decided the positions.

CCDC 753567 - 753570 contain the supplementary crystallographic data for this paper. These data can be obtained free of charge from The Cambridge Crystallographic Data Centre via www.ccdc.cam.ac.uk/data_request/cif.

Physical Measurements. The IR spectra were measured by an FTIR 6200 instrument (JASCO) with a infrared microscope (IRT-3000). The Raman study was carried out in back scattering geometry at the temperature between 300 K and 90 K with LabRAM HR-800 (HORIBA). The 785 nm line laser was used for excitation source. Scattered light was detected by a Jobin-Yvon triple monochromator T64000 and a Jobin-Yvon Spex Spectrum-one CCD (charge-coupled device) system.

Sorption Measurements. The adsorption isotherms of several gas molecules were measured with BELSORP-CRYO (O_2, N_2, Ar, NO) and BELSORP-MAX (CO_2, CO) volumetric adsorption equipment from Bel Japan and AUTOSORB-1 (C_2H_2) volumetric adsorption equipment from

Quantachrome instruments. The host sample was obtained by treating under reduced pressure (< 10^{-2} Pa) at 398K for more than 12 h. Each point in the adsorption isotherms has an error of ±0.25, which is caused by the resolution of the pressure gauge.

XRPD experiments. The XRPD patterns with good counting statistics were measured by the synchrotron radiation XRPD experiment with the large Debye-Scherrer camera and imaging plate as detectors on the BL02B2 beam line at the Super Photon Ring (SPring-8, Hyogo, Japan) (Proposal Nos. 2008B1263). The gas-vapor pressure control system was used to adjust the pressure of adsorbate. XRPD of **1** was measured under several atmospheres. The X-ray wavelength is 0.80235 Å (no guest), and 0.80130 Å (O_2, NO). Lattice parameters of each state by Le Bail method are as follows: (no guest) orthorhombic crystal system *P*222, a = 22.015(2) Å, b = 12.569(1) Å, c = 15.815(2) Å, V = 4376.0(8) Å^3, R_{wp} = 0.01861. (O_2 adsorbed) orthorhombic crystal system *Pccm*, a = 11.424(1) Å, b = 12.252(2) Å, c = 14.809(2) Å, V = 2072.8(5) Å^3, R_{wp} = 0.03097. (NO adsorbed) orthorhombic crystal system *Pccm*, a = 11.402(1) Å, b = 12.348(2) Å, c = 14.809(2) Å, V = 2072.8(5) Å^3, R_{wp} = 0.02136.

Table 2. Crystal data and Structure Solution and Refinement of **1**⊃anisole.

Empirical Formula	$C_{41}H_{16}N_{10}OZn$
Formula Weight	730.02
Crystal System	orthorhombic
Lattice Parameters	a = 11.419(4) Å
	b = 12.670(5) Å
	c = 14.752(5) Å
	V = 2134.3(13) $Å^3$
Space Group	Pccm (#49)
Z value	2
D_{calc}	1.136 g/cm^3
F_{000}	740.00
μ (MoKα)	6.158 cm^{-1}
Radiation	MoKα (λ = 0.71070 Å)
	graphite monochromated
$2\theta_{max}$	55.0^o
No. of Reflections Measured	Total: 18071
	Unique: 2548 (R_{int} = 0.022)
Completeness	99.8%
Refinement	Full-matrix least-squares on F
$2\theta_{max}$ cutoff	55.0^o
Anomalous Dispersion	All non-hydrogen atoms
No. Observations (I>2.50σ(I))	2130
No. Variables	156
Reflection/Parameter Ratio	13.65
Residuals: R1 (I>2.00σ(I))	0.0817
Residuals: wR2 (All reflections)	0.0955
Goodness of Fit Indicator	0.917
Max Shift/Error in Final Cycle	0.000
Maximum peak in Final Diff. Map	1.67 $e^-/Å^3$
Minimum peak in Final Diff. Map	−0.75 $e^-/Å^3$

Table 3. Crystal data and Structure Solution and Refinement of **1**⊃benzonitrile.

Empirical Formula	$C_{41}H_{20}N_{11}Zn$
Formula Weight	732.06
Crystal System	orthorhombic
Lattice Parameters	a = 11.4341(13) Å
	b = 12.5791(14) Å
	c = 14.7759(14) Å
	V = 2125.2(4) $Å^3$
Space Group	Pccm (#49)
Z value	2
D_{calc}	1.144 g/cm^3
F_{000}	746.00
μ (MoKα)	6.175 cm^{-1}
Radiation	MoKα (λ = 0.71070 Å)
	graphite monochromated
$2\theta_{max}$	55.0^o
No. of Reflections Measured	Total: 18032
	Unique: 2527 (R_{int} = 0.020)
Completeness	99.8%
Refinement	Full-matrix least-squares on F
$2\theta_{max}$ cutoff	55.0^o
Anomalous Dispersion	All non-hydrogen atoms
No. Observations (I>2.00σ(I))	2223
No. Variables	148
Reflection/Parameter Ratio	15.02
Residuals: R1 (I>2.00σ(I))	0.0711
Residuals: wR2 (I>2.00σ(I))	0.0814
Goodness of Fit Indicator	0.852
Max Shift/Error in Final Cycle	0.000
Maximum peak in Final Diff. Map	1.66 $e^-/Å^3$
Minimum peak in Final Diff. Map	−0.37 $e^-/Å^3$

Table 4. Crystal data and Structure Solution and Refinement of **1**⊃*p*-xylene.

Empirical Formula	$C_{42}H_{26}N_{10}Zn$
Formula Weight	736.11
Crystal System	orthorhombic
Lattice Parameters	a = 11.3749(17) Å
	b = 12.7239(19) Å
	c = 14.801(2) Å
	V = 2142.2(6) Å^3
Space Group	Pccm (#49)
Z value	2
D_{calc}	1.142 g/cm^3
F_{000}	756.00
μ (MoKα)	6.122 cm^{-1}
Radiation	MoKα (λ = 0.71070 Å)
	graphite monochromated
$2\theta_{max}$	55.0°
No. of Reflections Measured	Total: 17921
	Unique: 2561 (R_{int} = 0.052)
Completeness	99.8%
Refinement	Full-matrix least-squares on F
$2\theta_{max}$ cutoff	55.0°
Anomalous Dispersion	All non-hydrogen atoms
No. Observations (I>3.00σ(I))	1587
No. Variables	146
Reflection/Parameter Ratio	10.87
Residuals: R1 (I>3.00σ(I))	0.0672
Residuals: Rw (I>3.00σ(I))	0.0678
Goodness of Fit Indicator	0.894
Max Shift/Error in Final Cycle	0.000
Maximum peak in Final Diff. Map	2.04 e$^-$/Å^3
Minimum peak in Final Diff. Map	−0.40 e$^-$/Å^3

Table 5. Crystal data and Structure Solution and Refinement of **1**⊃ 1,2,4,5-Tetrafluorobenzene.

Empirical Formula	$C_{46}H_{16}N_{10}F_8Zn$
Formula Weight	926.07
Crystal System	orthorhombic
Lattice Parameters	a = 22.857(6) Å
	b = 12.614(3) Å
	c = 14.604(4) Å
	V = 4211(2) $Å^3$
Space Group	Pcca (#54)
Z value	4
D_{calc}	1.461 g/cm^3
F_{000}	1856.00
μ (MoKα)	6.658 cm^{-1}
Radiation	MoKα (λ = 0.71070 Å)
	graphite monochromated
$2\theta_{max}$	55.0^o
No. of Reflections Measured	Total: 26904
	Unique: 4648 (R_{int} = 0.019)
Completeness	99.8%
Refinement	Full-matrix least-squares on F
$2\theta_{max}$ cutoff	55.0^o
Anomalous Dispersion	All non-hydrogen atoms
No. Observations (I>3.00σ(I))	3526
No. Variables	327
Reflection/Parameter Ratio	10.78
Residuals: R1 (I>3.00σ(I))	0.0678
Residuals: Rw (I>3.00σ(I))	0.0832
Goodness of Fit Indicator	0.927
Max Shift/Error in Final Cycle	0.000
Maximum peak in Final Diff. Map	1.92 $e^-/Å^3$
Minimum peak in Final Diff. Map	−0.79 $e^-/Å^3$

References

[1] Batten, S. R.; Robson, R., *Angew. Chem. Int. Ed.* **1998,** *37*, 1460-1494.

[2] Blake, A. J.; Champness, N. R.; Hubberstey, P.; Li, W. S.; Withersby, M. A.; Schroder, M., *Coord. Chem. Rev.* **1999,** *183*, 117-138.

[3] Eddaoudi, M.; Moler, D. B.; Li, H. L.; Chen, B. L.; Reineke, T. M.; O'Keeffe, M.; Yaghi, O. M., *Acc. Chem. Res.* **2001,** *34*, 319-330.

[4] Kitagawa, S.; Kitaura, R.; Noro, S., *Angew. Chem. Int. Ed.* **2004,** *43*, 2334-2375.

[5] Fletcher, A. J.; Thomas, K. M.; Rosseinsky, M. J., *J. Solid State Chem.* **2005,** *178*, 2491-2510.

[6] Lee, J.; Farha, O. K.; Roberts, J.; Scheidt, K. A.; Nguyen, S. T.; Hupp, J. T., *Chem. Soc. Rev.* **2009,** *38*, 1450-1459.

[7] Ferey, G.; Serre, C., *Chem. Soc. Rev.* **2009,** *38*, 1380-1399.

[8] Murray, L. J.; Dinca, M.; Long, J. R., *Chem. Soc. Rev.* **2009,** *38*, 1294-1314.

[9] Li, J. R.; Kuppler, R. J.; Zhou, H. C., *Chem. Soc. Rev.* **2009,** *38*, 1477-1504.

[10] Matsuda, R.; Kitaura, R.; Kitagawa, S.; Kubota, Y.; Belosludov, R. V.; Kobayashi, T. C.; Sakamoto, H.; Chiba, T.; Takata, M.; Kawazoe, Y.; Mita, Y., *Nature* **2005,** *436*, 238-241.

[11] Mulfort, K. L.; Hupp, J. T., *J. Am. Chem. Soc.* **2007,** *129*, 9604-9605.

[12] Zhang, J. P.; Kitagawa, S., *J. Am. Chem. Soc.* **2008,** *130*, 907-917.

[13] Tanabe, K. K.; Wang, Z. Q.; Cohen, S. M., *J. Am. Chem. Soc.* **2008,** *130*, 8508-8517.

[14] Li, Q. W.; Zhang, W. Y.; Miljanic, O. S.; Sue, C. H.; Zhao, Y. L.; Liu, L. H.; Knobler, C. B.; Stoddart, J. F.; Yaghi, O. M., *Science* **2009,** *325*, 855-859.

[15] Horike, S.; Shimomura, S.; Kitagawa, S., *Nature Chem.* **2009,** *1*, 695-704.

[16] Kitaura, R.; Seki, K.; Akiyama, G.; Kitagawa, S., *Angew. Chem. Int. Ed.* **2003,** *42*, 428-+.

[17] Tanaka, D.; Nakagawa, K.; Higuchi, M.; Horike, S.; Kubota, Y.; Kobayashi, L. C.; Takata, M.; Kitagawa, S., *Angew. Chem. Int. Ed.* **2008,** *47*, 3914-3918.

[18] Hamon, L.; Llewellyn, P. L.; Devic, T.; Ghoufi, A.; Clet, G.; Guillerm, V.; Pirngruber, G. D.; Maurin, G.; Serre, C.; Driver, G.; van Beek, W.; Jolimaitre, E.; Vimont, A.; Daturi, M.; Ferey, G., *J. Am. Chem. Soc.* **2009,** *131*, 17490-17499.

[19] Kim, H.; Samsonenko, D. G.; Yoon, M.; Yoon, J. W.; Hwang, Y. K.; Chang, J. S.; Kim, K., *Chem. Commun.* **2008**, 4697-4699.

[20] Koros, W. J.; Fleming, G. K., *J. Membr. Sci.* **1993,** *83*, 1-80.

[21] Stern, S. A., *J. Membr. Sci.* **1994,** *94*, 1-65.

[22] Reid, C. R.; Thomas, K. M., *Langmuir* **1999,** *15*, 3206-3218.

[23] Bae, Y. S.; Lee, C. H., *Carbon* **2005,** *43*, 95-107.

[24] Yoon, J. W.; Jhung, S. H.; Hwang, Y. K.; Humphrey, S. M.; Wood, P. T.; Chang, J. S., *Adv. Mater.* **2007,** *19*, 1830-1834.

[25] Bastin, L.; Barcia, P. S.; Hurtado, E. J.; Silva, J. A. C.; Rodrigues, A. E.; Chen, B., *J. Phys. Chem. C* **2008,** *112*, 1575-1581.

[26] Cheon, Y. E.; Park, J.; Suh, M. P., *Chem. Commun.* **2009**, 5436-5438.

[27] Xiao, B.; Byrne, P. J.; Wheatley, P. S.; Wragg, D. S.; Zhao, X. B.; Fletcher, A. J.; Thomas, K. M.; Peters, L.; Evans, J. S. O.; Warren, J. E.; Zhou, W. Z.; Morris, R. E., *Nature Chem.* **2009,** *1*, 289-294.

[28] Vaidhyanathan, R.; Iremonger, S. S.; Dawson, K. W.; Shimizu, G. K. H., *Chem. Commun.* **2009**, 5230-5232.

[29] Golden, T. C.; Sircar, S., *J. Colloid Interface Sci.* **1994,** *162*, 182-188.

[30] Shimomura, S.; Horike, S.; Matsuda, R.; Kitagawa, S., *J. Am. Chem. Soc.* **2007,** *129*, 10990-10991.

[31] Meyer, E. A.; Castellano, R. K.; Diederich, F., *Angew. Chem. Int. Ed.* **2003,** *42*, 1210-1250.

[32] Zhao, H.; Heintz, R. A.; Ouyang, X.; Dunbar, K. R.; Campana, C. F.; Rogers, R. D., *Chem. Mater.* **1999,** *11*, 736-746.

[33] Ballester, L.; Gutierrez, A.; Perpinan, M. F.; Azcondo, M. T.; Sanchez, A. E., *Synth. Met.* **2001,** *120*, 965-966.

[34] Khatkale, M. S.; Devlin, J. P., *J. Chem. Phys.* **1979,** *70*, 1851-1859.

[35] Kaim, W.; Moscherosch, M., *Coord. Chem. Rev.* **1994,** *129*, 157-193.

[36] Ballester, L.; Gutierrez, A.; Perpinan, M. F.; Azcondo, M. T., *Coord. Chem. Rev.* **1999,** *192*, 447-470.

[37] Shamir, J.; Binenboy, J.; Claassen, H. H., *J. Am. Chem. Soc.* **1968,** *90*, 6223-6224.

[38] Smardzew, R. R.; Andrews, L., *J. Chem. Phys.* **1972,** *57*, 1327-1333.

[39] Bier, K. D.; Jodl, H. J., *J. Chem. Phys.* **1984,** *81*, 1192-1197.

[40] Vogel, K. M.; Kozlowski, P. M.; Zgierski, M. Z.; Spiro, T. G., *J. Am. Chem. Soc.* **1999,** *121*, 9915-9921.

[41] Imai, J.; Souma, M.; Ozeki, S.; Suzuki, T.; Kaneko, K., *J. Phys. Chem.* **1991,** *95*, 9955-9960.

[42] Honda, H.; Yang, C. M.; Kanoh, H.; Tanaka, H.; Ohba, T.; Hattori, Y.; Utsumi, S.; Kaneko, K., *J. Phys. Chem. C* **2007,** *111*, 3220-3223.

[43] Creighton, J. A.; Lippincott, E. R., *J. Chem. Phys.* **1964,** *40*, 1779-1780.

[44] Gao, Z. X.; Kim, H. S.; Sun, Q.; Stair, P. C.; Sachtler, W. M. H., *J. Phys. Chem. B* **2001,** *105*, 6186-6190.

[45] Fujita, S.; Suzuki, K.; Ohkawa, M.; Mori, T.; Iida, Y.; Miwa, Y.; Masuda, H.; Shimada, S., *Chem. Mater.* **2003,** *15*, 255-263.

Chapter 5

Flexibility of porous coordination polymers strongly linked to selective sorption mechanism

Abstract

Comparison of the properties of two porous coordination polymers consisting of the same components except for the metal cations and forming identical structures shows that flexible natures of them have a critical role in the selective sorption and separation mechanism.

Introduction

Soft porous crystals have received increasing attention as new functional porous systems because of their unique molecular accommodation characteristics.[1] Dynamic guest sorption by a highly ordered framework provides unique porous properties, which are not seen in other porous materials, and has created a platform for synthetic approaches to new functional materials. In this field, porous coordination polymers (PCPs) (or metal–organic frameworks) are among the most evolving classes of materials in recent decades,[2-5] and there has been much research published on their potential applications in gas storage,[6-19] separation,[20-26] sensing,[27-33] and catalysis.[34-39]

In contrast to robust porous frameworks, guest sorption processes with a structural change have a highly complex mechanism, in which guest accommodation and structural transformation proceed simultaneously. This means that flexibility and transformability of the framework have significant influences on the sorption properties, and for that reason, this may lead to an unconventional methodology to control the porous properties. The sorption properties of PCPs could be changed without tuning the pore sizes and/or pore surface properties, even if they have identical structures. Therefore, we focus on coordination bonds in the framework, which mainly affect the dynamic phenomena of PCPs. Two PCPs consisting of the same components except for the metal cations and forming identical structures were prepared to compare their structural flexibilities and guest sorption properties.

Results and discussion

The PCPs $[M(TCNQ\text{-}TCNQ)bpy]_n$ (M = Mn, Zn) [TCNQ = 7,7,8,8-tetracyano-*p*-quinodimethane, bpy = 4,4′-bipyridyl] were obtained from methanol and benzene solutions of the metal nitrate, LiTCNQ, and bpy at room temperature.[22] In this solution, TCNQ radical anions spontaneously form a σ-bond by using their unpaired electrons, and coalesce into a TCNQ dimer in the complexation process. These components assemble to produce a three-dimensional open framework with undulating channels filled with benzene molecules. They have virtually identical structures, but the bond lengths between metal and organic ligands are slightly different. In contrast to the isotropic coordination geometry of the Zn complex, the presence of tetragonal distortion, with the Mn–N(bpy) axial bonds being longer than the Mn–N(TCNQ) equatorial bonds, can be observed in the Mn complex (Figures 1(a) and (b)). In this connection, the pore diameter of undulating channels is slightly different between them. It is interesting how these subtle differences in coordination bond and porous structure affect the guest sorption capability of the complexes.

The as-synthesized crystals of the Zn complex transform to a guest-free crystal phase in the guest removal process, and this transformation is reversible. In contrast, the crystals of the Mn complex show a significant decrease in crystallinity in the guest removal process and transform to an amorphous-like phase. This transformation is also reversible and both of these complexes are classified as third-generation compounds[6] (Figures 1(c) and (d)). By using these flexible PCPs with different transformability, we compared their sorption properties.

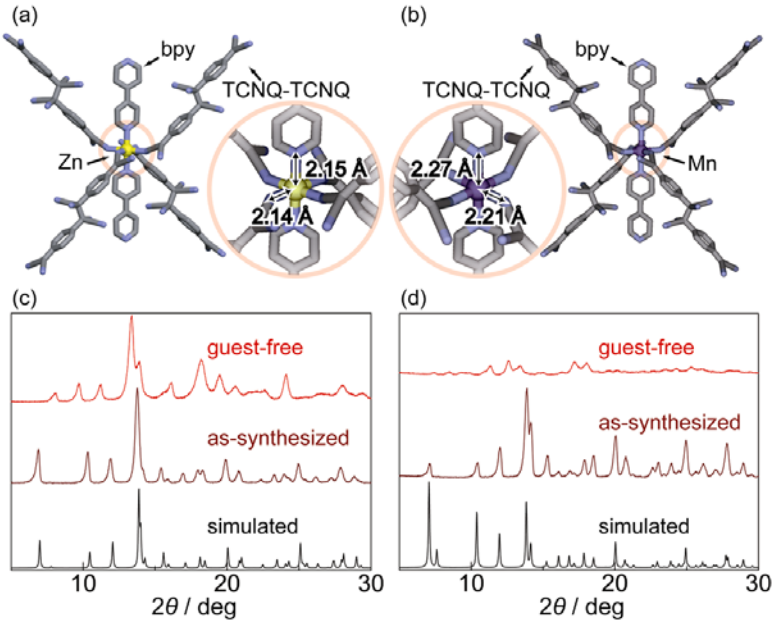

Figure 1. Crystal structures of (a) Zn complex and (b) Mn complex showing the coordination geometries of as-synthesized phases. XRPD patterns of (c) Zn complex and (d) Mn complex.

Figures 2(a) and (c) show the benzene and cyclohexane sorption isotherms of the Zn and Mn complexes. The Zn complex shows apparent selective sorption properties; no uptake of cyclohexane and a gate-open-type sorption behavior for benzene were observed. A previous study showed that the Zn complex has a good affinity for benzene based on H–π interactions between TCNQ dimers and benzene molecules, and this should be true for the isomorphic Mn complex. However, although a similar tendency is observed in the affinity of the Mn complex for benzene, there are some notable differences in the details of the sorption behavior. Benzene was adsorbed in the low relative pressure region ($P < 0.1$) and a Type I adsorption profile without a gate-opening phenomenon was obtained.[40] In addition, cyclohexane was gradually adsorbed as the pressure increased and a large hysteretic desorption curve was observed. We measured the X-ray powder diffraction (XRPD) patterns of these complexes before and after the cyclohexane sorption measurement. In contrast to no change in the Zn complex, several broad peaks appeared in the pattern of the Mn complex at the simulated peak positions of the as-synthesized complex after the sorption measurement. This result indicates that the Mn complex transforms from an amorphous-like phase to a roughly ordered phase that has a similar structure to the as-synthesized compound in the accommodation process of cyclohexane. Their gas sorption isotherms are shown in Figures 2(b) and (d). The selective gas sorption property of the Zn complex is very specific; the Zn complex shows a high uptake with gate-open-type sorption behavior only in the case of O_2. In contrast, the Mn complex has no selectivity and shows uptake for any gas molecules in the low-pressure region, despite some small differences such as adsorption steps. In addition, it turns out that the Mn complex adsorbed these gas molecules through the gate-opening process, as seen by examining the sorption isotherms in the low-pressure region (Figure 3). This means that the Mn complex also transforms from a nonporous structure to a porous structure accompanying guest accommodation, as was observed with the Zn complex.

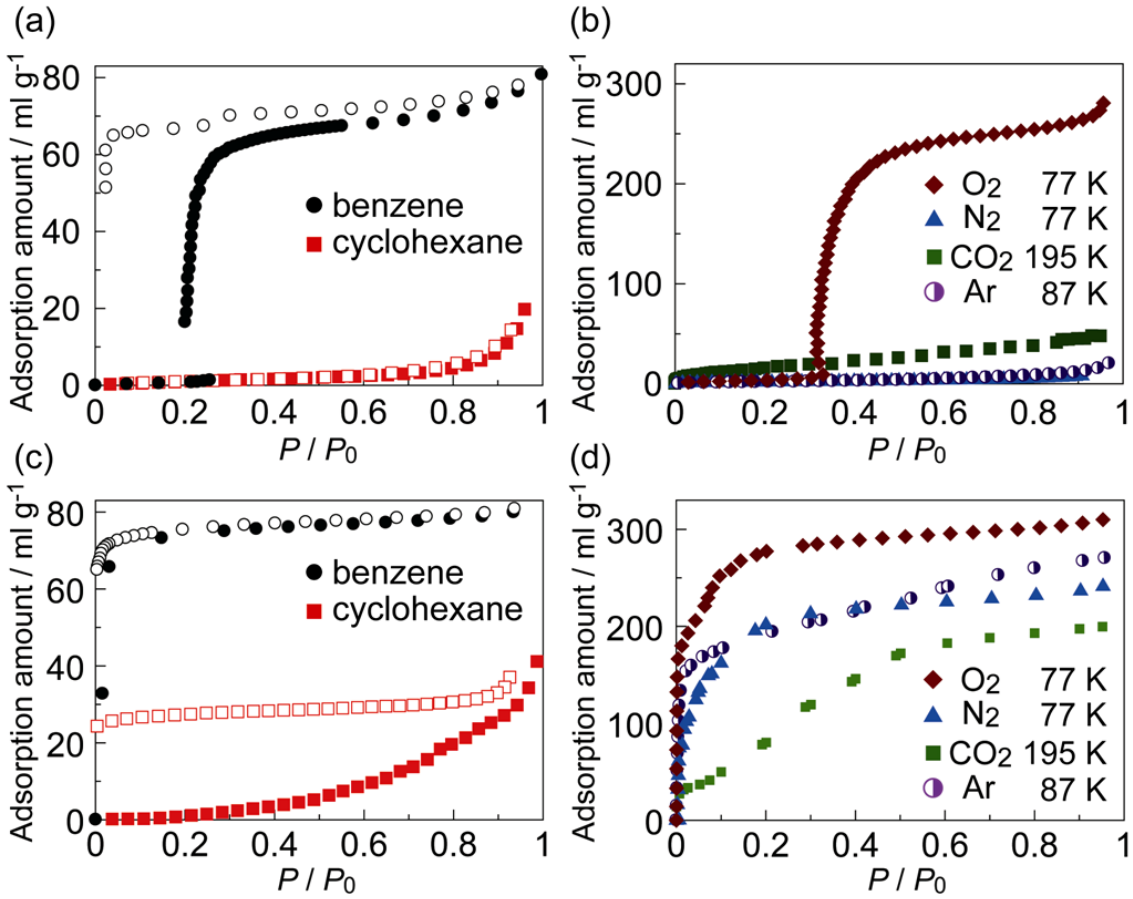

Figure 2. Sorption isotherms of several molecules for (a)(b) Zn complex and (c)(d) Mn complex. The sorption measurements of benzene and cyclohexane were conducted at 298 K. The filled and open symbols show the adsorption and desorption profiles, respectively.

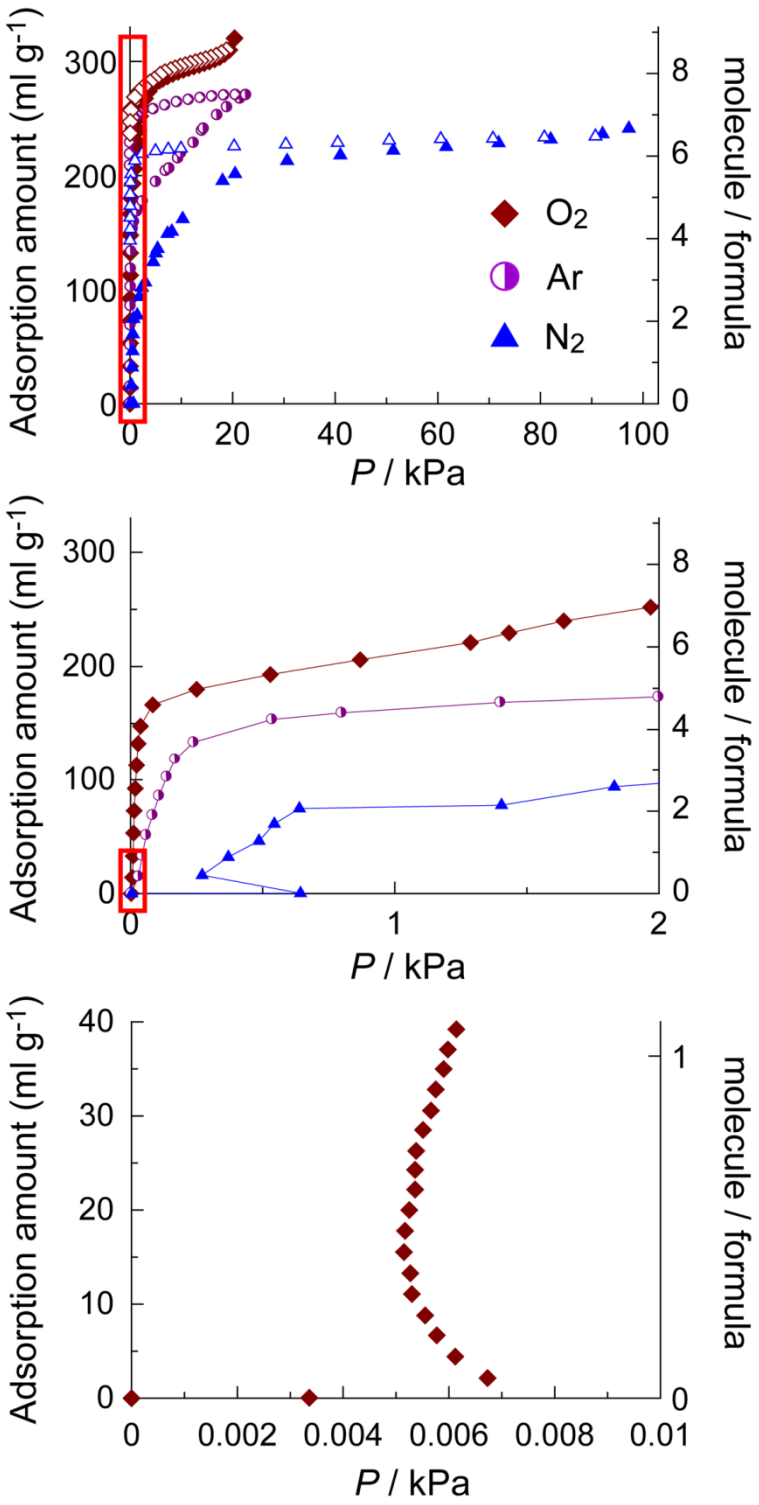

Figure 3. The details of the gas sorption isotherms of [Mn(TCNQ-TCNQ)bpy] in the low-pressure region.

Based on these results, the distinct differences in sorption properties between Zn and Mn complexes should be explainable by reference to their structural transformability; the structural change of the Mn complex can be induced easier than that of the Zn complex. To determine the reason for this phenomenon, we checked the heat balance in the guest desorption processes by using differential scanning calorimetry (DSC). Figure 4 shows the DSC curves observed for the first heating processes on the as-synthesized Mn and Zn complexes. The DSC scan for the Mn complex presented a broad endothermic peak at 87.2 °C for the release of benzene. On the other hand, in the case of the Zn complex, not only a broad endothermic peak at about 110 °C for the guest release but also an exothermic peak at 98.1 °C overlapping each other were observed. This exothermic peak should be derived from the structural transformation accompanying with the guest removal. The differences in the DSC curves between these complexes indicate that an energy gap between the guest-accommodating phase and the guest-free phase of Zn complex is larger than that of Mn complex. Considering the almost same as-synthesized structures of them, stabilities of the guest-free phases are critical elements of the thermal behaviors. The Zn complex is more stabilized thermodynamically through the structural transformation from the guest-accommodating phase to the guest-free phase with long-range structural order than is the Mn complex, whose guest-free phase has no ordered structure. By the cooperative transformation with maintenance of the ordered structure, the Zn complex produces a high energy barrier for guest sorption and only those guest molecules that can supply the adsorption energy produced by a good interaction with the framework, such as charge transfer or CH–π interactions, are able to overcome the energy barrier, induce the structural transformation and be accommodated. However, these results suggest that transformability of PCPs is one of the important factors for selective sorption properties.

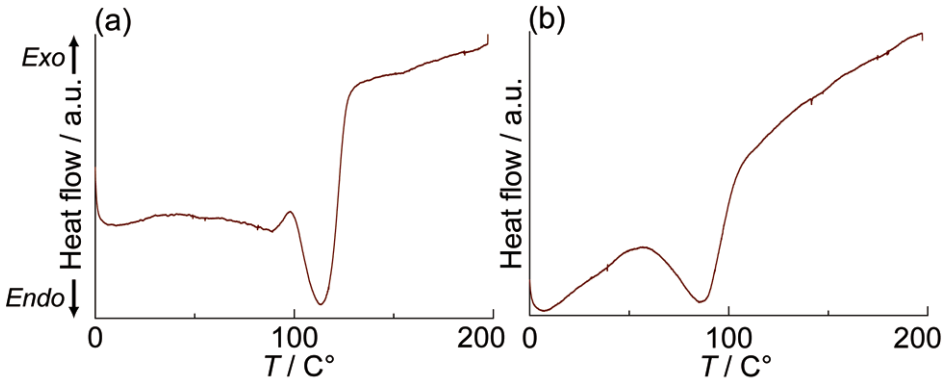

Figure 4. DSC curves observed for the first heating process on the as-synthesized sample of (a) Zn complex and (b) Mn complex at a scan rate of 2 K min^{-1}.

We also compared their separation properties by using a benzene/cyclohexane mixture (Figure 5). Because of their chemical similarities and industrial importance, their separation is important.[41]

Their guest-free phases were exposed to the vapor of mixtures at various mixture ratios at room temperature for 24 h. The ratio of benzene to cyclohexane in the complexes was determined by ^{1}H NMR spectroscopy. The Zn complex showed a quite high separation ability for benzene at all mixture ratios. Over 90% of the adsorbed guest molecules were benzene, even when the mixture ratio of benzene was a mere 0.1%. These complexes can be reused for separation after a desolvation treatment. The Mn complex also showed good separation ability for benzene, although the ability pales compared with that of the Zn complex. The results provide interesting insights into porous systems for the design of separation applications. Introducing a good affinity for the target molecule into the framework, in this case CH–π interaction for the benzene molecule, is an effective approach for a good separation ability for the Mn complex, but not enough to gain a high selectivity. A blocking effect or a gate effect to prevent the accommodation of the other molecules, found in the sorption isotherms of the Zn complex, is the important factor to achieve highly selective separation ability. Structural flexibility, which can be configured by designability of PCPs, is useful for introducing these effects into the sorption process.

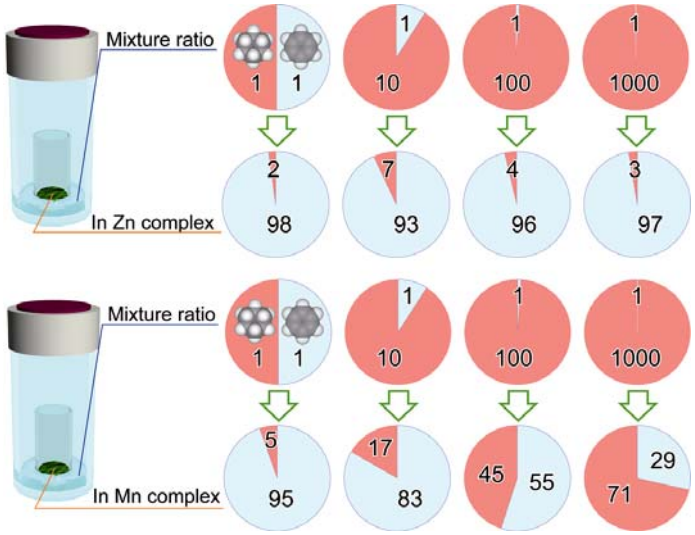

Figure 5. Separation properties of (a) Zn complex and (b) Mn complex. The red parts and the blue parts of circle graphs show the rates of cyclohexane and benzene, respectively.

Conclusion

In conclusion, two PCPs consisting of the same components except for the metal cations and forming identical structures have been prepared to compare their selective sorption and separation properties. The structural changes accompanying guest removal vary widely and the differences strongly affect the selective sorption behavior. In this system, the high selective guest accommodation of the Zn complex is based on the crystal-to-crystal transformation with a large energy gap. The results indicate that the flexibility of the framework is one of the important factors determining the porous properties. Tuning the flexibility of PCPs based on designability of the frameworks will offer a new approach to control sorption behavior and a new function based on the dynamic properties of PCPs.

Experimental Section

Synthesis of [Mn(TCNQ-TCNQ)bpy]•benzene.

Single crystal of **1** was prepared by the following procedure. All procedure were carried out under N_2 atmosphere using Schlenk technique. A solution of LiTCNQ (0.1 mmol, 21 mg) and bpy (0.1 mmol, 16 mg) in MeOH/benzene mixture (20 ml) was carefully layered on the top of a solution of $Mn(NO_3)_2 \cdot 6H_2O$ (0.1 mmol, 29 mg) in MeOH/benzene mixture (20 ml). Green crystals began to form in a few days. The bulk product was obtained by the following procedure. Slow addition of a solution of LiTCNQ (2 mmol, 422 mg) and bpy (1 mmol, 156 mg) in MeOH/benzene mixture (1:1, 100 ml) to a solution of $Mn(NO_3)_2 \bullet 6H_2O$ (1 mmol, 284 mg) in MeOH/benzene mixture (1:1, 100 ml) at 293 K under N_2 atmosphere. The green powder obtained was collected by filtration, washed with MeOH/benzene mixture (1:20), and dried under reduced pressure. Elemental analysis calcd. for C34H16N10Mn: C, 65.91; H, 2.60; N, 22.61, Found: C, 64.74; H, 2.65; N, 21.70.

Crystal Structure Determination.

Single crystal X-ray diffraction data collection was carried out on a Rigaku mercury diffractometer with a graphite monochromated MoKα radiation (γ = 0.71069 Å) and a CCD detector. The crystal structure was solved by a direct method (SIR2002) and refined by full-matrix least-squares refinement using the CRYSTALS computer program. The positions of non-hydrogen atoms were refined with anisotropic displacement factors. The hydrogen atoms were positioned geometrically and refined using a riding model. The void space of all compounds along the *c* axis is occupied by the disordered guest molecules.

Physical Measurements.

The elemental analysis was carried out on a Flash EA 1112 series, Thermo Finnigan instrument. X-ray powder diffraction (XRPD) data were collected on a Rigaku RINT-2200HF (Ultima) diffractometer with Cu-Kα radiation. The adsorption isotherms of gas molecules (O_2, CO_2, N_2, Ar), and solvent molecules (benzene, cyclohexane) were measured in the gaseous state by using BELSORP-MAX and BELSORP18-Plus volumetric adsorption equipment from BEL Japan, Inc. Different scanning calorimetric measurements were measured on a DSC 6220 (Seiko Instruments Inc.) under N_2 atmosphere, where the sample was placed between an aluminum DSC pan and lid.

Table 1. Crystal data and Structure Solution and Refinement of [Mn(TCNQ-TCNQ)bpy]• benzene.

Empirical Formula	C40H22N10Mn
Formula Weight	697.62
Crystal System	orthorhombic
Lattice Parameters	a = 11.616(3) Å
b = 12.503(3) Å	
c = 14.891(4) Å	
V = 2162.6(9) Å3	
Space Group	Pccm (#49)
Z value	2
Dcalc	1.071 g/cm^3
F000	714.00
μ (MoKα)	3.412 cm^{-1}
Radiation	MoKα (λ = 0.71070 Å)
graphite monochromated	
2θmax	55º
No. of Reflections Measured	Total: 16064
Unique: 2584 (Rint = 0.052)	
Completeness	99.8%
Refinement	Full-matrix least-squares on F
2θmax cutoff	55.0º
Anomalous Dispersion	All non-hydrogen atoms
No. Observations (I>1.80σ(I))	1442
No. Variables	138
Reflection/Parameter Ratio	10.73
Residuals: R1 (I>1.80σ(I))	0.0848
Residuals: wR2 (I>1.80σ(I))	0.0945
Goodness of Fit Indicator	0.974
Max Shift/Error in Final Cycle	0.000
Maximum peak in Final Diff. Map	1.34 e-/Å^3
Minimum peak in Final Diff. Map	-0.54 e-/Å^3

References

[1] Horike, S.; Shimomura, S.; Kitagawa, S., *Nature Chem.* **2009,** *1*, 695.

[2] Batten, S. R.; Robson, R., *Angew. Chem. Int. Ed.* **1998,** *37*, 1460.

[3] Kitagawa, S.; Kitaura, R.; Noro, S., *Angew. Chem. Int. Ed.* **2004,** *43*, 2334.

[4] Ferey, G.; Serre, C., *Chem. Soc. Rev.* **2009,** *38*, 1380.

[5] Phan, A.; Doonan, C. J.; Uribe-Romo, F. J.; Knobler, C. B.; O'Keeffe, M.; Yaghi, O. M., *Acc. Chem. Res.* **2010,** *43*, 58.

[6] Kitagawa, S.; Kondo, M., *Bull. Chem. Soc. Jpn.* **1998,** *71*, 1739.

[7] Li, H.; Eddaoudi, M.; Groy, T. L.; Yaghi, O. M., *J. Am. Chem. Soc.* **1998,** *120*, 8571.

[8] Llewellyn, P. L.; Bourrelly, S.; Serre, C.; Filinchuk, Y.; Ferey, G., *Angew. Chem. Int. Ed.* **2006,** *45*, 7751.

[9] Mulfort, K. L.; Hupp, J. T., *J. Am. Chem. Soc.* **2007,** *129*, 9604.

[10] Ma, S. Q.; Sun, D. F.; Simmons, J. M.; Collier, C. D.; Yuan, D. Q.; Zhou, H. C., *J. Am. Chem. Soc.* **2008,** *130*, 1012.

[11] Choi, H. J.; Dinca, M.; Long, J. R., *J. Am. Chem. Soc.* **2008,** *130*, 7848.

[12] Dietzel, P. D. C.; Johnsen, R. E.; Fjellvag, H.; Bordiga, S.; Groppo, E.; Chavan, S.; Blom, R., *Chem. Commun.* **2008**, 5125.

[13] Zhang, J. P.; Chen, X. M., *J. Am. Chem. Soc.* **2008,** *130*, 6010.

[14] Wang, Z. Q.; Cohen, S. M., *J. Am. Chem. Soc.* **2009,** *131*, 16675.

[15] Klein, N.; Senkovska, I.; Gedrich, K.; Stoeck, U.; Henschel, A.; Mueller, U.; Kaskel, S., *Angew. Chem. Int. Ed.* **2009,** *48*, 9954.

[16] Cheon, Y. E.; Park, J.; Suh, M. P., *Chem. Commun.* **2009**, 5436.

[17] Ahnfeldt, T.; Guillou, N.; Gunzelmann, D.; Margiolaki, I.; Loiseau, T.; Ferey, G.; Senker, J.; Stock, N., *Angew. Chem. Int. Ed.* **2009,** *48*, 5163.

[18] Yang, S. H.; Lin, X.; Blake, A. J.; Walker, G. S.; Hubberstey, P.; Champness, N. R.; Schroder, M., *Nature Chem.* **2009,** *1*, 487.

[19] Deng, H. X.; Doonan, C. J.; Furukawa, H.; Ferreira, R. B.; Towne, J.; Knobler, C. B.; Wang, B.; Yaghi, O. M., *Science* **2010,** *327*, 846.

[20] Chen, B. L.; Liang, C. D.; Yang, J.; Contreras, D. S.; Clancy, Y. L.; Lobkovsky, E. B.; Yaghi, O. M.; Dai, S., *Angew. Chem. Int. Ed.* **2006,** *45*, 1390.

(21) Alaerts, L.; Kirschhock, C. E. A.; Maes, M.; van der Veen, M. A.; Finsy, V.; Depla, A.; Martens, J. A.; Baron, G. V.; Jacobs, P. A.; Denayer, J. E. M.; De Vos, D. E., *Angew. Chem. Int. Ed.* **2007,** *46*, 4293.

[22] Shimomura, S.; Horike, S.; Matsuda, R.; Kitagawa, S., *J. Am. Chem. Soc.* **2007,** *129*, 10990.

[23] Yoon, J. W.; Jhung, S. H.; Hwang, Y. K.; Humphrey, S. M.; Wood, P. T.; Chang, J. S., *Adv. Mater.* **2007,** *19*, 1830.

[24] Couck, S.; Denayer, J. F. M.; Baron, G. V.; Remy, T.; Gascon, J.; Kapteijn, F., *J. Am. Chem. Soc.* **2009,** *131*, 6326.

[25] Li, Y. S.; Liang, F. Y.; Bux, H.; Feldhoff, A.; Yang, W. S.; Caro, J., *Angew. Chem. Int. Ed.* **2010,** *49*, 548.

[26] Venna, S. R.; Carreon, M. A., *J. Am. Chem. Soc.* **2010,** *132*, 76.

[27] McManus, G. J.; Perry, J. J.; Perry, M.; Wagner, B. D.; Zaworotko, M. J., *J. Am. Chem. Soc.* **2007,** *129*, 9094.

[28] Chen, B. L.; Yang, Y.; Zapata, F.; Lin, G. N.; Qian, G. D.; Lobkovsky, E. B., *Adv. Mater.* **2007,** *19*, 1693.

[29] Ohba, M.; Yoneda, K.; Agusti, G.; Munoz, M. C.; Gaspar, A. B.; Real, J. A.; Yamasaki, M.; Ando, H.; Nakao, Y.; Sakaki, S.; Kitagawa, S., *Angew. Chem. Int. Ed.* **2009,** *48*, 4767.

[30] Harbuzaru, B. V.; Corma, A.; Rey, F.; Jorda, J. L.; Ananias, D.; Carlos, L. D.; Rocha, J., *Angew. Chem. Int. Ed.* **2009,** *48*, 6476.

[31] Xiao, B.; Byrne, P. J.; Wheatley, P. S.; Wragg, D. S.; Zhao, X. B.; Fletcher, A. J.; Thomas, K. M.; Peters, L.; Evans, J. S. O.; Warren, J. E.; Zhou, W. Z.; Morris, R. E., *Nature Chem.* **2009,** *1*, 289.

[32] Southon, P. D.; Liu, L.; Fellows, E. A.; Price, D. J.; Halder, G. J.; Chapman, K. W.; Moubaraki, B.; Murray, K. S.; Letard, J. F.; Kepert, C. J., *J. Am. Chem. Soc.* **2009,** *131*, 10998.

[33] Xie, Z. G.; Ma, L. Q.; deKrafft, K. E.; Jin, A.; Lin, W. B., *J. Am. Chem. Soc.* **2010,** *132*, 922.

[34] Cho, S. H.; Ma, B. Q.; Nguyen, S. T.; Hupp, J. T.; Albrecht-Schmitt, T. E., *Chem. Commun.* **2006**, 2563.

[35] Wu, C. D.; Lin, W. B., *Angew. Chem. Int. Ed.* **2007,** *46*, 1075.

[36] Muller, M.; Hermes, S.; Kaehler, K.; van den Berg, M. W. E.; Muhler, M.; Fischer, R. A., *Chem. Mater.* **2008,** *20*, 4576.

[37] Alkordi, M. H.; Liu, Y. L.; Larsen, R. W.; Eubank, J. F.; Eddaoudi, M., *J. Am. Chem. Soc.* **2008,** *130*, 12639.

[38] Sun, C. Y.; Liu, S. X.; Liang, D. D.; Shao, K. Z.; Ren, Y. H.; Su, Z. M., *J. Am. Chem. Soc.* **2009,** *131*, 1883.

[39] Tonigold, M.; Lu, Y.; Bredenkotter, B.; Rieger, B.; Bahnmuller, S.; Hitzbleck, J.; Langstein, G.; Volkmer, D., *Angew. Chem. Int. Ed.* **2009,** *48*, 7546.

[40] Sing, K. S. W.; Everett, D. H.; Haul, R. A. W.; Moscou, L.; Pierotti, R. A.; Rouquerol, J.; Siemieniewska, T., *Pure Appl. Chem.* **1985,** *57*, 603.

[41] Bai, Y. X.; Qian, J. W.; Zhao, Q.; Xu, Y.; Ye, S. R., *J. Appl. Poly. Sci.* **2006,** *102*, 2832.

List of Publications

General Introduction

TCNQ based hybrid porous coordination polymers
Satoru Shimomura, Susumu Kitagawa
Journal of Material Chemistry submitted.

Chapter 1

(1) TCNQ Dianion-Based Coordination Polymer Whose Open Framework Shows Charge-Transfer Type Guest Inclusion
Satoru Shimomura, Ryotaro Matsuda, Takashi Tsujino, Takashi Kawamura, and Susumu Kitagawa
Journal of the American Chemical Society **2006**, *128*, 16416-16417.
(2) Chemistry and application of porous coordination polymers
Satoru Shimomura, Satoshi Horike, and Susumu Kitagawa
Studies in Surface Science and Catalysis **2007**, *170* (B), 1983-1990.

Chapter 2

Impact of Metal-ion Dependence on the Porous and Electronic Properties of TCNQ-dianion-based Porous Coordination Polymers
Satoru Shimomura, Nobuhiro Yanai, Ryotaro Matsuda, and Susumu Kitagawa
Inorganic Chemistry **2011**, *50*, 172-177.

Chapter 3

Guest-Specific Function of a Flexible Undulating Channel in a 7,7,8,8-Tetracyano-p-quinodimethane Dimer-based Porous Coordination Polymer
Satoru Shimomura, Satoshi Horike, Ryotaro Matsuda, and Susumu Kitagawa
Journal of the American Chemical Society **2007**, *129*, 10990-10991.

Chapter 4

Selective Sorption of Oxygen and Nitric Oxide by an Electron-Donating Flexible Porous Coordination Polymer
Satoru Shimomura, Masakazu Higuchi, Ryotaro Matsuda, Ko Yoneda, Yuh Hijikata, Yoshiki Kubota, Yoshimi Mita, Jungeun Kim, Masaki Takata, and

Susumu Kitagawa
Nature Chemistry **2010**, *2*, 633-637.

Chapter 5

Flexibility of Porous Coordination Polymers Strongly Linked to Selective Sorption Mechanism
Satoru Shimomura, Ryotaro Matsuda, and Susumu Kitagawa
Chemistry of Materials **2010**, *22*, 4129-4131.

Other Publications

(1) Chemistry and application of flexible porous coordination polymers
Sareeya Bureekaew, Satoru Shimomura, Susumu Kitagawa
Science and Technology of Advanced Materials **2008**, *9*, no. 014108.

(2) Soft porous crystals
Satoshi Horike, Satoru Shimomura and Susumu Kitagawa
Nature Chemistry **2009**, *1*, 695-704.

(3) Porous coordination polymers towards gas technology
Satoru Shimomura, Sareeya Bureekaew, Susumu Kitagawa
Structure and Bonding **2009**, *132*, 51-86.

(4) Selective Gas Adsorption in One-Dimensional, Flexible CuII Coordination Polymers with Polar Units
Shin-ichiro Noro, Daisuke Tanaka, Hirotoshi Sakamoto, Satoru Shimomura, Susumu Kitagawa, Sadamu Takeda, Kazuhiro Uemura, Hidetoshi Kita, Tomoyuki Akutagawa and Takayoshi Nakamura
Chemistry of Materials **2009**, *21*, 3346-3355.

(5) Heterogeneously Hybridized Porous Coordination Polymer Crystals: Fabrication of Heterometallic Core-Shell Single Crystals with an In-Plane Rotational Epitaxial Relationship
Shuhei Furukawa, Kenji Hirai, Keiji Nakagawa, Yohei Takashima, Ryotaro

Matsuda, Takaaki Tsuruoka, Mio Kondo, Rie Haruki, Daisuke Tanaka, Hirotoshi Sakamoto, Satoru Shimomura, Osami Sakata, Susumu Kitagawa
Angewandte Chemie-International Edition **2009**, *48*, 1766-1770.

(6) Enhanced Selectivity of CO_2 from a Ternary Gas Mixture in an Interdigitated Porous Framework
Keiji Nakagawa, Daisuke Tanaka, Satoshi Horike, Satoru Shimomura, Masakazu Higuchi, Susumu Kitagawa
Chemical Communications **2010**, *46*, 4258-4260.

(7) Inclusion and Dynamics of a Polymer–Li Salt Complex in Coordination Nanochannels
Nobuhiro Yanai, Takashi Uemura, Satoshi Horike, Satoru Shimomura and Susumu Kitagawa
Chemical Communications **2011**, Advance Article.